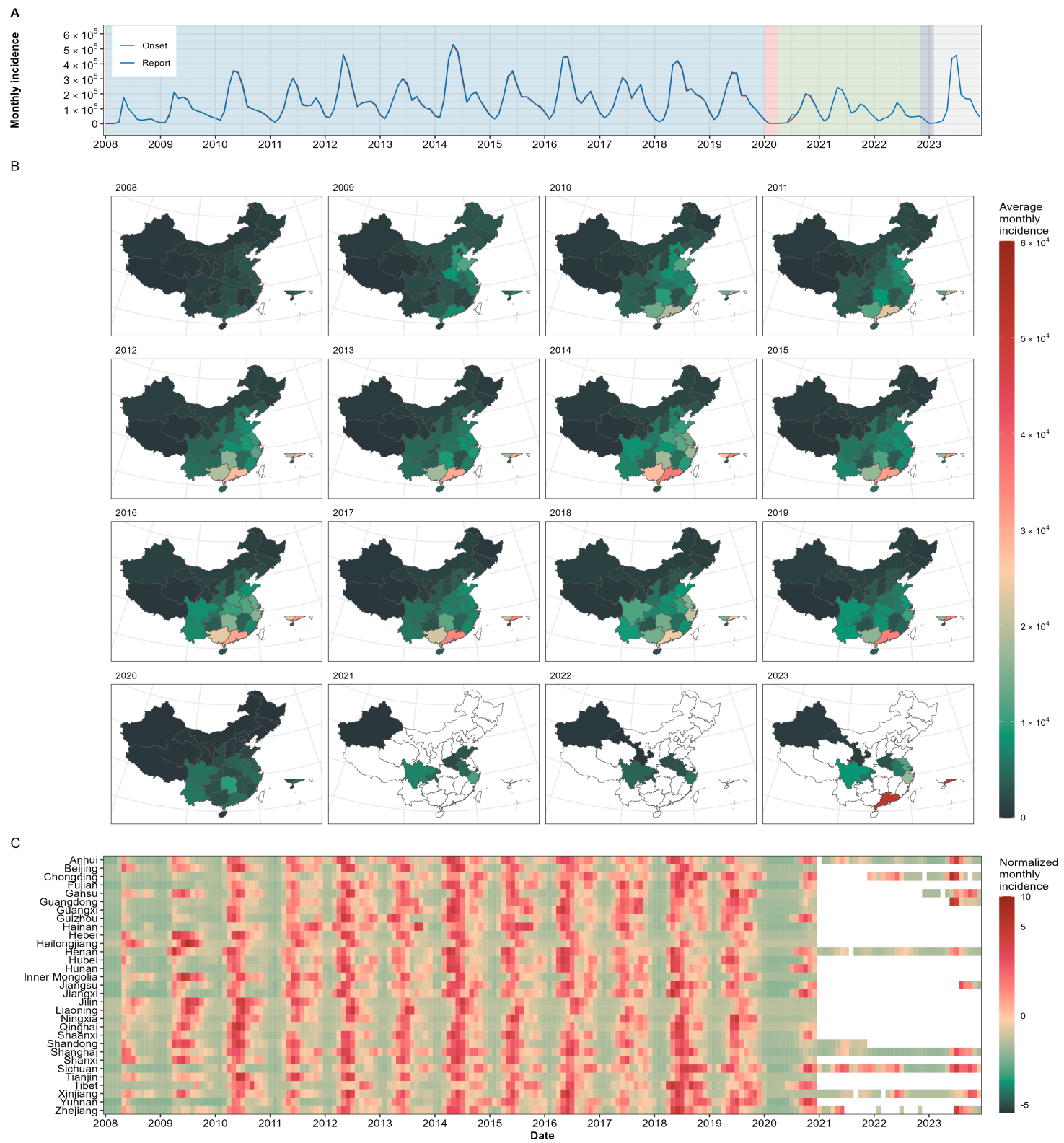


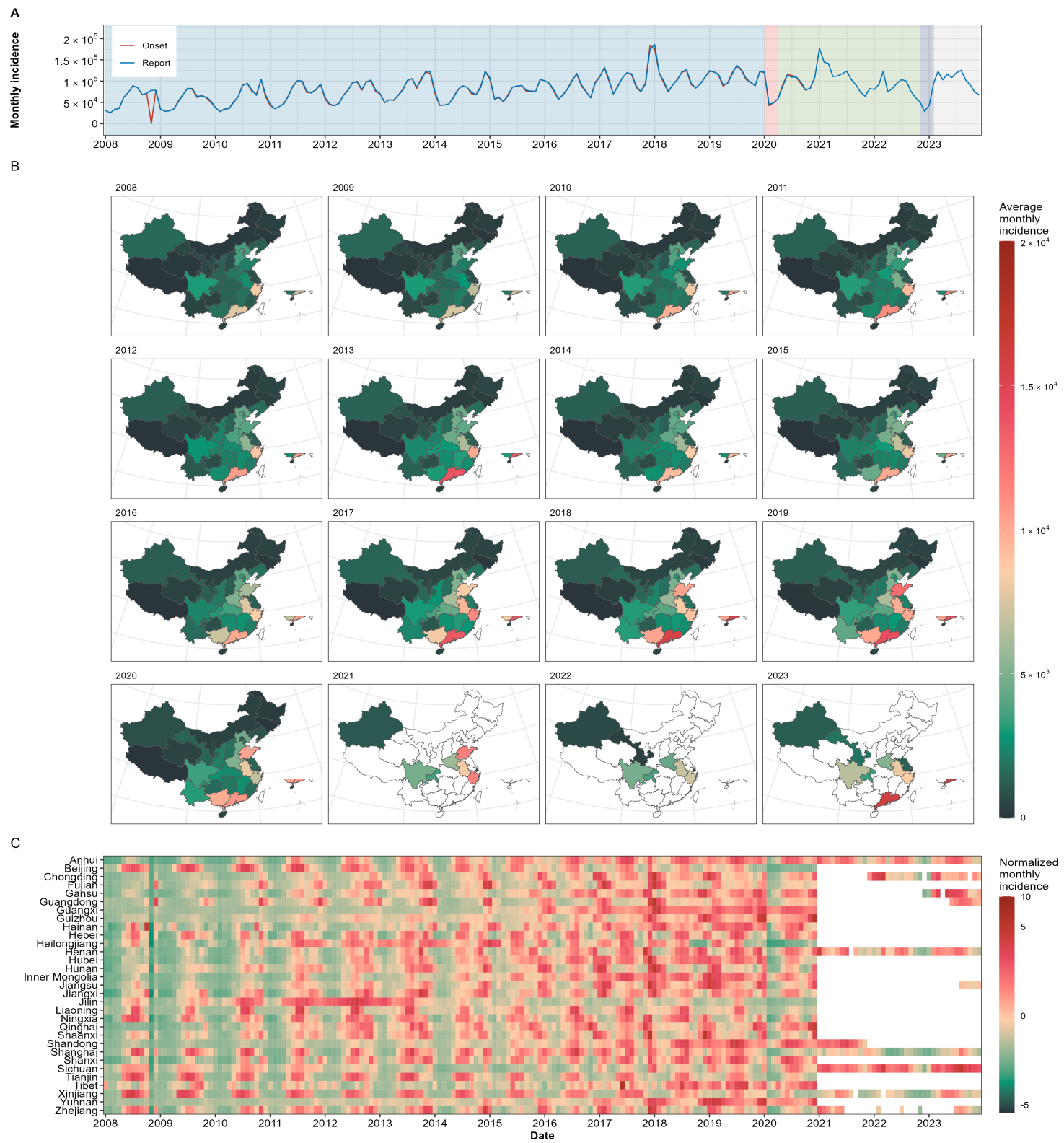
Supplementary Appendix 1:

**Temporal trends and shifts of 24 notifiable infectious diseases in China
before and after the COVID-19 epidemic**



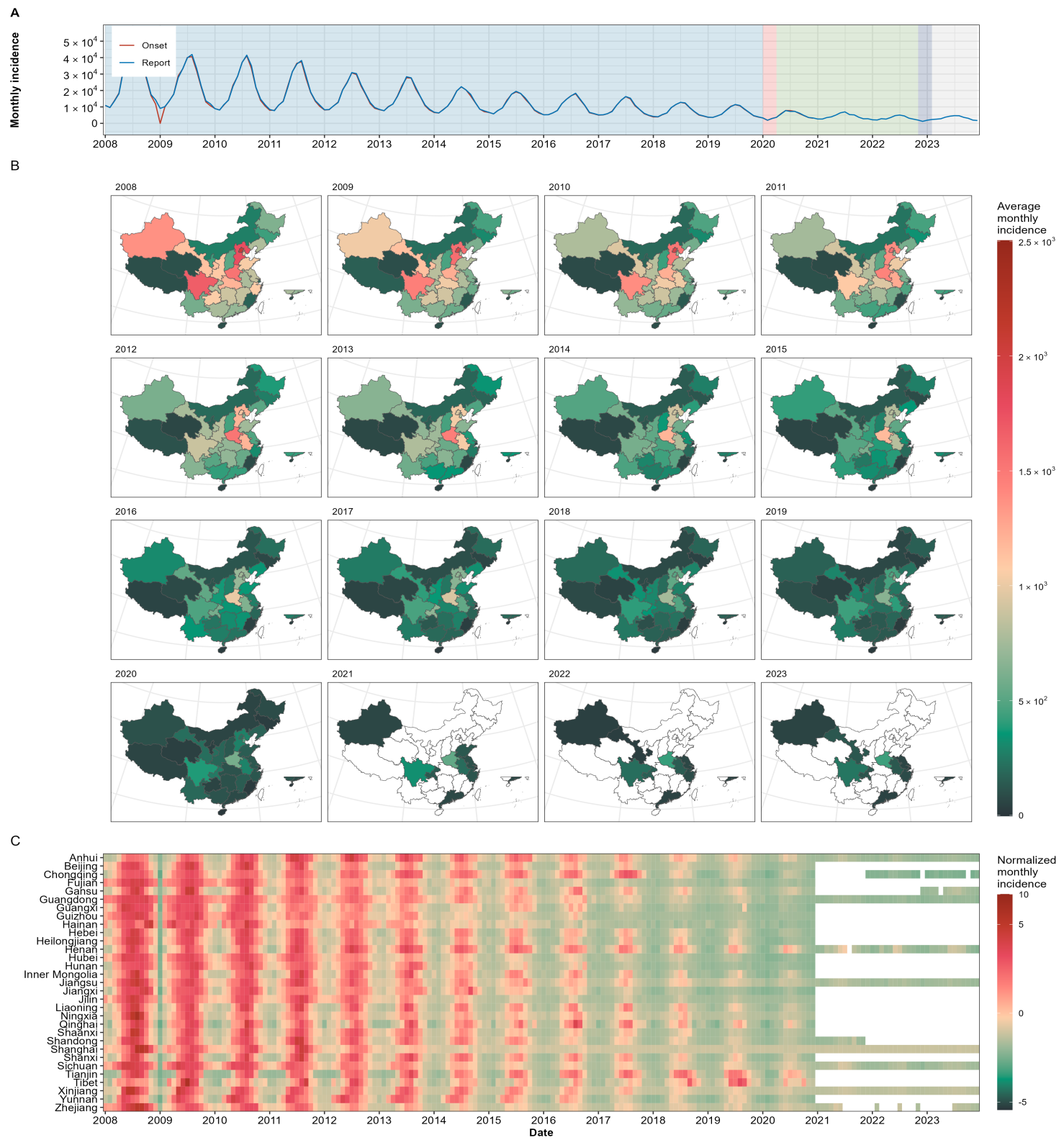
Supplementary Fig. 1. Temporal variation in the monthly incidence of hand, foot, and mouth disease (HFMD) in China from January 2008 to December 2023.

(A) The incidence of hand, foot, and mouth disease (HFMD) in China from January 2008 to December 2023; (B) The spatial distribution of cases in China; (C) Temporal variation in the monthly incidence between different provinces. The heatmap represents normalized monthly incidence data for each province, with color intensity corresponding to the normalized monthly incidence. Provincial data in panel (B) and (C) before January 2020 sourced from the Chinese Public Health Science Data Center, and data after January 2020 sourced from the provincial Notifiable Infectious Diseases Reports. * Normalized monthly incidence > 10.



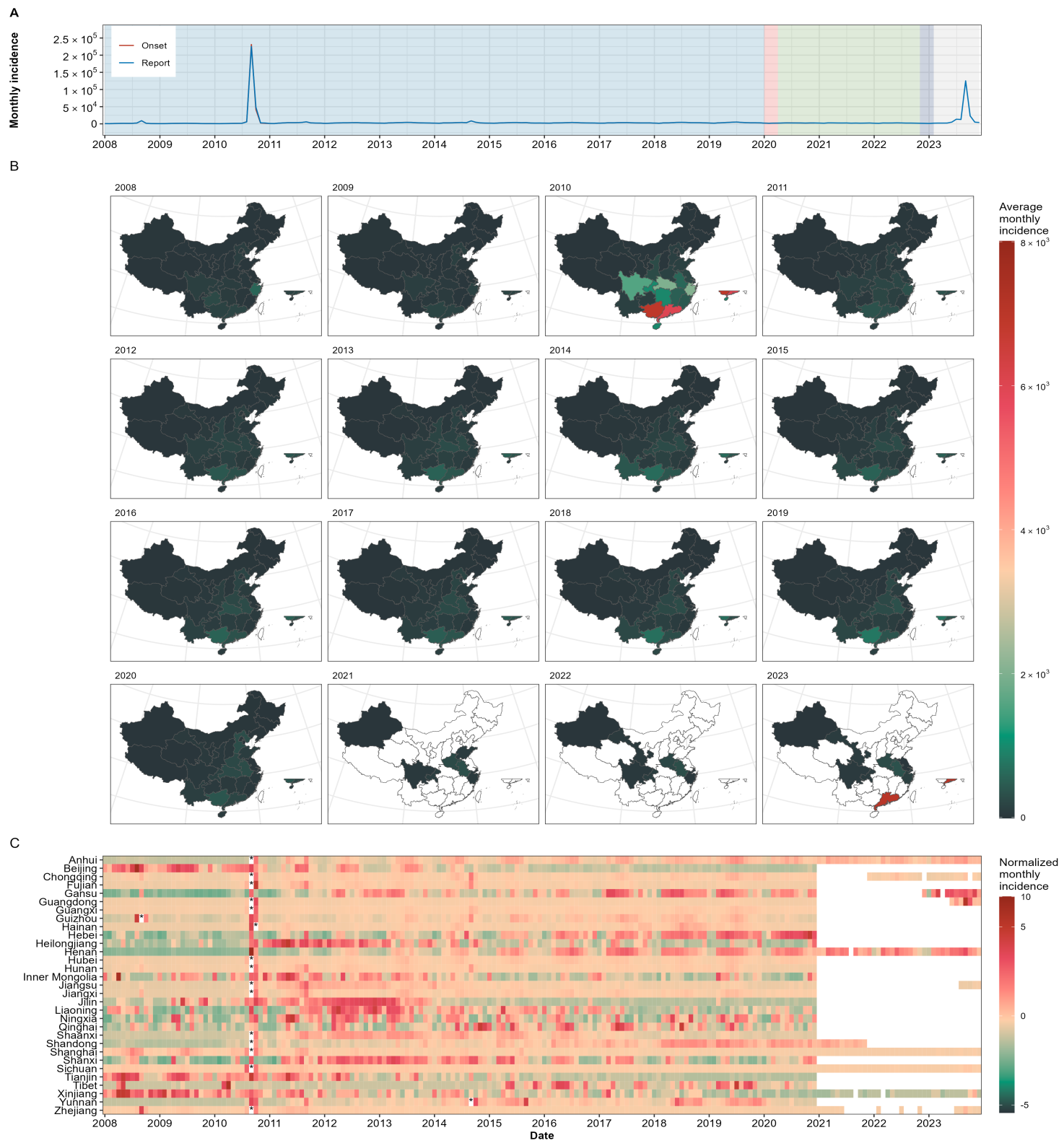
Supplementary Fig. 2. Temporal variation in the monthly incidence of infectious diarrhea in China from January 2008 to December 2023.

(A) The incidence of infectious diarrhea in China from January 2008 to December 2023; (B) The spatial distribution of cases in China; (C) Temporal variation in the monthly incidence between different provinces. The heatmap represents normalized monthly incidence data for each province, with color intensity corresponding to the normalized monthly incidence. Provincial data in panel (B) and (C) before January 2020 sourced from the Chinese Public Health Science Data Center, and data after January 2020 sourced from the provincial Notifiable Infectious Diseases Reports. * Normalized monthly incidence > 10.



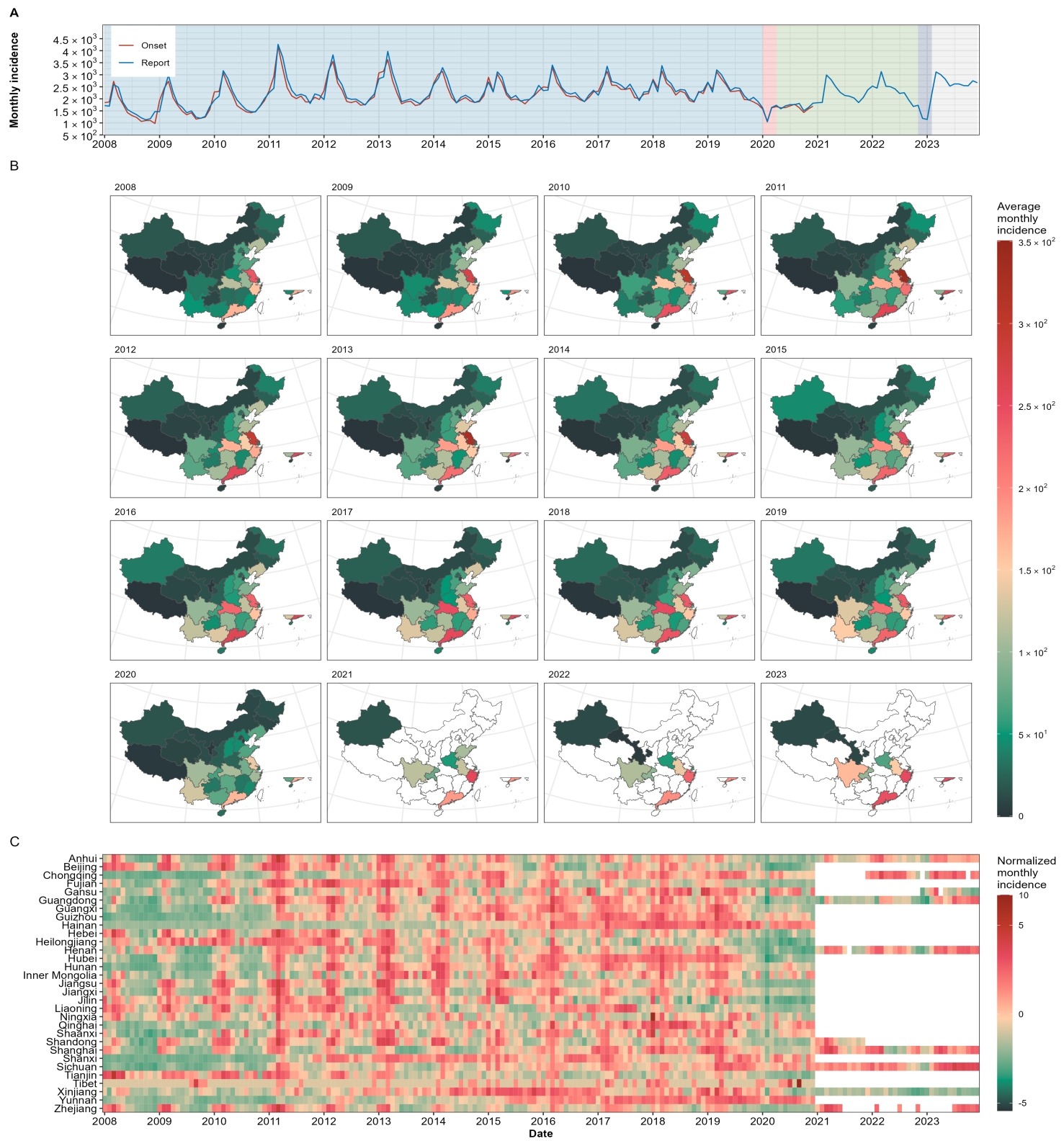
Supplementary Fig. 3. Temporal variation in the monthly incidence of dysentery in China from January 2008 to December 2023.

(A) The incidence of dysentery in China from January 2008 to December 2023; **(B)** The spatial distribution of cases in China; **(C)** Temporal variation in the monthly incidence between different provinces. The heatmap represents normalized monthly incidence data for each province, with color intensity corresponding to the normalized monthly incidence. Provincial data in panel **(B)** and **(C)** before January 2020 sourced from the Chinese Public Health Science Data Center, and data after January 2020 sourced from the provincial Notifiable Infectious Diseases Reports. * Normalized monthly incidence > 10.



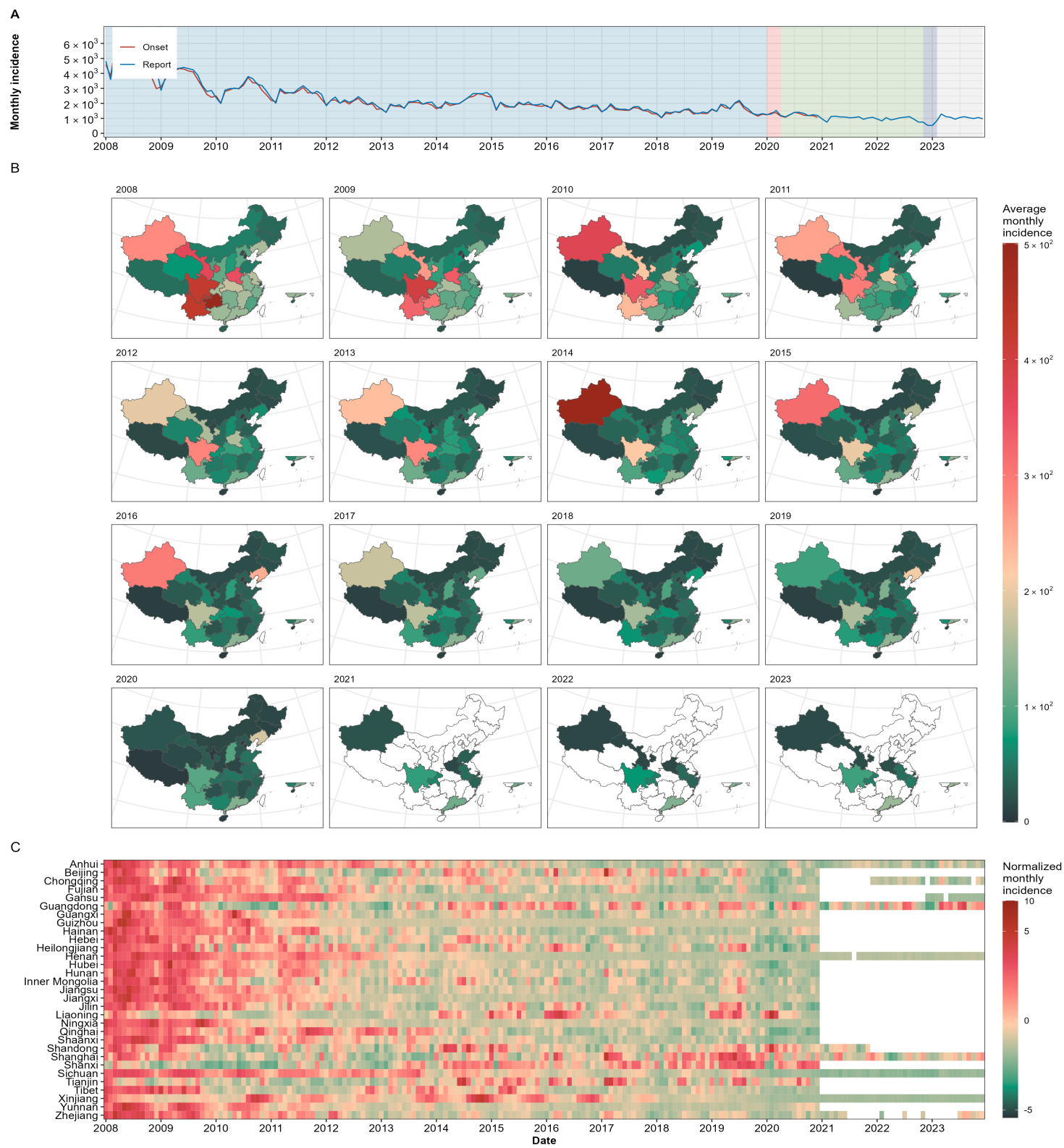
Supplementary Fig. 4. Temporal variation in the monthly incidence of acute hemorrhagic conjunctivitis (AHC) in China from January 2008 to December 2023.

(A) The incidence of acute hemorrhagic conjunctivitis (AHC) in China from January 2008 to December 2023; (B) The spatial distribution of cases in China; (C) Temporal variation in the monthly incidence between different provinces. The heatmap represents normalized monthly incidence data for each province, with color intensity corresponding to the normalized monthly incidence. Provincial data in panel (B) and (C) before January 2020 sourced from the Chinese Public Health Science Data Center, and data after January 2020 sourced from the provincial Notifiable Infectious Diseases Reports. * Normalized monthly incidence > 10.



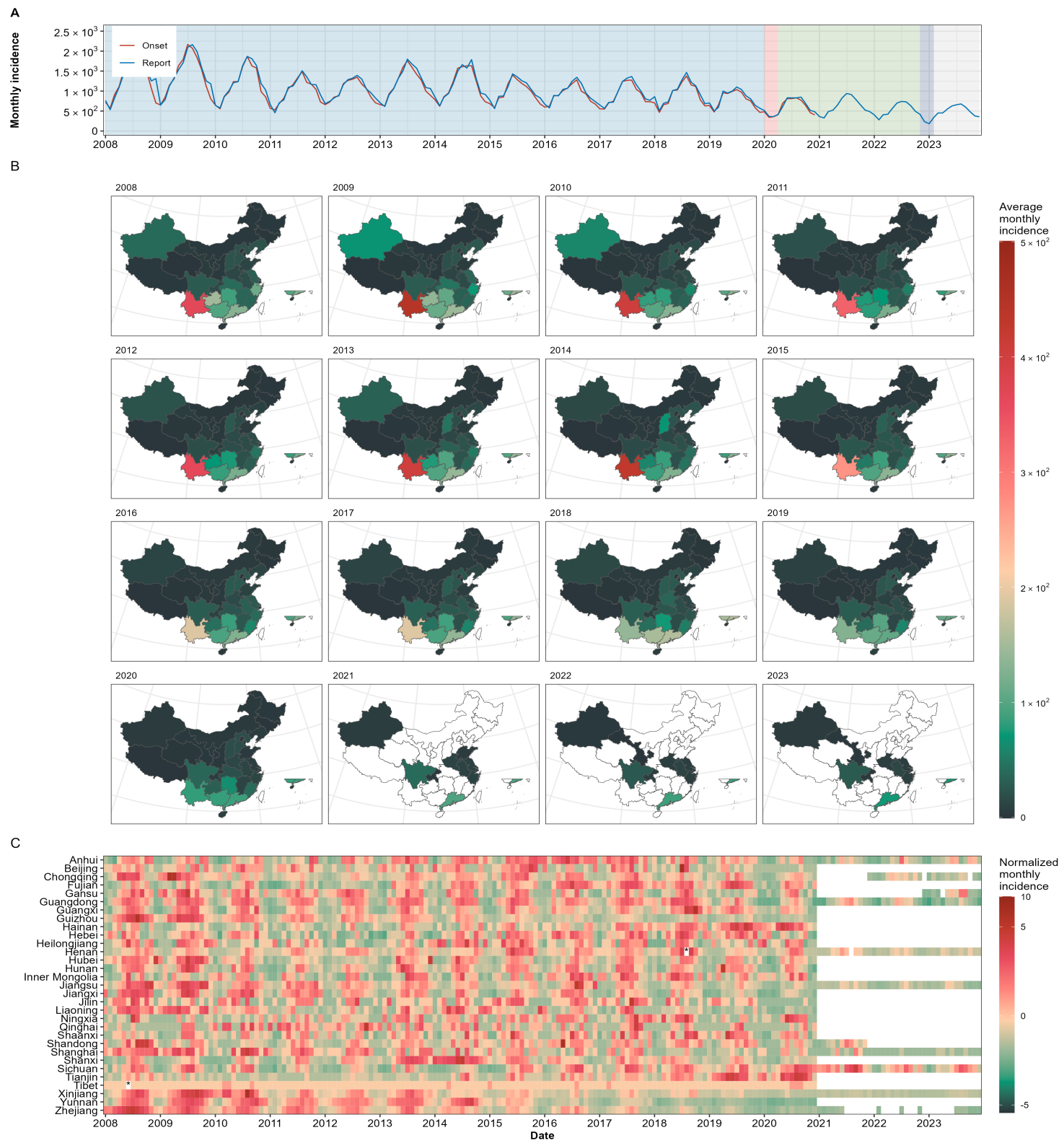
Supplementary Fig. 5. Temporal variation in the monthly incidence of hepatitis E in China from January 2008 to December 2023.

(A) The incidence of hepatitis E in China from January 2008 to December 2023; **(B)** The spatial distribution of cases in China; **(C)** Temporal variation in the monthly incidence between different provinces. The heatmap represents normalized monthly incidence data for each province, with color intensity corresponding to the normalized monthly incidence. Provincial data in panel **(B)** and **(C)** before January 2020 sourced from the Chinese Public Health Science Data Center, and data after January 2020 sourced from the provincial Notifiable Infectious Diseases Reports. * Normalized monthly incidence > 10.



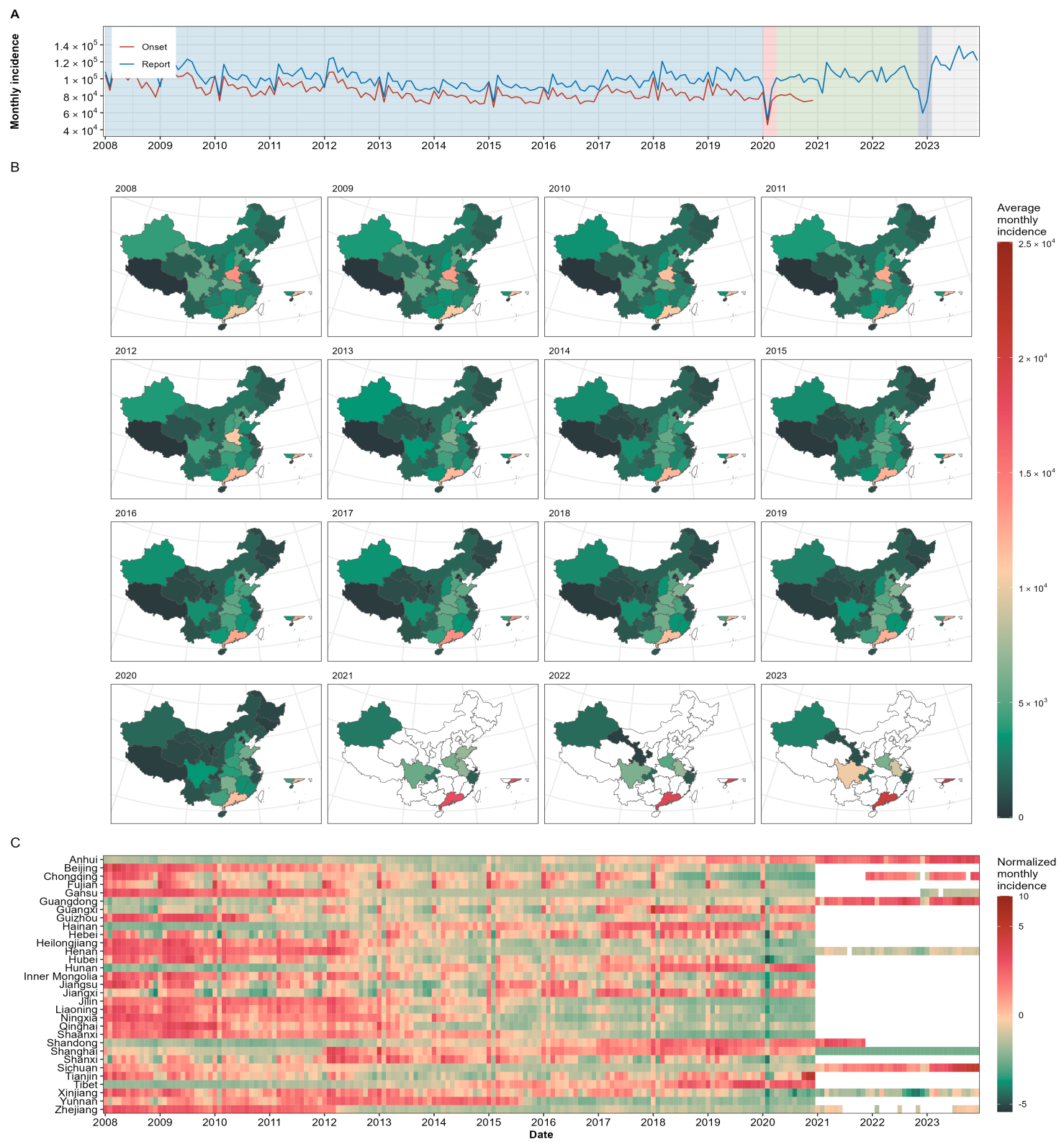
Supplementary Fig. 6. Temporal variation in the monthly incidence of hepatitis A in China from January 2008 to December 2023.

(A) The incidence of hepatitis A in China from January 2008 to December 2023; (B) The spatial distribution of cases in China; (C) Temporal variation in the monthly incidence between different provinces. The heatmap represents normalized monthly incidence data for each province, with color intensity corresponding to the normalized monthly incidence. Provincial data in panel (B) and (C) before January 2020 sourced from the Chinese Public Health Science Data Center, and data after January 2020 sourced from the provincial Notifiable Infectious Diseases Reports. * Normalized monthly incidence > 10.



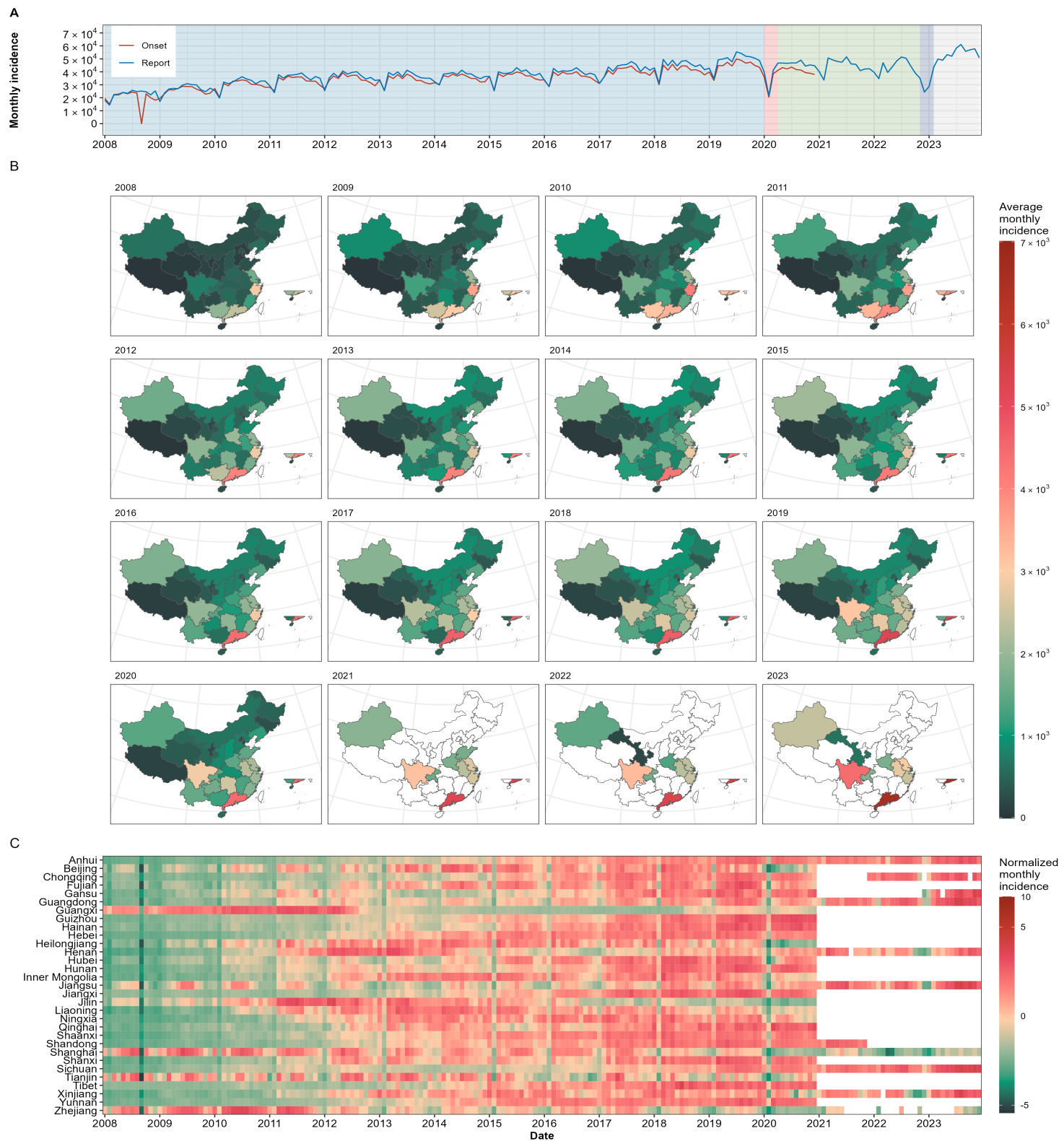
Supplementary Fig. 7. Temporal variation in the monthly incidence of enteric fever in China from January 2008 to December 2023.

(A) The incidence of enteric fever in China from January 2008 to December 2023; **(B)** The spatial distribution of cases in China; **(C)** Temporal variation in the monthly incidence between different provinces. The heatmap represents normalized monthly incidence data for each province, with color intensity corresponding to the normalized monthly incidence. Provincial data in panel **(B)** and **(C)** before January 2020 sourced from the Chinese Public Health Science Data Center, and data after January 2020 sourced from the provincial Notifiable Infectious Diseases Reports. * Normalized monthly incidence > 10.



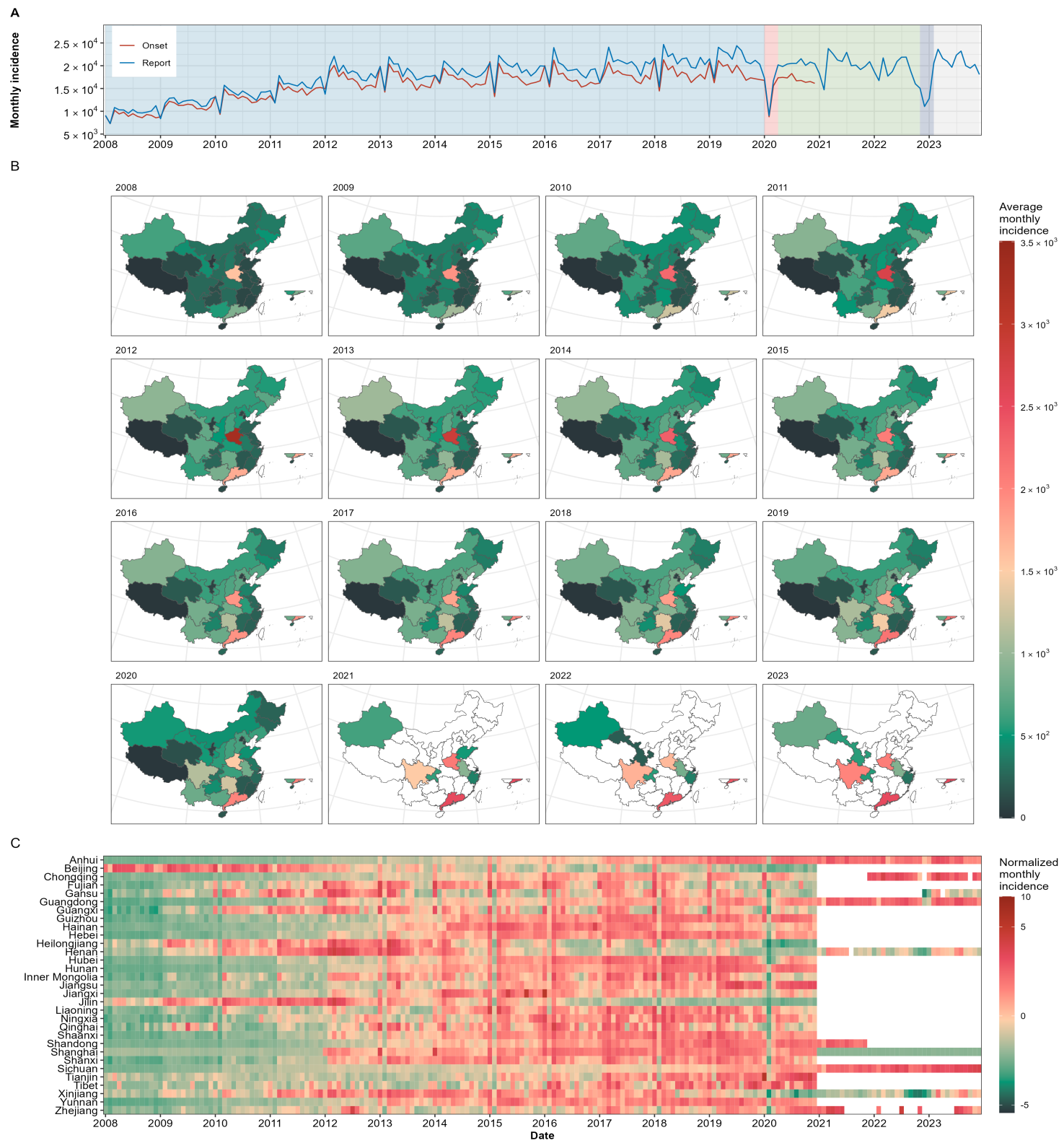
Supplementary Fig. 8. Temporal variation in the monthly incidence of hepatitis B in China from January 2008 to December 2023.

(A) The incidence of hepatitis B in China from January 2008 to December 2023; **(B)** The spatial distribution of cases in China; **(C)** Temporal variation in the monthly incidence between different provinces. The heatmap represents normalized monthly incidence data for each province, with color intensity corresponding to the normalized monthly incidence. Provincial data in panel **(B)** and **(C)** before January 2020 sourced from the Chinese Public Health Science Data Center, and data after January 2020 sourced from the provincial Notifiable Infectious Diseases Reports. * Normalized monthly incidence > 10.



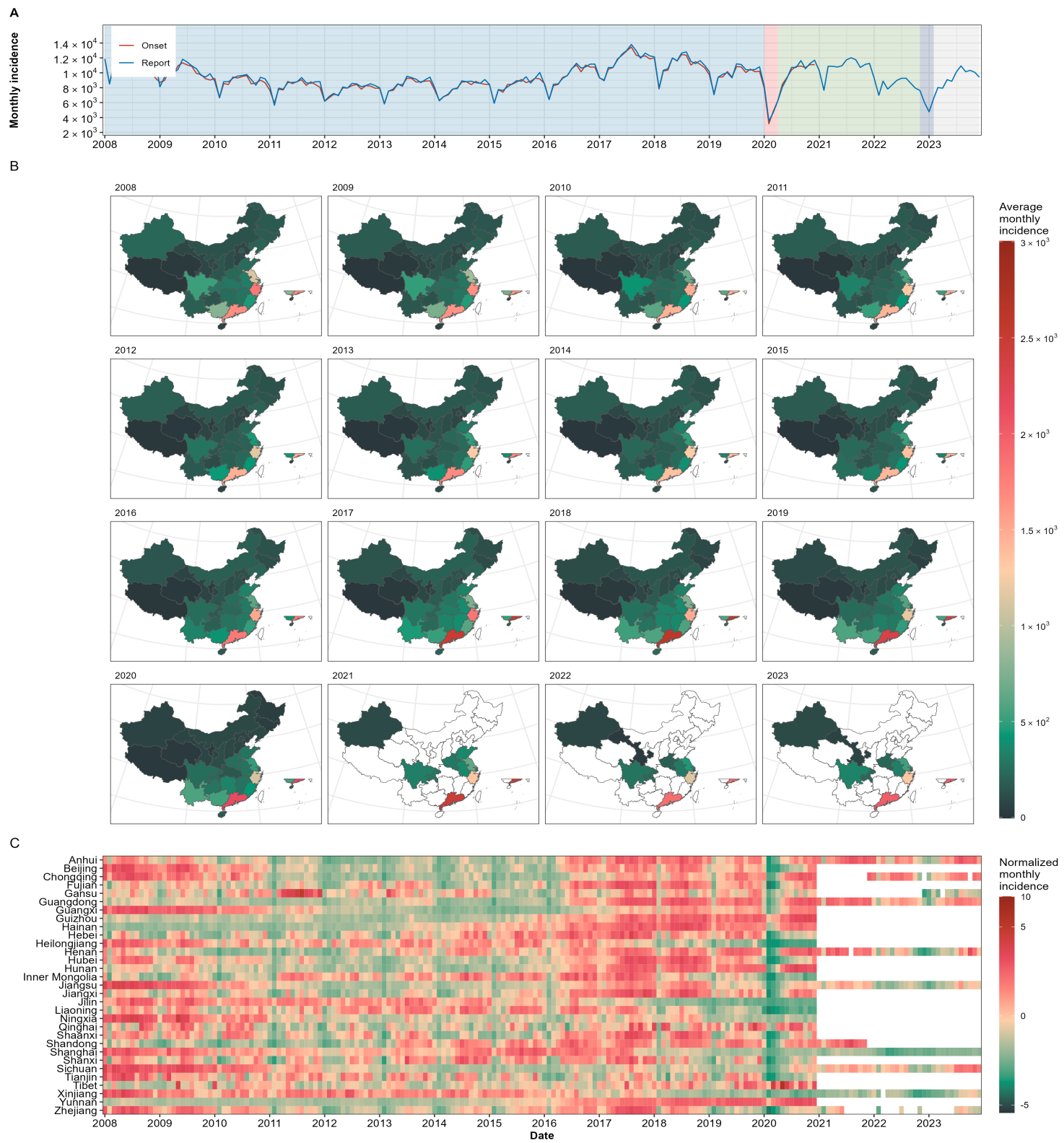
Supplementary Fig. 9. Temporal variation in the monthly incidence of syphilis in China from January 2008 to December 2023.

(A) The incidence of syphilis in China from January 2008 to December 2023; **(B)** The spatial distribution of cases in China; **(C)** Temporal variation in the monthly incidence between different provinces. The heatmap represents normalized monthly incidence data for each province, with color intensity corresponding to the normalized monthly incidence. Provincial data in panel **(B)** and **(C)** before January 2020 sourced from the Chinese Public Health Science Data Center, and data after January 2020 sourced from the provincial Notifiable Infectious Diseases Reports. * Normalized monthly incidence > 10.



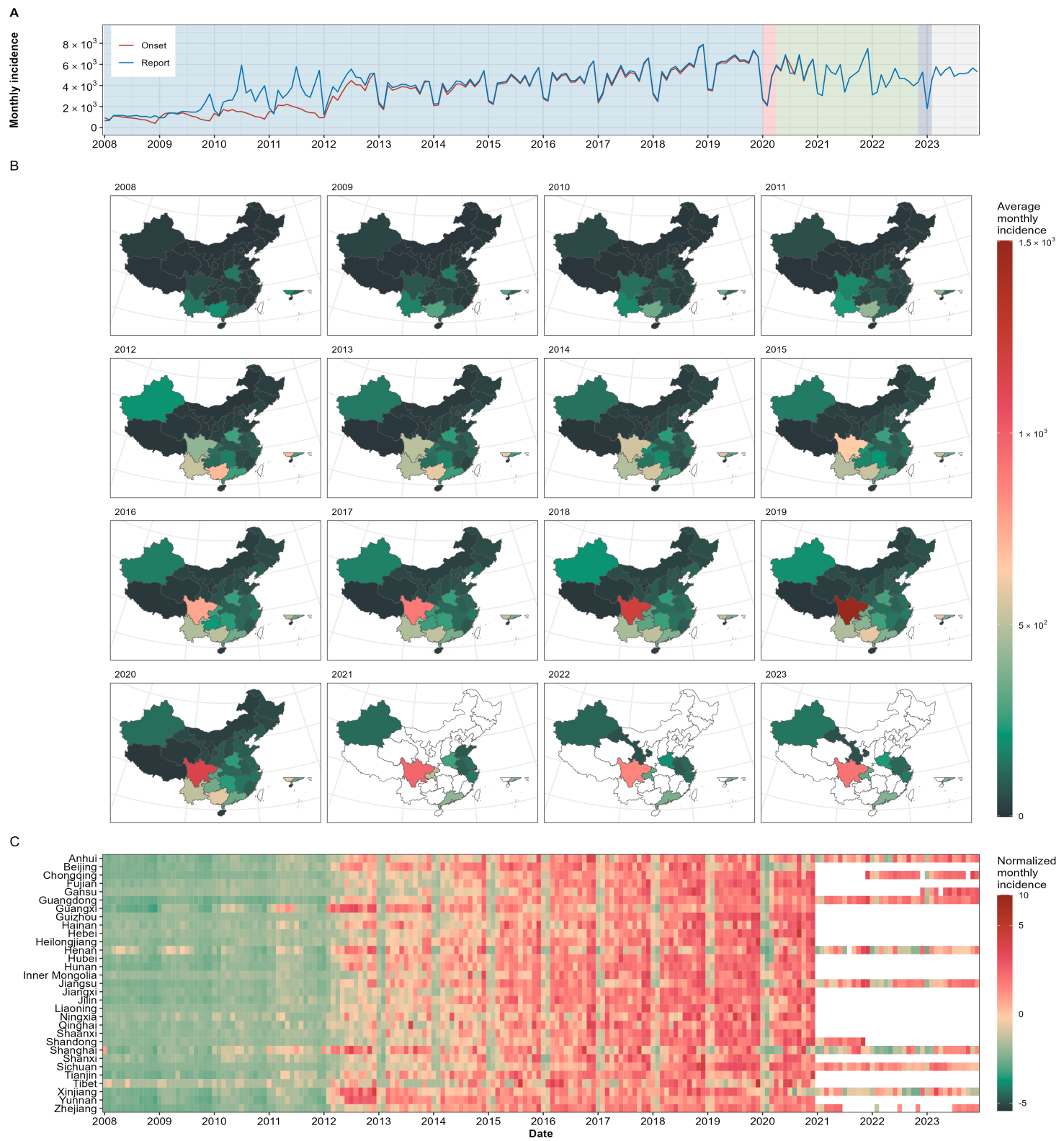
Supplementary Fig. 10. Temporal variation in the monthly incidence of hepatitis C in China from January 2008 to December 2023.

(A) The incidence of hepatitis C in China from January 2008 to December 2023; **(B)** The spatial distribution of cases in China; **(C)** Temporal variation in the monthly incidence between different provinces. The heatmap represents normalized monthly incidence data for each province, with color intensity corresponding to the normalized monthly incidence. Provincial data in panel **(B)** and **(C)** before January 2020 sourced from the Chinese Public Health Science Data Center, and data after January 2020 sourced from the provincial Notifiable Infectious Diseases Reports. * Normalized monthly incidence > 10.



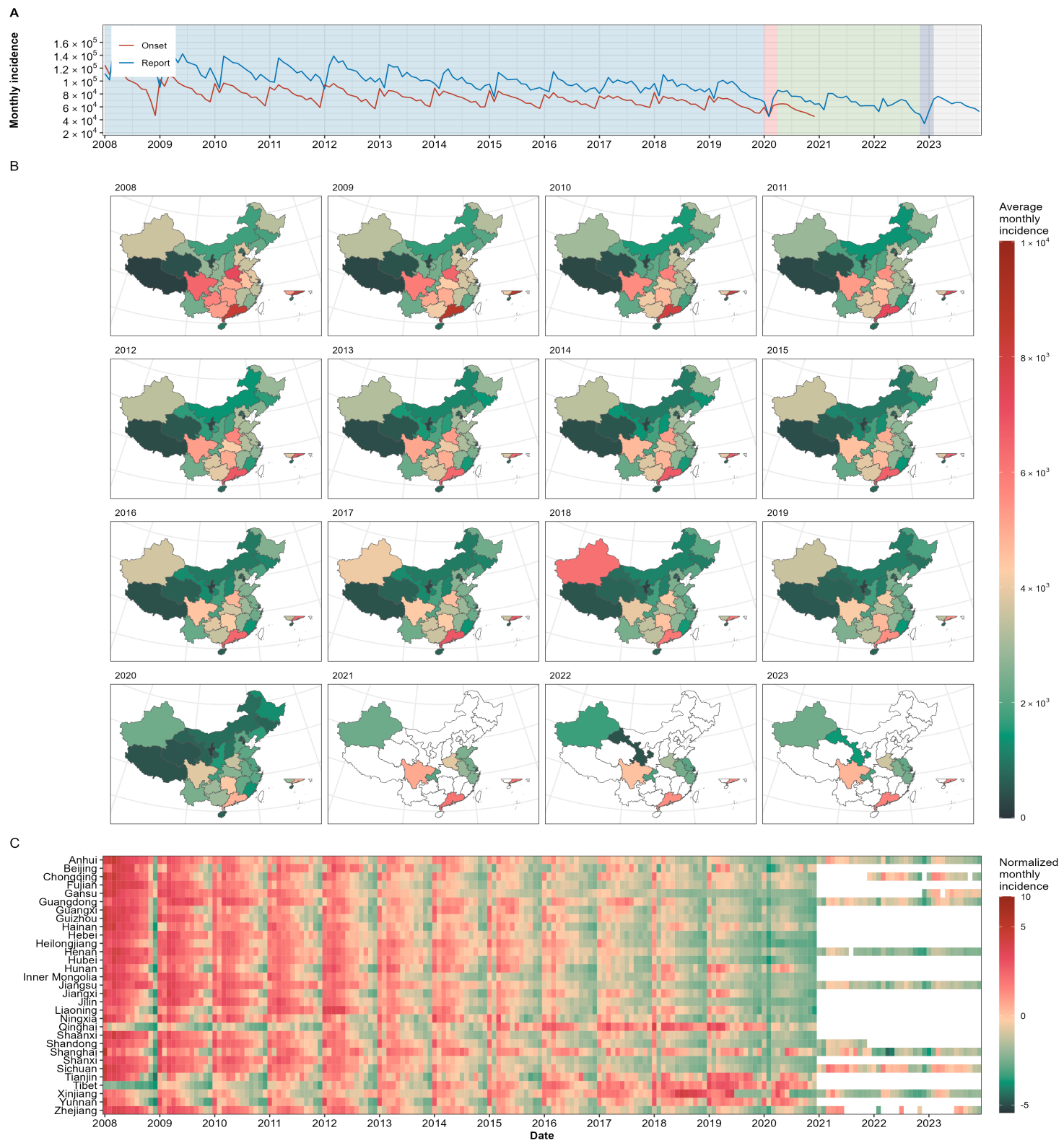
Supplementary Fig. 11. Temporal variation in the monthly incidence of gonorrhea in China from January 2008 to December 2023.

(A) The incidence of gonorrhea in China from January 2008 to December 2023; (B) The spatial distribution of cases in China; (C) Temporal variation in the monthly incidence between different provinces. The heatmap represents normalized monthly incidence data for each province, with color intensity corresponding to the normalized monthly incidence. Provincial data in panel (B) and (C) before January 2020 sourced from the Chinese Public Health Science Data Center, and data after January 2020 sourced from the provincial Notifiable Infectious Diseases Reports. * Normalized monthly incidence > 10.



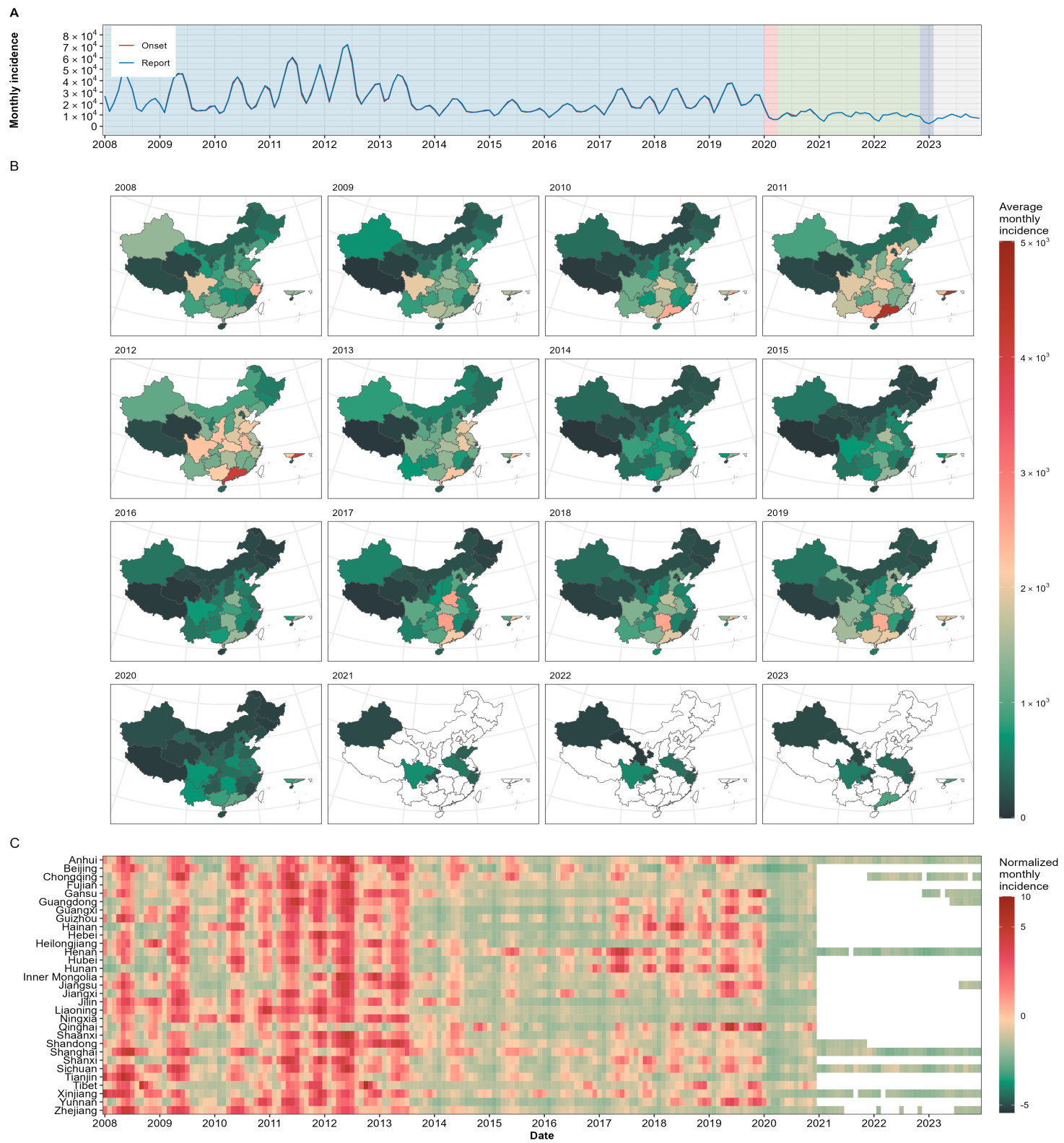
Supplementary Fig. 12. Temporal variation in the monthly incidence of acquired immunodeficiency syndrome (AIDS) in China from January 2008 to December 2023.

(A) The incidence of acquired immunodeficiency syndrome (AIDS) in China from January 2008 to December 2023; (B) The spatial distribution of cases in China; (C) Temporal variation in the monthly incidence between different provinces. The heatmap represents normalized monthly incidence data for each province, with color intensity corresponding to the normalized monthly incidence. Provincial data in panel (B) and (C) before January 2020 sourced from the Chinese Public Health Science Data Center, and data after January 2020 sourced from the provincial Notifiable Infectious Diseases Reports. * Normalized monthly incidence > 10.



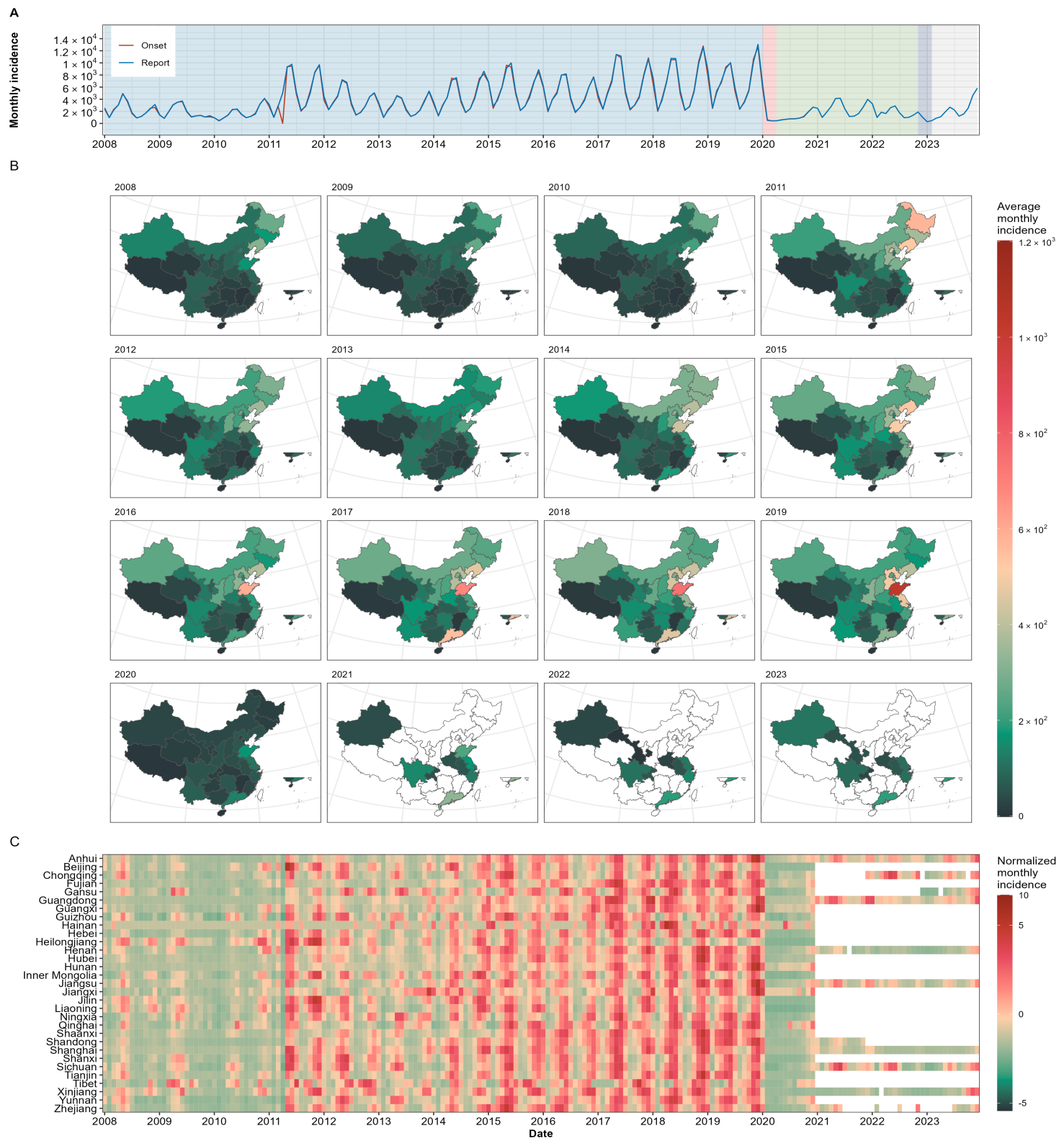
Supplementary Fig. 13. Temporal variation in the monthly incidence of tuberculosis in China from January 2008 to December 2023.

(A) The incidence of tuberculosis in China from January 2008 to December 2023; **(B)** The spatial distribution of cases in China; **(C)** Temporal variation in the monthly incidence between different provinces. The heatmap represents normalized monthly incidence data for each province, with color intensity corresponding to the normalized monthly incidence. Provincial data in panel **(B)** and **(C)** before January 2020 sourced from the Chinese Public Health Science Data Center, and data after January 2020 sourced from the provincial Notifiable Infectious Diseases Reports. * Normalized monthly incidence > 10.



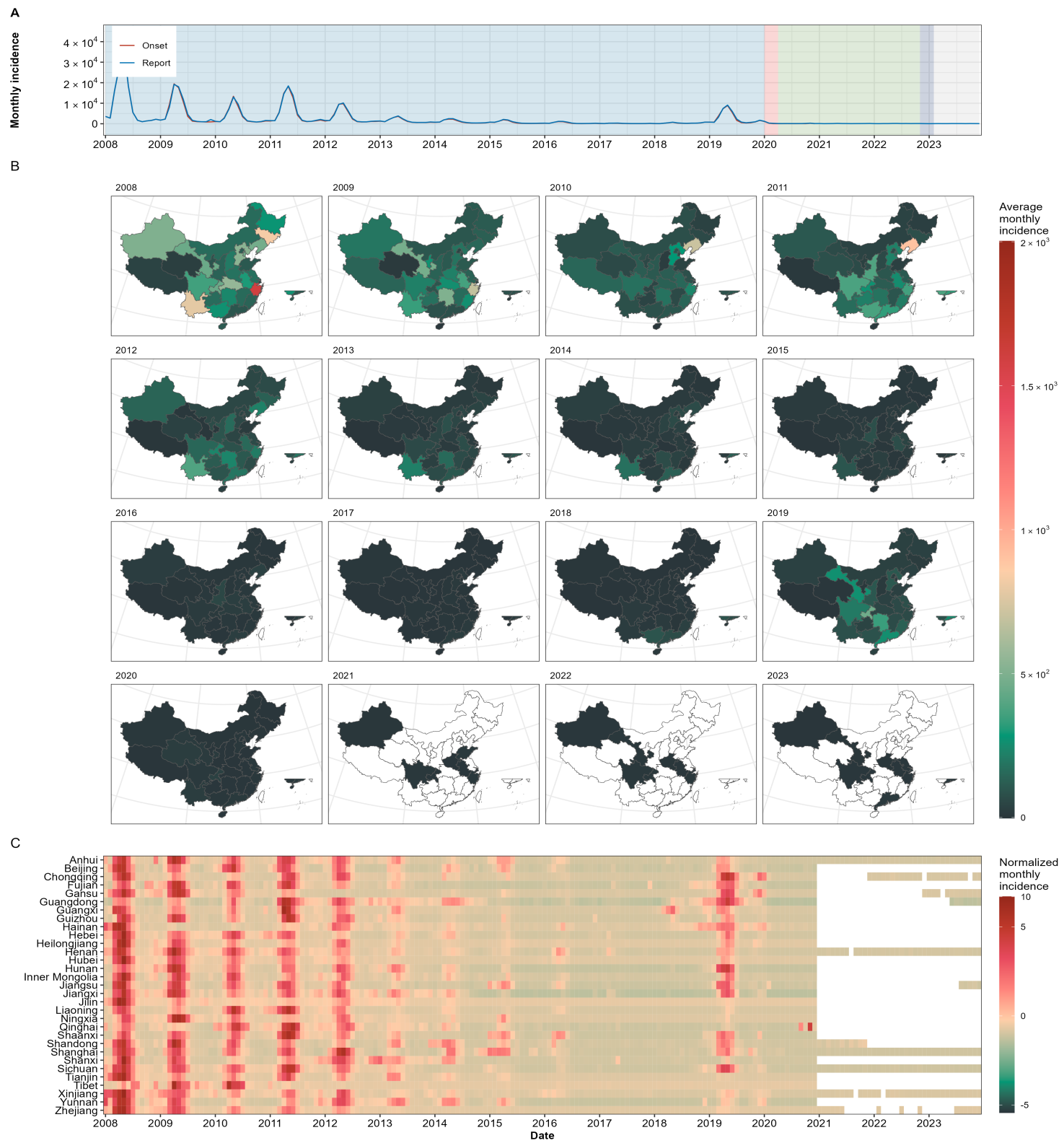
Supplementary Fig. 14. Temporal variation in the monthly incidence of mumps in China from January 2008 to December 2023.

(A) The incidence of mumps in China from January 2008 to December 2023; (B) The spatial distribution of cases in China; (C) Temporal variation in the monthly incidence between different provinces. The heatmap represents normalized monthly incidence data for each province, with color intensity corresponding to the normalized monthly incidence. Provincial data in panel (B) and (C) before January 2020 sourced from the Chinese Public Health Science Data Center, and data after January 2020 sourced from the provincial Notifiable Infectious Diseases Reports. * Normalized monthly incidence > 10.



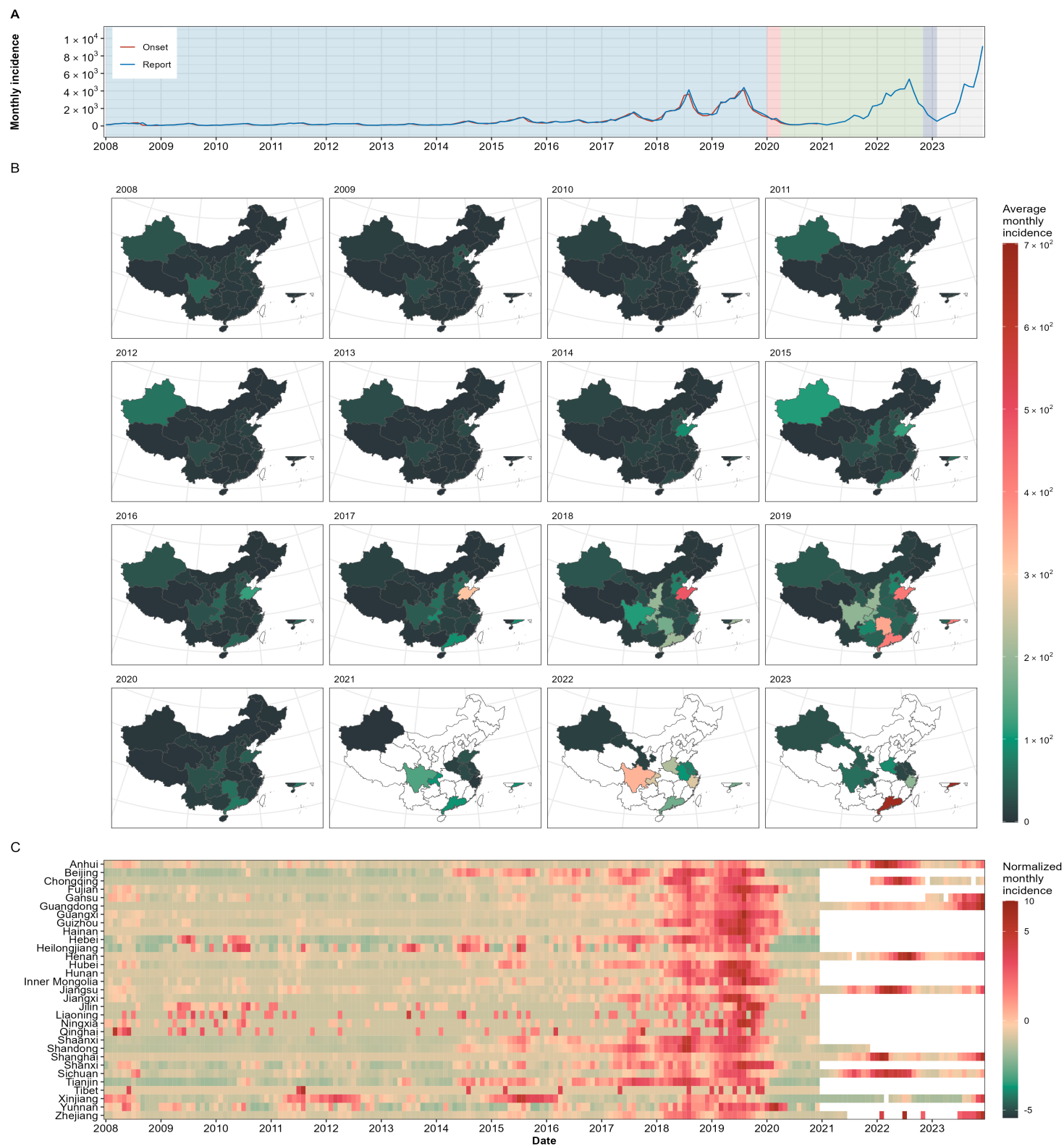
Supplementary Fig. 15. Temporal variation in the monthly incidence of scarlet fever in China from January 2008 to December 2023.

(A) The incidence of scarlet fever in China from January 2008 to December 2023; **(B)** The spatial distribution of cases in China; **(C)** Temporal variation in the monthly incidence between different provinces. The heatmap represents normalized monthly incidence data for each province, with color intensity corresponding to the normalized monthly incidence. Provincial data in panel **(B)** and **(C)** before January 2020 sourced from the Chinese Public Health Science Data Center, and data after January 2020 sourced from the provincial Notifiable Infectious Diseases Reports. * Normalized monthly incidence > 10.



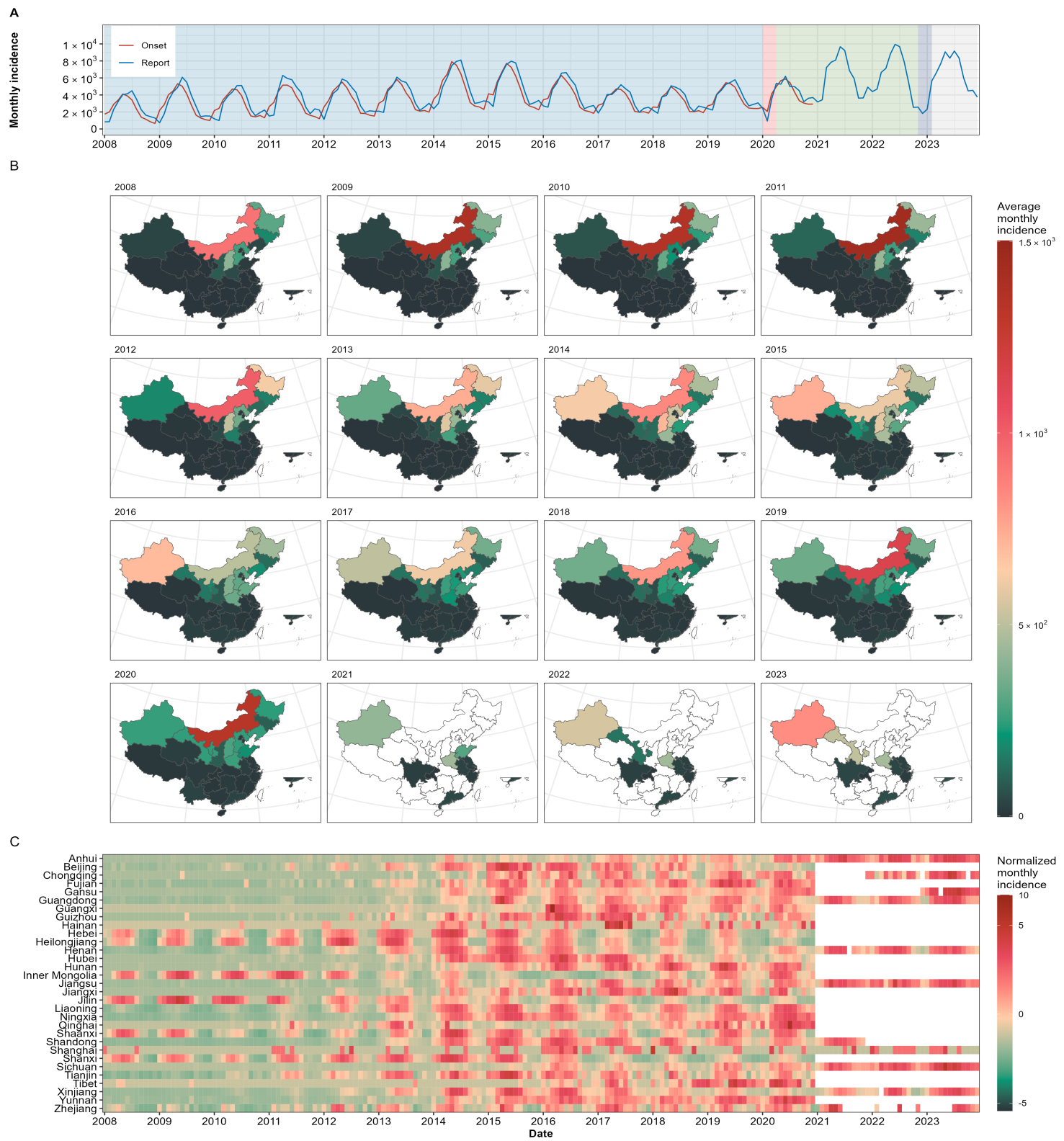
Supplementary Fig. 16. Temporal variation in the monthly incidence of rubella in China from January 2008 to December 2023.

(A) The incidence of rubella in China from January 2008 to December 2023; (B) The spatial distribution of cases in China; (C) Temporal variation in the monthly incidence between different provinces. The heatmap represents normalized monthly incidence data for each province, with color intensity corresponding to the normalized monthly incidence. Provincial data in panel (B) and (C) before January 2020 sourced from the Chinese Public Health Science Data Center, and data after January 2020 sourced from the provincial Notifiable Infectious Diseases Reports. * Normalized monthly incidence > 10.



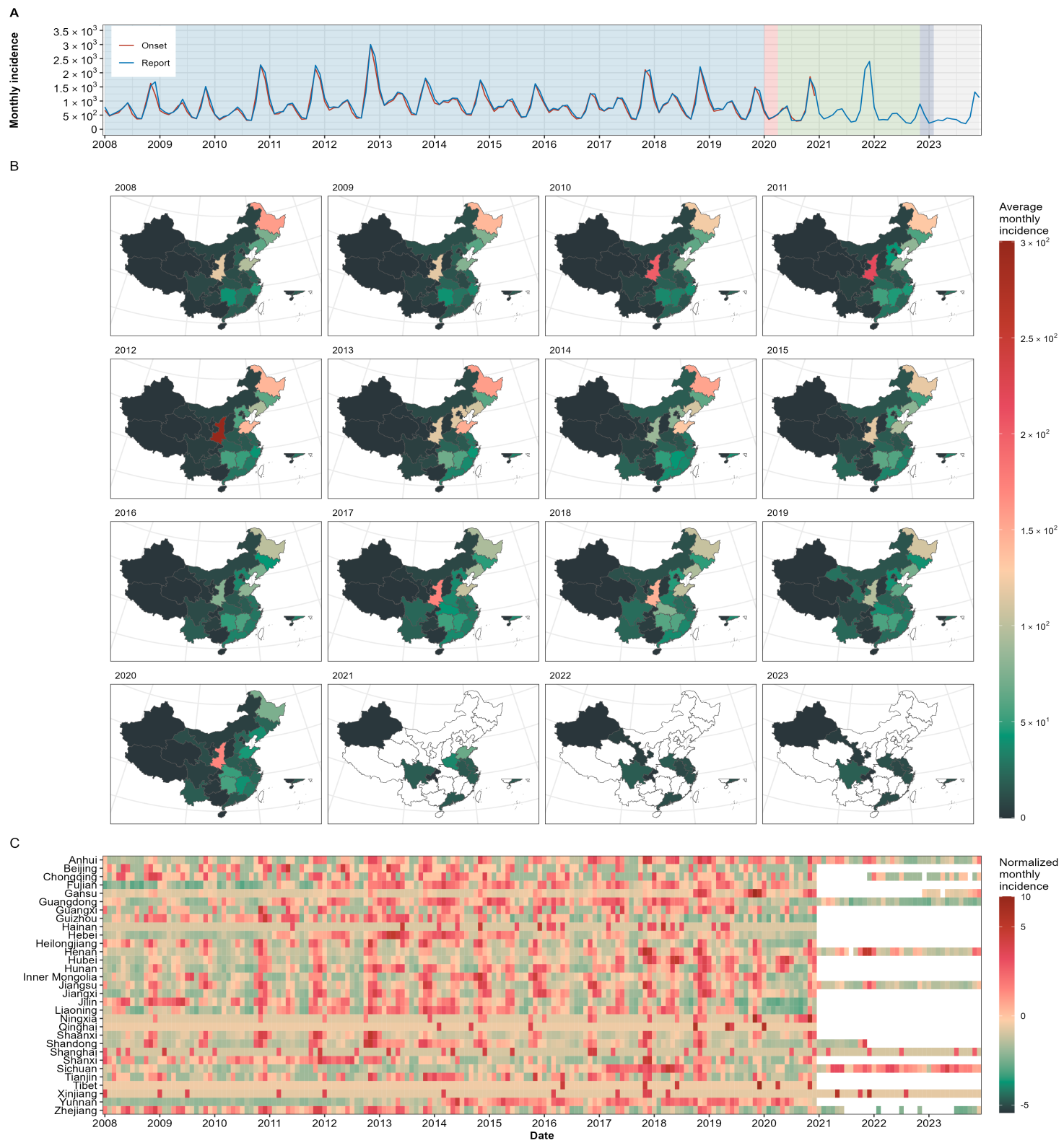
Supplementary Fig. 17. Temporal variation in the monthly incidence of pertussis in China from January 2008 to December 2023.

(A) The incidence of pertussis in China from January 2008 to December 2023; (B) The spatial distribution of cases in China; (C) Temporal variation in the monthly incidence between different provinces. The heatmap represents normalized monthly incidence data for each province, with color intensity corresponding to the normalized monthly incidence. Provincial data in panel (B) and (C) before January 2020 sourced from the Chinese Public Health Science Data Center, and data after January 2020 sourced from the provincial Notifiable Infectious Diseases Reports. * Normalized monthly incidence > 10.



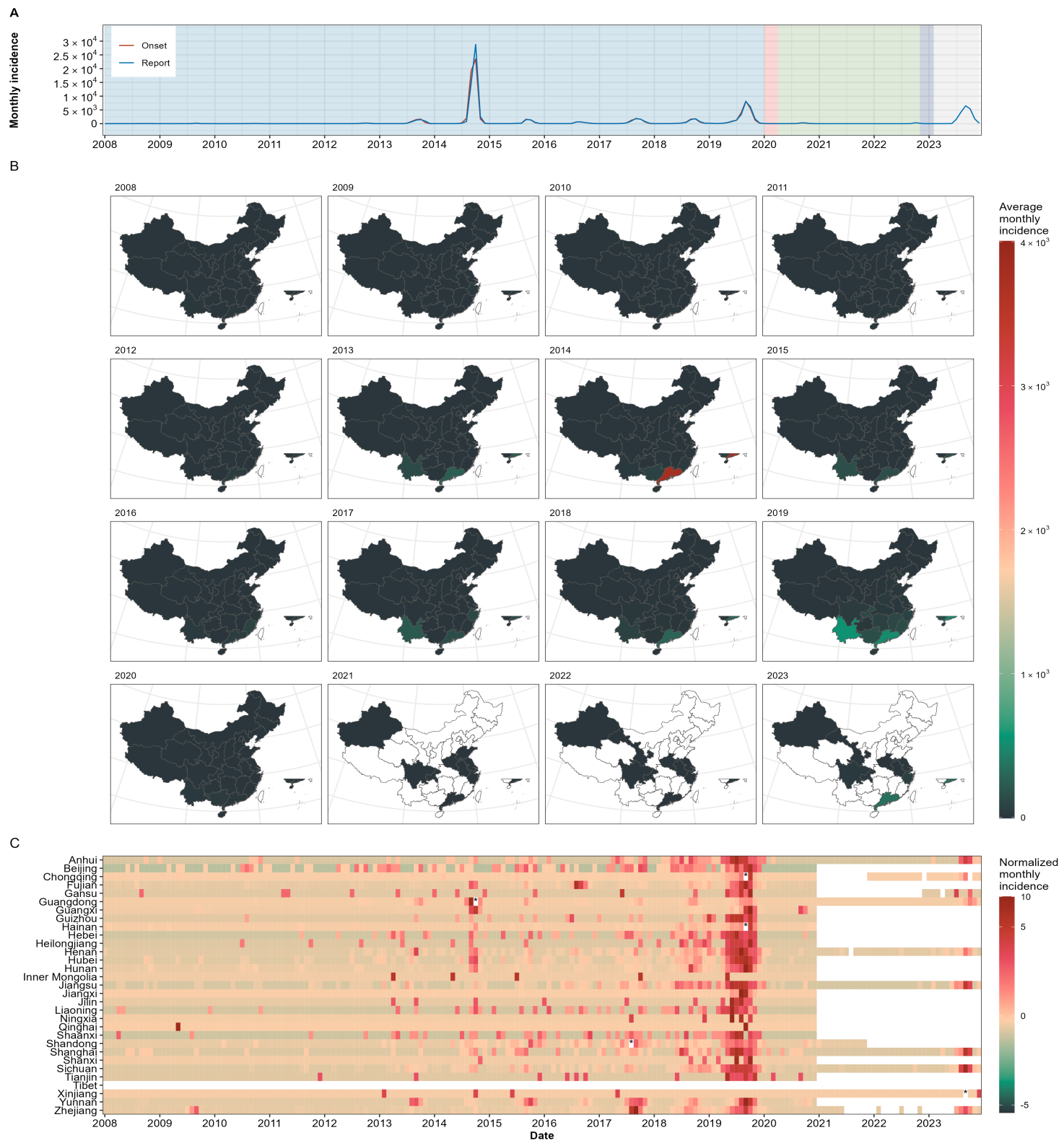
Supplementary Fig. 18. Temporal variation in the monthly incidence of brucellosis in China from January 2008 to December 2023.

(A) The incidence of brucellosis in China from January 2008 to December 2023; (B) The spatial distribution of cases in China; (C) Temporal variation in the monthly incidence between different provinces. The heatmap represents normalized monthly incidence data for each province, with color intensity corresponding to the normalized monthly incidence. Provincial data in panel (B) and (C) before January 2020 sourced from the Chinese Public Health Science Data Center, and data after January 2020 sourced from the provincial Notifiable Infectious Diseases Reports. * Normalized monthly incidence > 10.



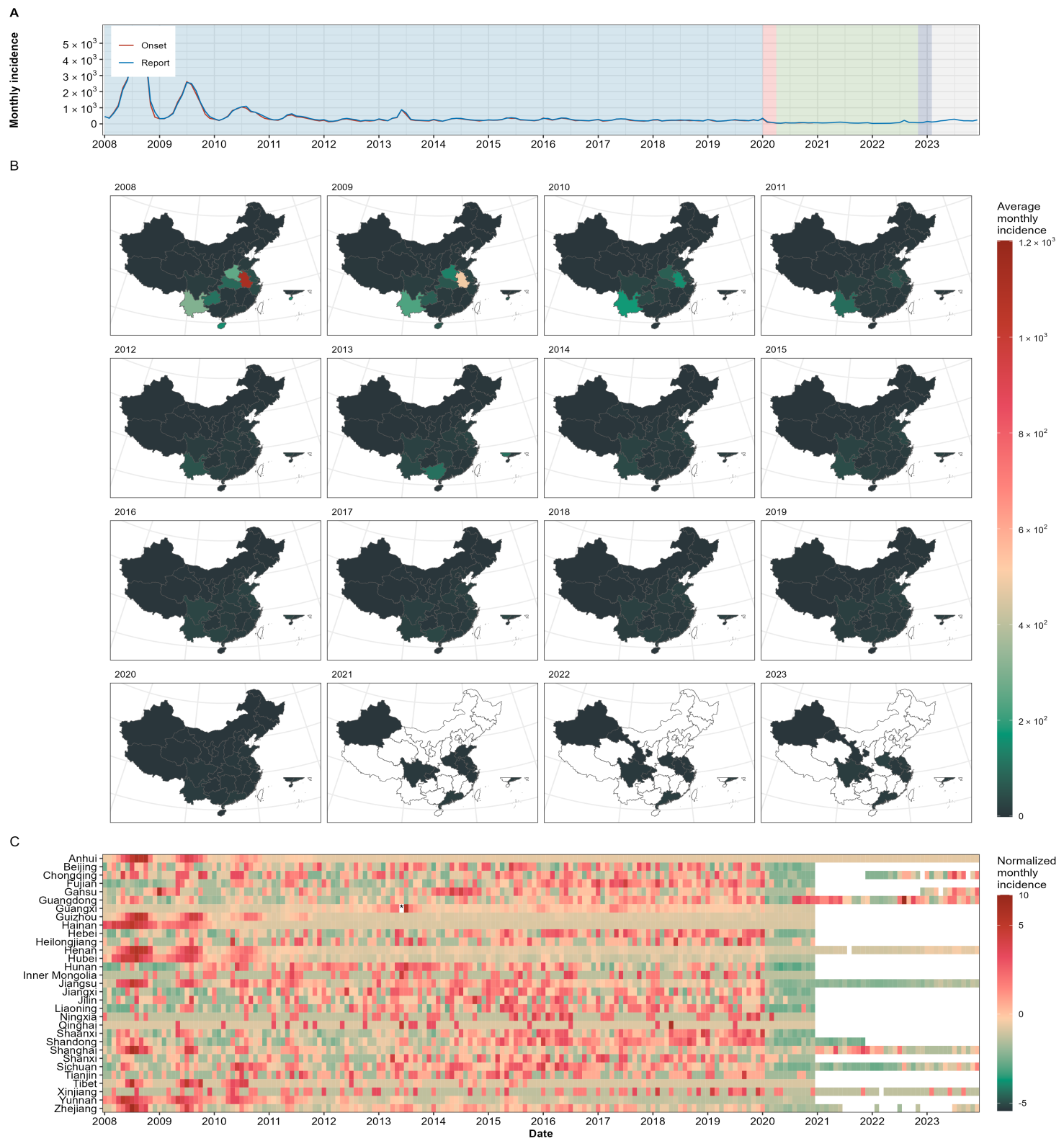
Supplementary Fig. 19. Temporal variation in the monthly incidence of hemorrhagic fever with renal syndrome (HFRS) in China from January 2008 to December 2023.

(A) The incidence of hemorrhagic fever with renal syndrome (HFRS) in China from January 2008 to December 2023; (B) The spatial distribution of cases in China; (C) Temporal variation in the monthly incidence between different provinces. The heatmap represents normalized monthly incidence data for each province, with color intensity corresponding to the normalized monthly incidence. Provincial data in panel (B) and (C) before January 2020 sourced from the Chinese Public Health Science Data Center, and data after January 2020 sourced from the provincial Notifiable Infectious Diseases Reports. * Normalized monthly incidence > 10.



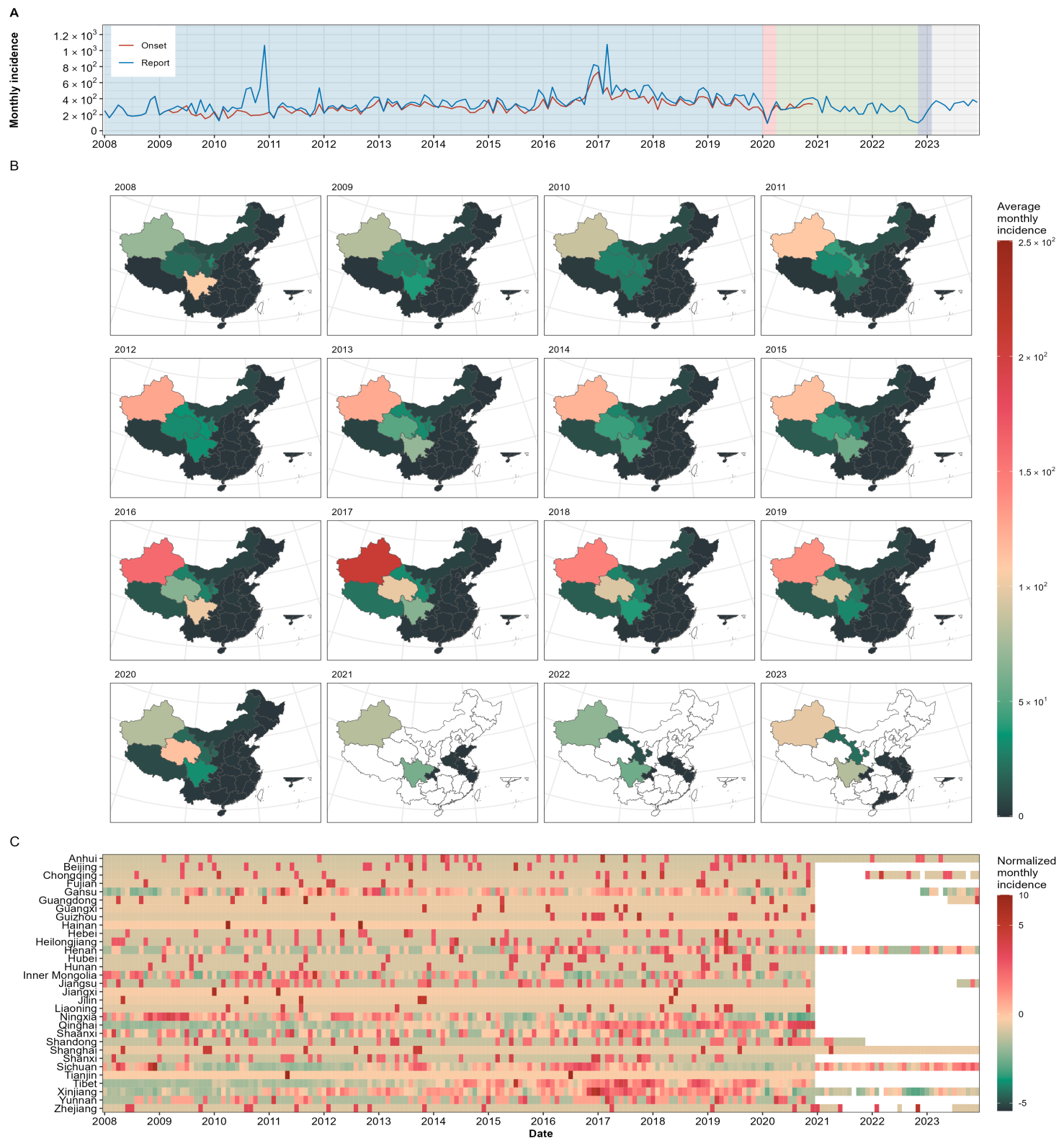
Supplementary Fig. 20. Temporal variation in the monthly incidence of dengue fever in China from January 2008 to December 2023.

(A) The incidence of dengue fever in China from January 2008 to December 2023; **(B)** The spatial distribution of cases in China; **(C)** Temporal variation in the monthly incidence between different provinces. The heatmap represents normalized monthly incidence data for each province, with color intensity corresponding to the normalized monthly incidence. Provincial data in panel **(B)** and **(C)** before January 2020 sourced from the Chinese Public Health Science Data Center, and data after January 2020 sourced from the provincial Notifiable Infectious Diseases Reports. * Normalized monthly incidence > 10.



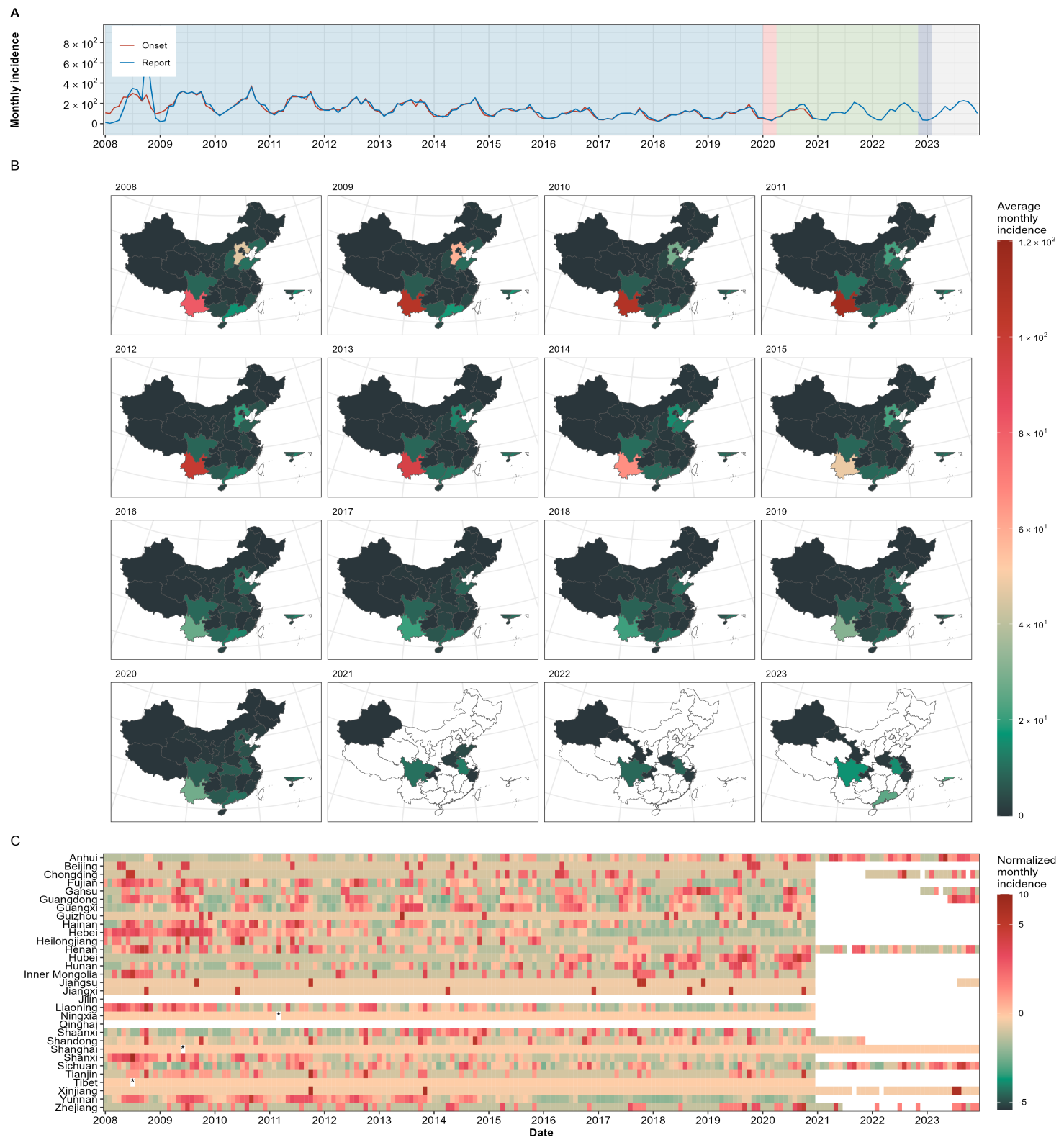
Supplementary Fig. 21. Temporal variation in the monthly incidence of malaria in China from January 2008 to December 2023.

(A) The incidence of malaria in China from January 2008 to December 2023; (B) The spatial distribution of cases in China; (C) Temporal variation in the monthly incidence between different provinces. The heatmap represents normalized monthly incidence data for each province, with color intensity corresponding to the normalized monthly incidence. Provincial data in panel (B) and (C) before January 2020 sourced from the Chinese Public Health Science Data Center, and data after January 2020 sourced from the provincial Notifiable Infectious Diseases Reports. * Normalized monthly incidence > 10.



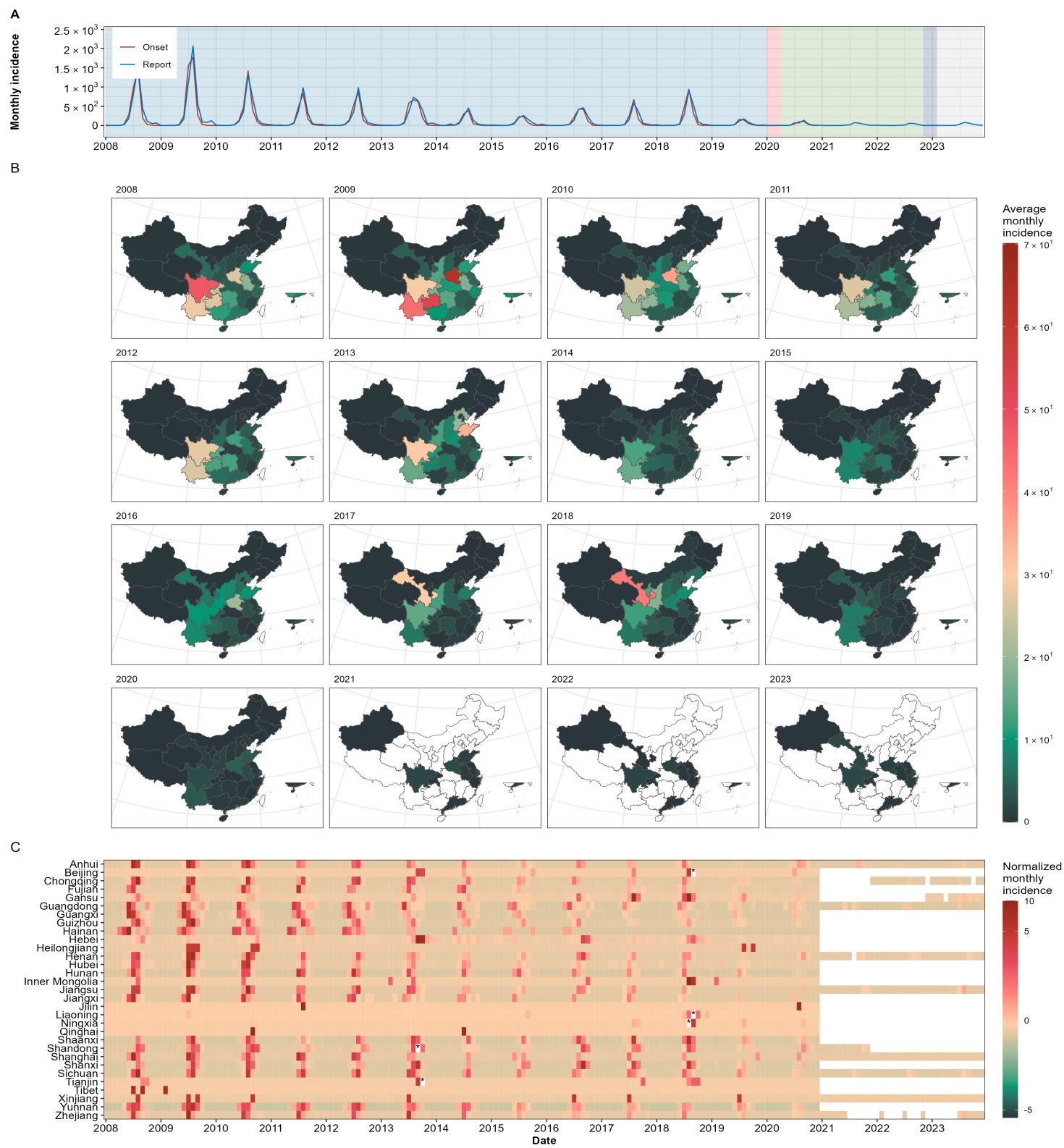
Supplementary Fig. 22. Temporal variation in the monthly incidence of echinococcosis in China from January 2008 to December 2023.

(A) The incidence of echinococcosis in China from January 2008 to December 2023; (B) The spatial distribution of cases in China; (C) Temporal variation in the monthly incidence between different provinces. The heatmap represents normalized monthly incidence data for each province, with color intensity corresponding to the normalized monthly incidence. Provincial data in panel (B) and (C) before January 2020 sourced from the Chinese Public Health Science Data Center, and data after January 2020 sourced from the provincial Notifiable Infectious Diseases Reports. * Normalized monthly incidence > 10.



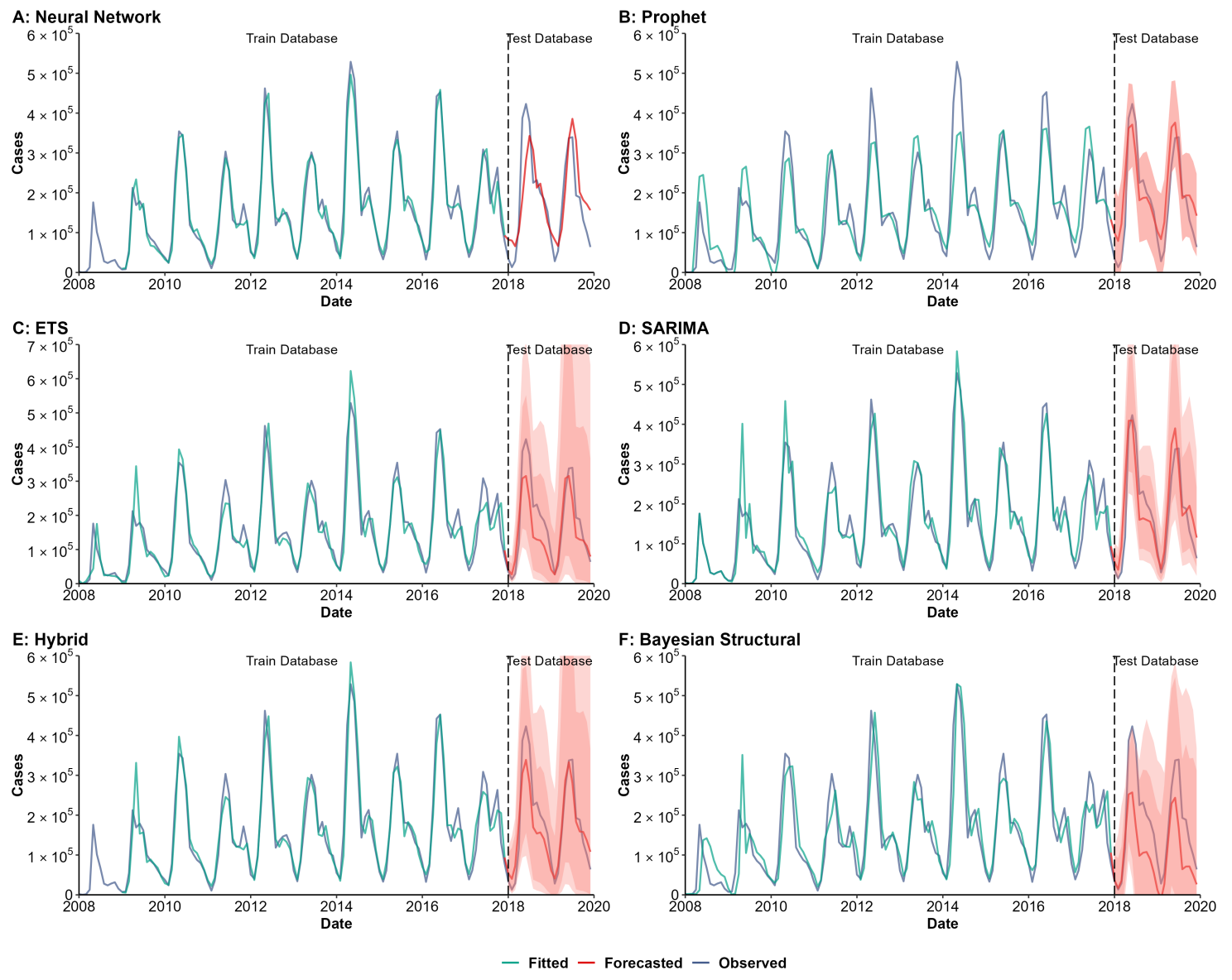
Supplementary Fig. 23. Temporal variation in the monthly incidence of typhus in China from January 2008 to December 2023.

(A) The incidence of typhus in China from January 2008 to December 2023; (B) The spatial distribution of cases in China; (C) Temporal variation in the monthly incidence between different provinces. The heatmap represents normalized monthly incidence data for each province, with color intensity corresponding to the normalized monthly incidence. Provincial data in panel (B) and (C) before January 2020 sourced from the Chinese Public Health Science Data Center, and data after January 2020 sourced from the provincial Notifiable Infectious Diseases Reports. * Normalized monthly incidence > 10.



Supplementary Fig. 24. Temporal variation in the monthly incidence of Japanese encephalitis (JE) in China from January 2008 to December 2023.

(A) The incidence of Japanese encephalitis (JE) in China from January 2008 to December 2023; (B) The spatial distribution of cases in China; (C) Temporal variation in the monthly incidence between different provinces. The heatmap represents normalized monthly incidence data for each province, with color intensity corresponding to the normalized monthly incidence. Provincial data in panel (B) and (C) before January 2020 sourced from the Chinese Public Health Science Data Center, and data after January 2020 sourced from the provincial Notifiable Infectious Diseases Reports. * Normalized monthly incidence > 10.



G : SMAPE of Models

| Method | Train | Test | All |
|---------------------|-------|-------|-------|
| Neural Network | 13.19 | 39.54 | 17.98 |
| ETS | 22.63 | 35.13 | 24.71 |
| SARIMA | 18.83 | 33.32 | 21.24 |
| Hybrid* | 15.83 | 31.71 | 18.71 |
| Bayesian Structural | 34.59 | 64.98 | 39.65 |
| Prophet | 37.35 | 42.58 | 38.22 |

*Hybrid: Combined SARIMA, ETS, STL and Neural Network model

H : RMSE of Models

| Method | Train | Test | All |
|---------------------|----------|----------|----------|
| Neural Network | 23323.90 | 72265.71 | 37344.47 |
| ETS | 40788.11 | 63677.84 | 45411.48 |
| SARIMA | 41585.44 | 53910.58 | 43880.70 |
| Hybrid* | 33188.04 | 48221.11 | 36386.27 |
| Bayesian Structural | 55537.49 | 98552.75 | 64723.40 |
| Prophet | 54513.95 | 62646.47 | 55951.52 |

*Hybrid: Combined SARIMA, ETS, STL and Neural Network model

I : MASE of Models

| Method | Train | Test | All |
|---------------------|-------|------|------|
| Neural Network | 0.30 | 1.10 | 0.43 |
| ETS | 0.47 | 1.07 | 0.56 |
| SARIMA | 0.44 | 0.71 | 0.49 |
| Hybrid* | 0.37 | 0.83 | 0.46 |
| Bayesian Structural | 0.67 | 1.80 | 0.85 |
| Prophet | 0.65 | 1.07 | 0.83 |

*Hybrid: Combined SARIMA, ETS, STL and Neural Network model

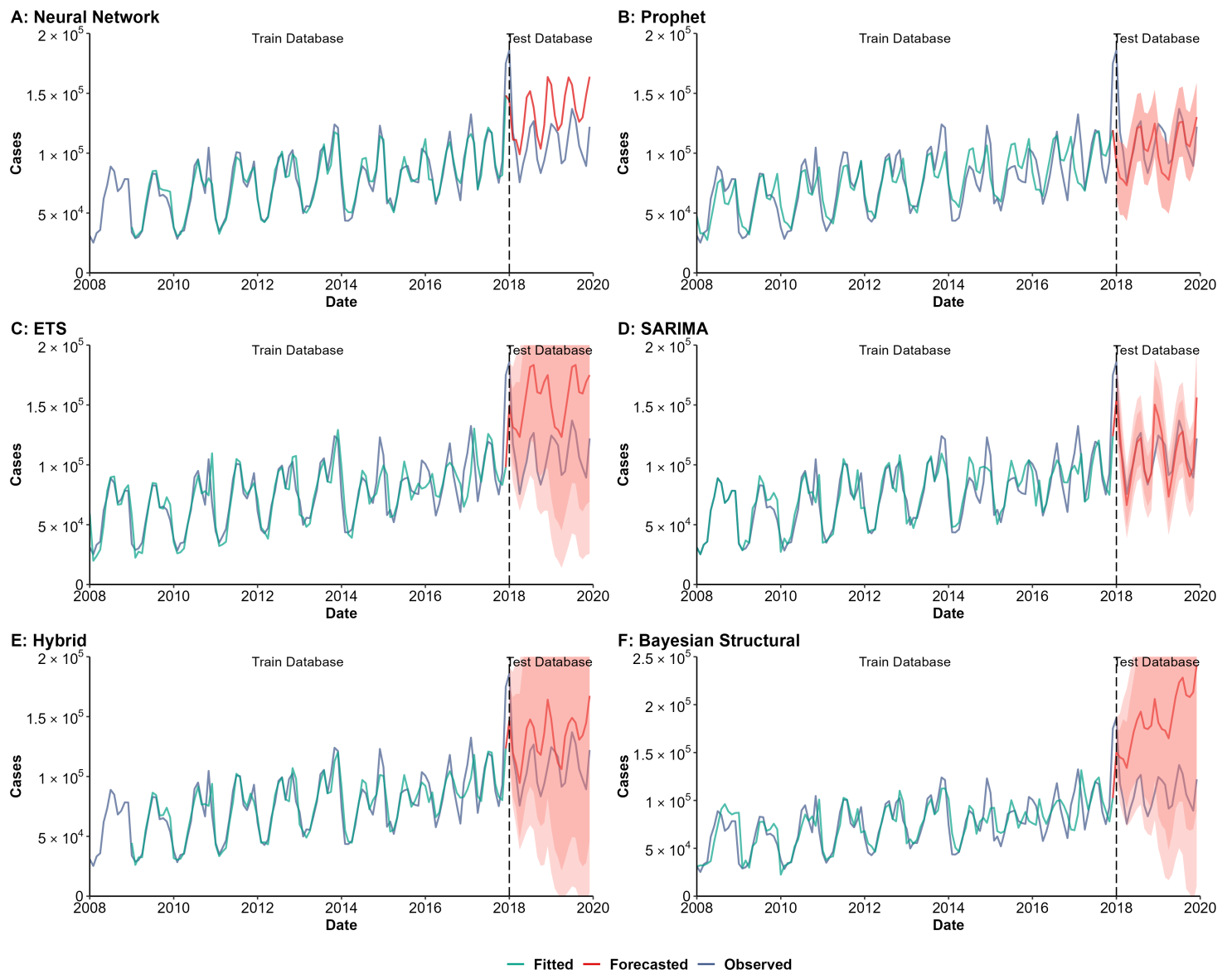
J : R_Squared of Models

| Method | Train | Test | All |
|---------------------|-------|------|------|
| Neural Network | 0.96 | 0.65 | 0.90 |
| ETS | 0.88 | 0.81 | 0.86 |
| SARIMA | 0.88 | 0.81 | 0.87 |
| Hybrid* | 0.92 | 0.89 | 0.90 |
| Bayesian Structural | 0.78 | 0.81 | 0.71 |
| Prophet | 0.78 | 0.79 | 0.77 |

*Hybrid: Combined SARIMA, ETS, STL and Neural Network model

Supplementary Fig. 25. Training and comparing variant time series models for hand, foot, and mouth disease (HFMD).

(A) Neural Network model; (B) Prophet model; (C) Exponential smoothing (ETS) model; (D) Seasonal autoregressive integrated moving average (SARIMA) model; (E) Hybrid models combining SARIMA, ETS, STL (seasonal and trend decomposition using loess), and neural network model; (F) Bayesian structural model; (G) Root mean square error (RMSE) of variant models; (H) Symmetric mean absolute percentage error (SMAPE) of variant models; (I) Mean absolute scaled error (MASE) of variant models; (J) R-squared of variant models.



G : SMAPE of Models

| Method | Train | Test | All |
|---------------------|-------|-------|-------|
| Neural Network | 6.56 | 23.06 | 9.56 |
| ETS | 13.26 | 36.59 | 17.15 |
| SARIMA | 10.37 | 9.05 | 10.15 |
| Hybrid* | 9.41 | 21.78 | 11.66 |
| Bayesian Structural | 15.32 | 52.15 | 21.46 |
| Prophet | 15.23 | 15.68 | 15.31 |

H : RMSE of Models

| Method | Train | Test | All |
|---------------------|----------|----------|----------|
| Neural Network | 6990.88 | 32511.72 | 15237.14 |
| ETS | 14680.65 | 52087.60 | 25135.38 |
| SARIMA | 12083.49 | 15076.35 | 12631.64 |
| Hybrid* | 10773.19 | 30462.76 | 16238.32 |
| Bayesian Structural | 16986.54 | 80925.42 | 36495.74 |
| Prophet | 15073.91 | 26207.03 | 17430.44 |

I : MASE of Models

| Method | Train | Test | All |
|---------------------|-------|------|------|
| Neural Network | 0.39 | 1.76 | 0.69 |
| ETS | 0.66 | 4.02 | 1.17 |
| SARIMA | 0.59 | 0.50 | 0.56 |
| Hybrid* | 0.49 | 1.80 | 0.83 |
| Bayesian Structural | 0.80 | 6.24 | 1.79 |
| Prophet | 0.76 | 1.54 | 1.06 |

J : R_Squared of Models

| Method | Train | Test | All |
|---------------------|-------|------|------|
| Neural Network | 0.93 | 0.22 | 0.79 |
| ETS | 0.69 | 0.06 | 0.61 |
| SARIMA | 0.79 | 0.63 | 0.81 |
| Hybrid* | 0.83 | 0.26 | 0.74 |
| Bayesian Structural | 0.59 | 0.02 | 0.47 |
| Prophet | 0.67 | 0.05 | 0.63 |

*Hybrid: Combined SARIMA, ETS, STL and Neural Network model

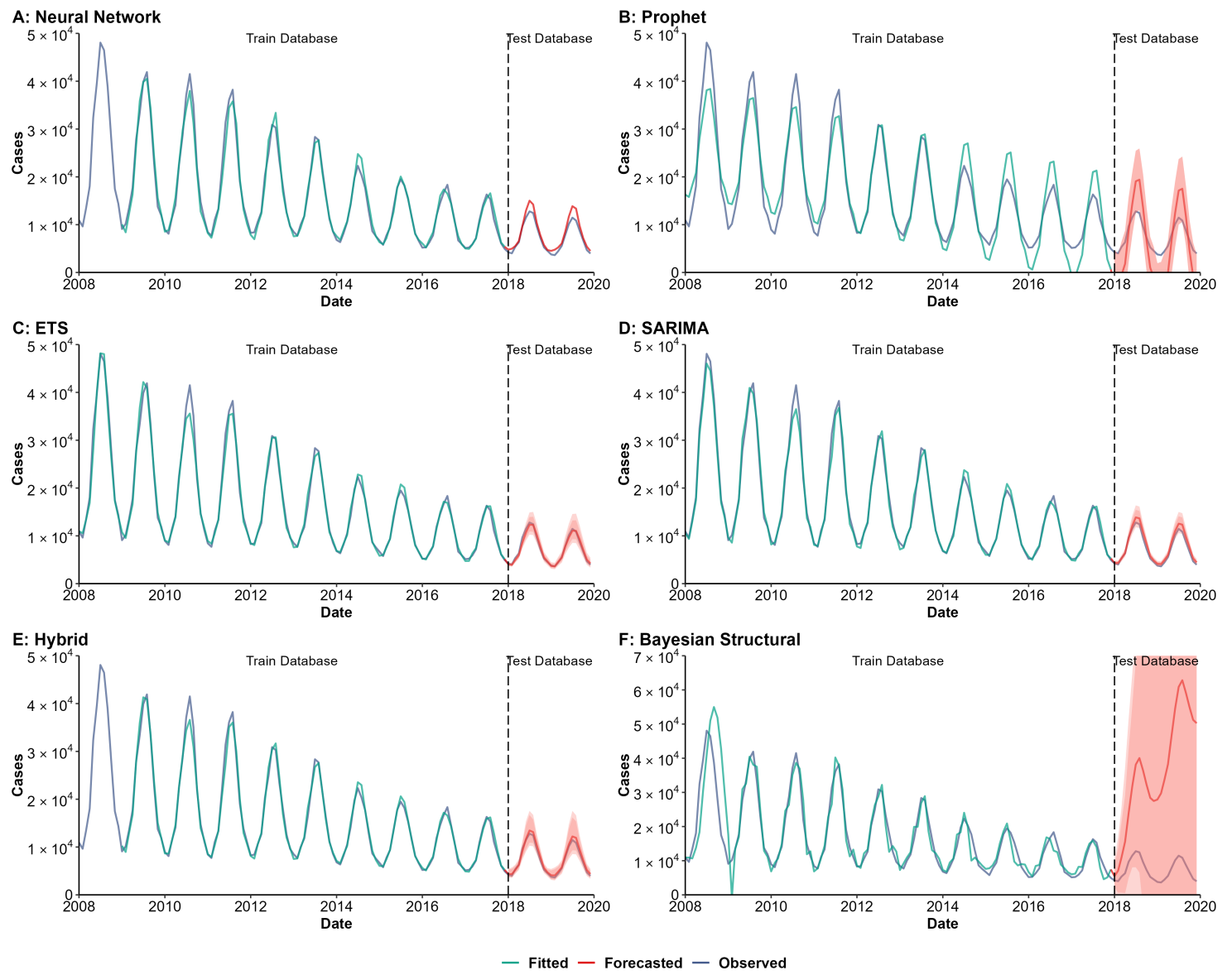
*Hybrid: Combined SARIMA, ETS, STL and Neural Network model

*Hybrid: Combined SARIMA, ETS, STL and Neural Network model

*Hybrid: Combined SARIMA, ETS, STL and Neural Network model

Supplementary Fig. 26. Training and comparing variant time series models for infectious diarrhea.

(A) Neural Network model; (B) Prophet model; (C) Exponential smoothing (ETS) model; (D) Seasonal autoregressive integrated moving average (SARIMA) model; (E) Hybrid models combining SARIMA, ETS, STL (seasonal and trend decomposition using loess), and neural network model; (F) Bayesian structural model; (G) Root mean square error (RMSE) of variant models; (H) Symmetric mean absolute percentage error (SMAPE) of variant models; (I) Mean absolute scaled error (MASE) of variant models; (J) R-squared of variant models.



G : SMAPE of Models

| Method | Train | Test | All |
|---------------------|-------|--------|-------|
| Neural Network | 5.97 | 12.00 | 7.07 |
| ETS | 4.49 | 4.43 | 4.48 |
| SARIMA | 4.92 | 8.70 | 5.55 |
| Hybrid* | 4.52 | 6.38 | 4.86 |
| Bayesian Structural | 17.83 | 123.02 | 35.36 |
| Prophet | 25.50 | 108.09 | 39.26 |

*Hybrid: Combined SARIMA, ETS, STL and Neural Network model

H : RMSE of Models

| Method | Train | Test | All |
|---------------------|---------|----------|----------|
| Neural Network | 1339.95 | 1163.71 | 1309.68 |
| ETS | 1258.85 | 417.50 | 1161.74 |
| SARIMA | 1202.91 | 776.69 | 1142.97 |
| Hybrid* | 1132.16 | 520.12 | 1047.81 |
| Bayesian Structural | 4875.02 | 32607.31 | 14036.06 |
| Prophet | 3405.75 | 5433.71 | 3819.27 |

*Hybrid: Combined SARIMA, ETS, STL and Neural Network model

I : MASE of Models

| Method | Train | Test | All |
|---------------------|-------|------|------|
| Neural Network | 0.26 | 0.55 | 0.29 |
| ETS | 0.20 | 0.24 | 0.21 |
| SARIMA | 0.22 | 0.43 | 0.23 |
| Hybrid* | 0.20 | 0.31 | 0.22 |
| Bayesian Structural | 0.71 | 6.98 | 1.66 |
| Prophet | 0.68 | 1.26 | 0.79 |

*Hybrid: Combined SARIMA, ETS, STL and Neural Network model

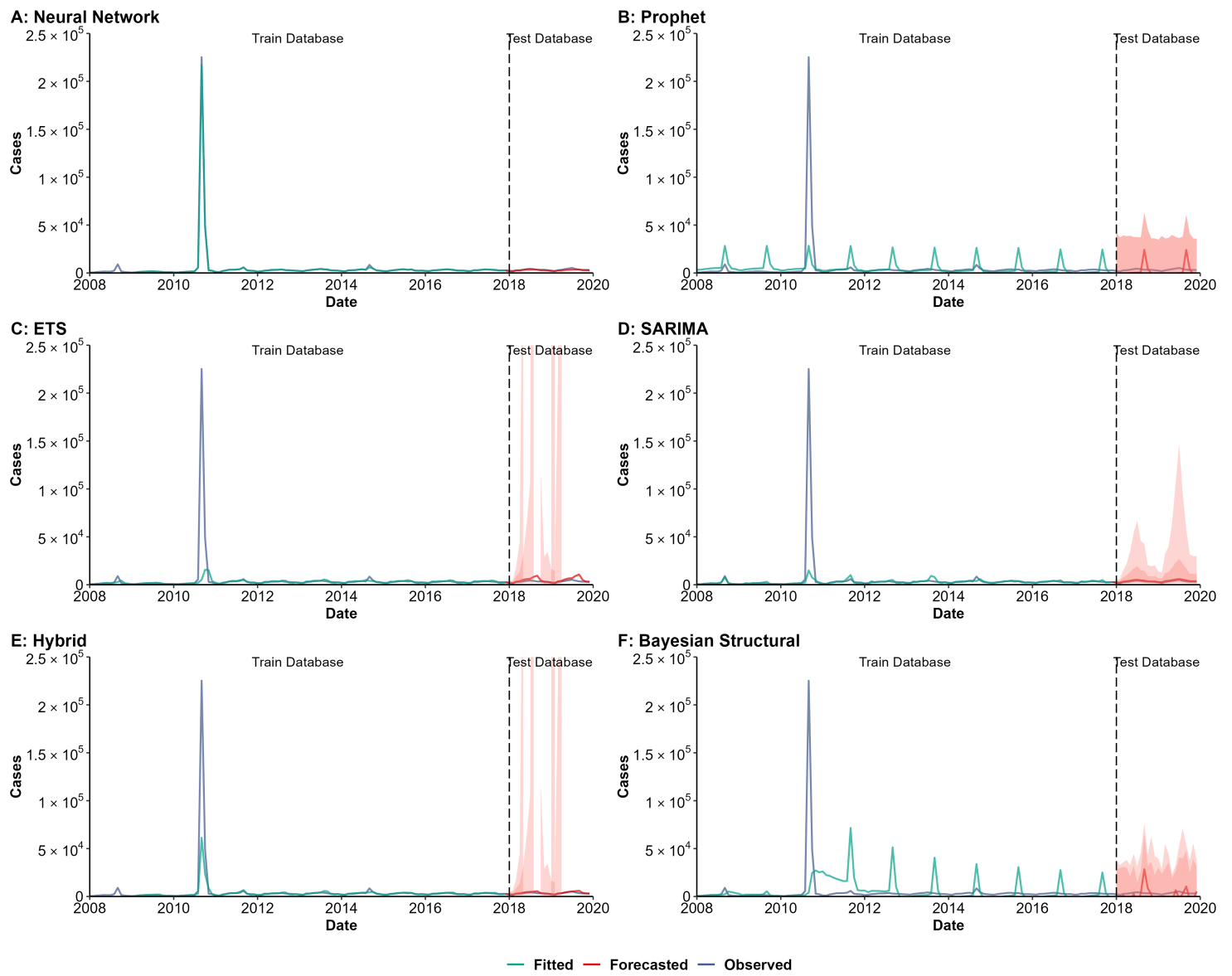
J : R_Squared of Models

| Method | Train | Test | All |
|---------------------|-------|------|------|
| Neural Network | 0.98 | 0.98 | 0.98 |
| ETS | 0.99 | 0.98 | 0.99 |
| SARIMA | 0.99 | 0.99 | 0.99 |
| Hybrid* | 0.99 | 0.99 | 0.99 |
| Bayesian Structural | 0.81 | 0.20 | 0.21 |
| Prophet | 0.89 | 0.97 | 0.87 |

*Hybrid: Combined SARIMA, ETS, STL and Neural Network model

Supplementary Fig. 27. Training and comparing variant time series models for dysentery.

(A) Neural Network model; (B) Prophet model; (C) Exponential smoothing (ETS) model; (D) Seasonal autoregressive integrated moving average (SARIMA) model; (E) Hybrid models combining SARIMA, ETS, STL (seasonal and trend decomposition using loess), and neural network model; (F) Bayesian structural model; (G) Root mean square error (RMSE) of variant models; (H) Symmetric mean absolute percentage error (SMAPE) of variant models; (I) Mean absolute scaled error (MASE) of variant models; (J) R-squared of variant models.



G : SMAPE of Models

H : RMSE of Models

I : MASE of Models

J : R_Squared of Models

| Method | Train | Test | All | Method | Train | Test | All |
|---------------------|--------|--------|--------|---------------------|----------|---------|----------|
| Neural Network | 2.33 | 15.99 | 4.83 | Neural Network | 845.24 | 682.80 | 817.89 |
| ETS | 23.46 | 32.23 | 24.92 | ETS | 20369.45 | 2571.36 | 18624.28 |
| SARIMA | 20.55 | 18.79 | 20.26 | SARIMA | 19596.50 | 750.74 | 17891.70 |
| Hybrid* | 14.04 | 14.44 | 14.11 | Hybrid* | 16051.37 | 837.24 | 14511.11 |
| Bayesian Structural | 119.92 | 145.03 | 124.11 | Bayesian Structural | 23230.53 | 7742.52 | 21440.75 |
| Prophet | 87.88 | 175.25 | 102.44 | Prophet | 19461.24 | 7003.92 | 17994.23 |

*Hybrid: Combined SARIMA, ETS, STL and Neural Network model

*Hybrid: Combined SARIMA, ETS, STL and Neural Network model

| Method | Train | Test | All |
|---------------------|-------|------|------|
| Neural Network | 0.04 | 2.03 | 0.06 |
| ETS | 0.64 | 1.23 | 2.94 |
| SARIMA | 2.39 | 1.38 | 2.31 |
| Hybrid* | 0.46 | 0.92 | 1.30 |
| Bayesian Structural | 1.82 | 0.81 | 1.37 |
| Prophet | 1.26 | 1.13 | 1.25 |

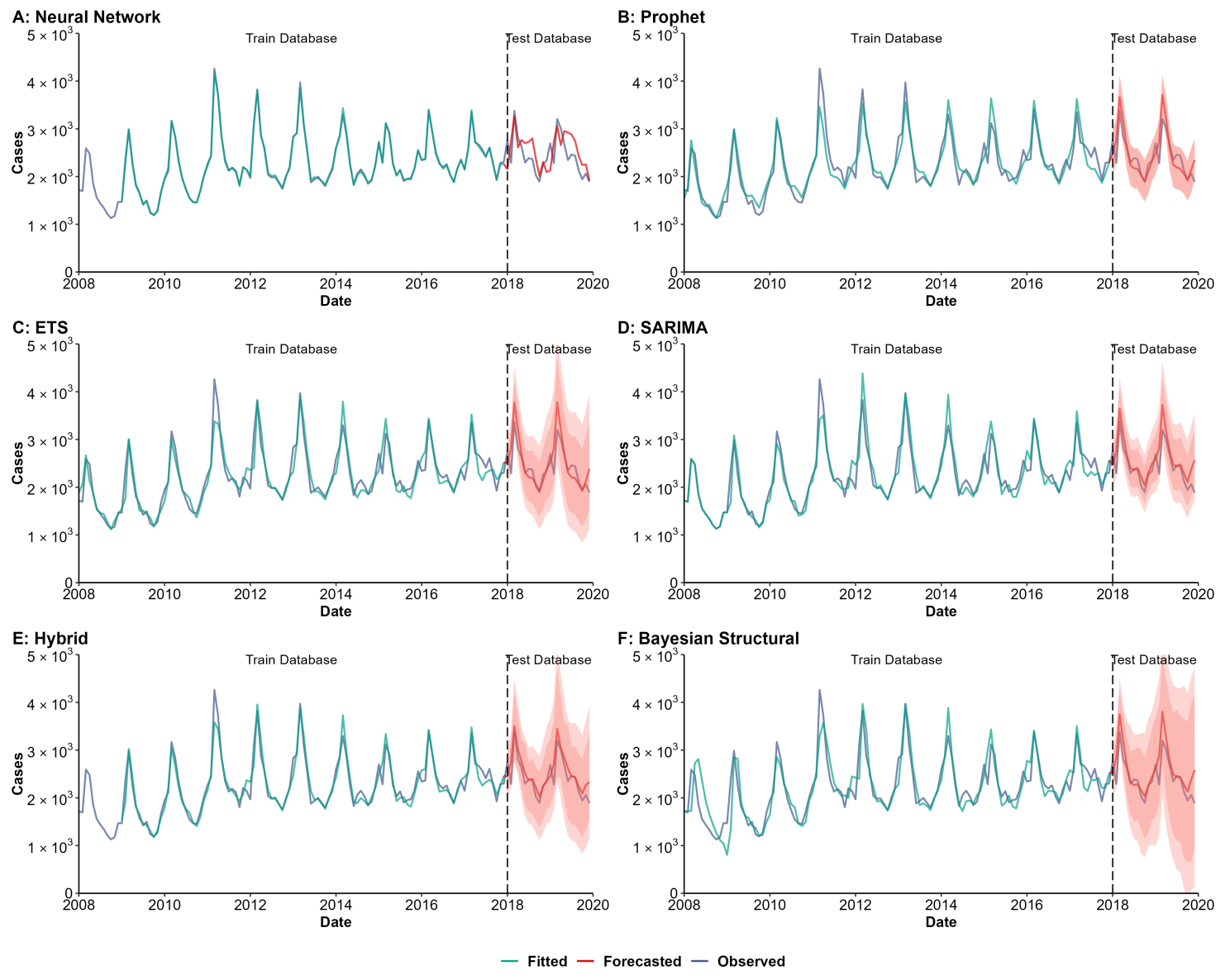
*Hybrid: Combined SARIMA, ETS, STL and Neural Network model

| Method | Train | Test | All |
|---------------------|-------|------|------|
| Neural Network | 1.00 | 0.70 | 1.00 |
| ETS | 0.06 | 0.48 | 0.04 |
| SARIMA | 0.37 | 0.91 | 0.34 |
| Hybrid* | 0.95 | 0.67 | 0.94 |
| Bayesian Structural | 0.00 | 0.02 | 0.00 |
| Prophet | 0.11 | 0.01 | 0.10 |

*Hybrid: Combined SARIMA, ETS, STL and Neural Network model

Supplementary Fig. 28. Training and comparing variant time series models for acute hemorrhagic conjunctivitis (AHC).

(A) Neural Network model; (B) Prophet model; (C) Exponential smoothing (ETS) model; (D) Seasonal autoregressive integrated moving average (SARIMA) model; (E) Hybrid models combining SARIMA, ETS, STL (seasonal and trend decomposition using loess), and neural network model; (F) Bayesian structural model; (G) Root mean square error (RMSE) of variant models; (H) Symmetric mean absolute percentage error (SMAPE) of variant models; (I) Mean absolute scaled error (MASE) of variant models; (J) R-squared of variant models.



G : SMAPE of Models

| Method | Train | Test | All |
|---------------------|-------|-------|------|
| Neural Network | 0.99 | 12.28 | 3.04 |
| ETS | 6.96 | 7.91 | 7.12 |
| SARIMA | 6.43 | 8.26 | 6.73 |
| Hybrid* | 5.13 | 7.15 | 5.49 |
| Bayesian Structural | 10.03 | 8.68 | 9.81 |
| Prophet | 7.37 | 7.85 | 7.45 |

*Hybrid: Combined SARIMA, ETS, STL and Neural Network model

H : RMSE of Models

| Method | Train | Test | All |
|---------------------|--------|--------|--------|
| Neural Network | 31.67 | 346.22 | 150.38 |
| ETS | 222.24 | 275.29 | 231.92 |
| SARIMA | 230.76 | 273.79 | 238.47 |
| Hybrid* | 168.61 | 222.28 | 179.57 |
| Bayesian Structural | 308.89 | 301.30 | 307.64 |
| Prophet | 222.36 | 254.26 | 227.99 |

*Hybrid: Combined SARIMA, ETS, STL and Neural Network model

I : MASE of Models

| Method | Train | Test | All |
|---------------------|-------|------|------|
| Neural Network | 0.07 | 1.15 | 0.23 |
| ETS | 0.48 | 0.65 | 0.55 |
| SARIMA | 0.47 | 0.71 | 0.51 |
| Hybrid* | 0.36 | 0.72 | 0.44 |
| Bayesian Structural | 0.66 | 0.75 | 0.70 |
| Prophet | 0.51 | 0.66 | 0.58 |

*Hybrid: Combined SARIMA, ETS, STL and Neural Network model

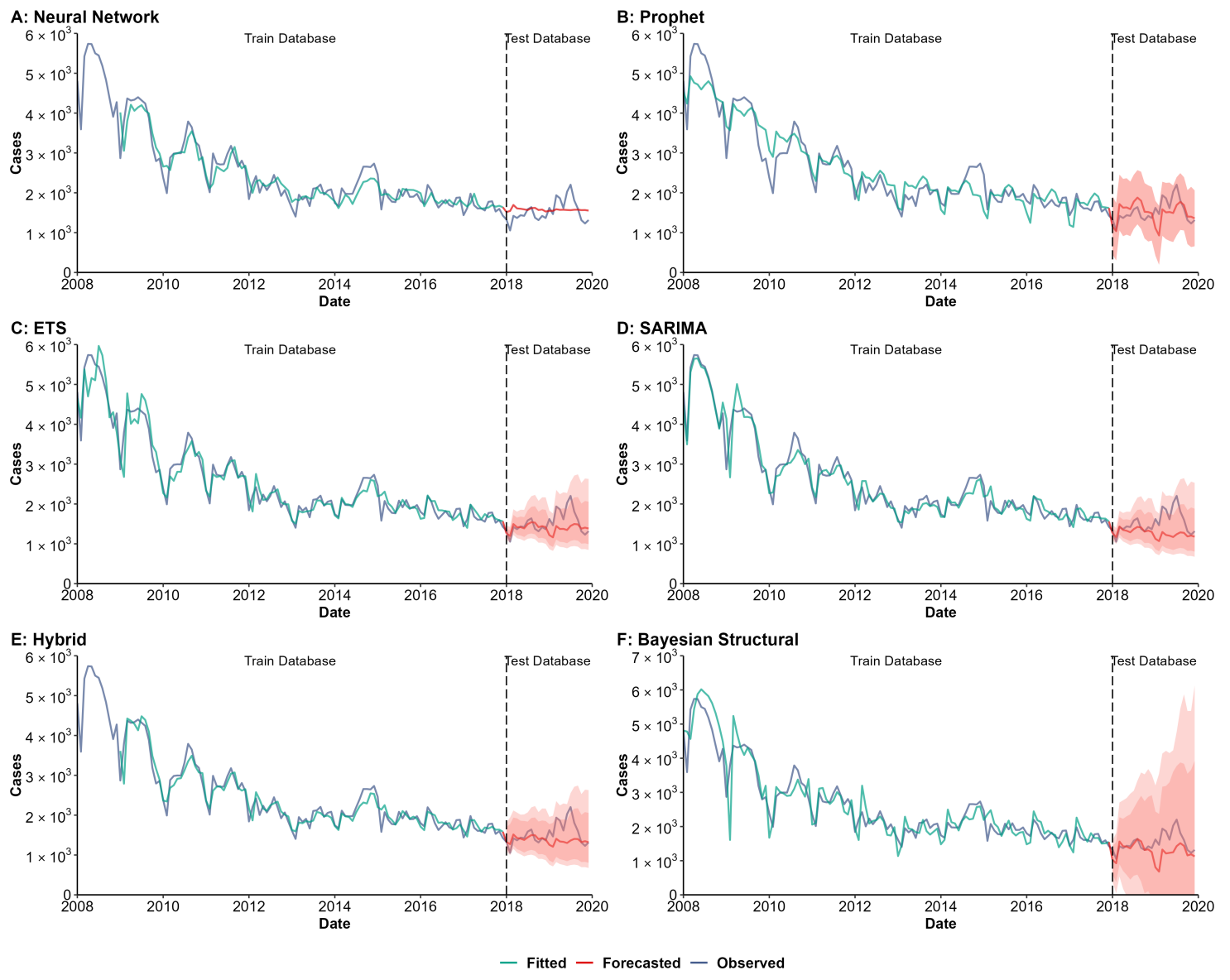
J : R_Squared of Models

| Method | Train | Test | All |
|---------------------|-------|------|------|
| Neural Network | 1.00 | 0.38 | 0.93 |
| ETS | 0.86 | 0.75 | 0.84 |
| SARIMA | 0.86 | 0.74 | 0.85 |
| Hybrid* | 0.91 | 0.78 | 0.89 |
| Bayesian Structural | 0.76 | 0.72 | 0.75 |
| Prophet | 0.86 | 0.75 | 0.84 |

*Hybrid: Combined SARIMA, ETS, STL and Neural Network model

Supplementary Fig. 29. Training and comparing variant time series models for hepatitis E.

(A) Neural Network model; (B) Prophet model; (C) Exponential smoothing (ETS) model; (D) Seasonal autoregressive integrated moving average (SARIMA) model; (E) Hybrid models combining SARIMA, ETS, STL (seasonal and trend decomposition using loess), and neural network model; (F) Bayesian structural model; (G) Root mean square error (RMSE) of variant models; (H) Symmetric mean absolute percentage error (SMAPE) of variant models; (I) Mean absolute scaled error (MASE) of variant models; (J) R-squared of variant models.



G : SMAPE of Models

| Method | Train | Test | All |
|---------------------|-------|-------|-------|
| Neural Network | 8.38 | 14.48 | 9.49 |
| ETS | 6.94 | 13.53 | 8.04 |
| SARIMA | 6.80 | 18.57 | 8.76 |
| Hybrid* | 6.46 | 14.06 | 7.85 |
| Bayesian Structural | 10.83 | 20.47 | 12.44 |
| Prophet | 10.68 | 15.57 | 11.50 |

*Hybrid: Combined SARIMA, ETS, STL and Neural Network model

H : RMSE of Models

| Method | Train | Test | All |
|---------------------|--------|--------|--------|
| Neural Network | 263.42 | 271.41 | 264.89 |
| ETS | 264.65 | 293.40 | 269.65 |
| SARIMA | 252.16 | 388.66 | 279.58 |
| Hybrid* | 209.55 | 316.97 | 232.80 |
| Bayesian Structural | 408.83 | 398.95 | 407.20 |
| Prophet | 360.64 | 288.37 | 349.64 |

*Hybrid: Combined SARIMA, ETS, STL and Neural Network model

I : MASE of Models

| Method | Train | Test | All |
|---------------------|-------|------|------|
| Neural Network | 1.29 | 8.67 | 1.56 |
| ETS | 0.71 | 2.74 | 0.86 |
| SARIMA | 0.73 | 3.81 | 0.91 |
| Hybrid* | 0.65 | 3.48 | 1.03 |
| Bayesian Structural | 1.05 | 1.78 | 0.88 |
| Prophet | 1.02 | 1.50 | 1.47 |

*Hybrid: Combined SARIMA, ETS, STL and Neural Network model

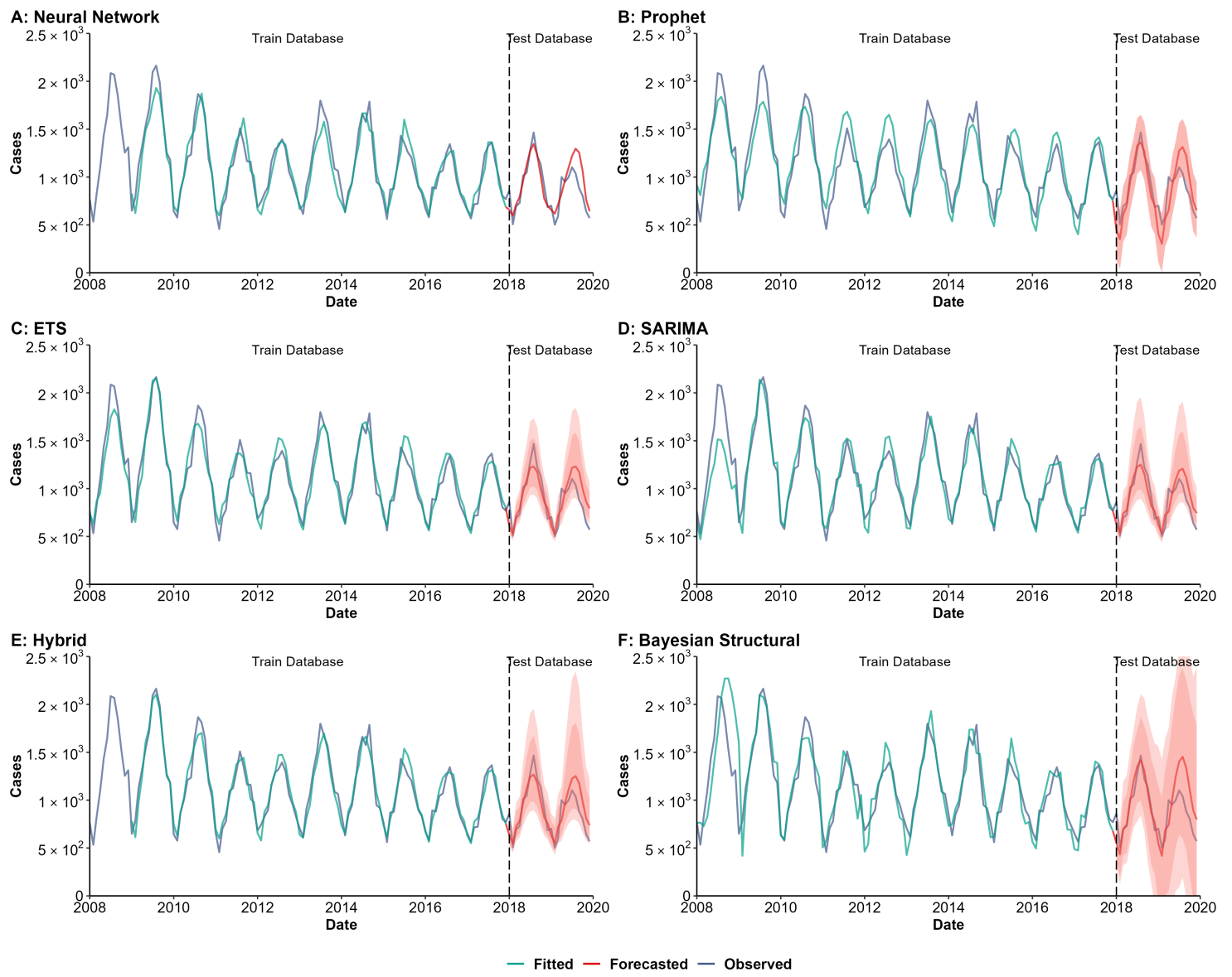
J : R_Squared of Models

| Method | Train | Test | All |
|---------------------|-------|------|------|
| Neural Network | 0.87 | 0.00 | 0.87 |
| ETS | 0.94 | 0.06 | 0.94 |
| SARIMA | 0.94 | 0.00 | 0.94 |
| Hybrid* | 0.92 | 0.00 | 0.91 |
| Bayesian Structural | 0.88 | 0.06 | 0.89 |
| Prophet | 0.88 | 0.13 | 0.89 |

*Hybrid: Combined SARIMA, ETS, STL and Neural Network model

Supplementary Fig. 30. Training and comparing variant time series models for hepatitis A.

(A) Neural Network model; (B) Prophet model; (C) Exponential smoothing (ETS) model; (D) Seasonal autoregressive integrated moving average (SARIMA) model; (E) Hybrid models combining SARIMA, ETS, STL (seasonal and trend decomposition using loess), and neural network model; (F) Bayesian structural model; (G) Root mean square error (RMSE) of variant models; (H) Symmetric mean absolute percentage error (SMAPE) of variant models; (I) Mean absolute scaled error (MASE) of variant models; (J) R-squared of variant models.



G : SMAPE of Models

| Method | Train | Test | All |
|---------------------|-------|-------|-------|
| Neural Network | 8.48 | 12.72 | 9.25 |
| ETS | 8.21 | 13.65 | 9.12 |
| SARIMA | 9.43 | 12.75 | 9.98 |
| Hybrid* | 6.86 | 13.23 | 8.02 |
| Bayesian Structural | 12.74 | 17.62 | 13.56 |
| Prophet | 12.04 | 18.88 | 13.18 |

*Hybrid: Combined SARIMA, ETS, STL and Neural Network model

H : RMSE of Models

| Method | Train | Test | All |
|---------------------|--------|--------|--------|
| Neural Network | 118.27 | 142.29 | 122.99 |
| ETS | 114.56 | 146.43 | 120.45 |
| SARIMA | 148.46 | 131.32 | 145.75 |
| Hybrid* | 91.41 | 138.18 | 101.53 |
| Bayesian Structural | 205.33 | 203.74 | 205.07 |
| Prophet | 157.24 | 180.16 | 161.29 |

*Hybrid: Combined SARIMA, ETS, STL and Neural Network model

I : MASE of Models

| Method | Train | Test | All |
|---------------------|-------|------|------|
| Neural Network | 0.57 | 0.90 | 0.62 |
| ETS | 0.48 | 1.05 | 0.59 |
| SARIMA | 0.61 | 0.96 | 0.65 |
| Hybrid* | 0.42 | 0.97 | 0.52 |
| Bayesian Structural | 0.74 | 0.96 | 0.72 |
| Prophet | 0.71 | 0.85 | 0.77 |

*Hybrid: Combined SARIMA, ETS, STL and Neural Network model

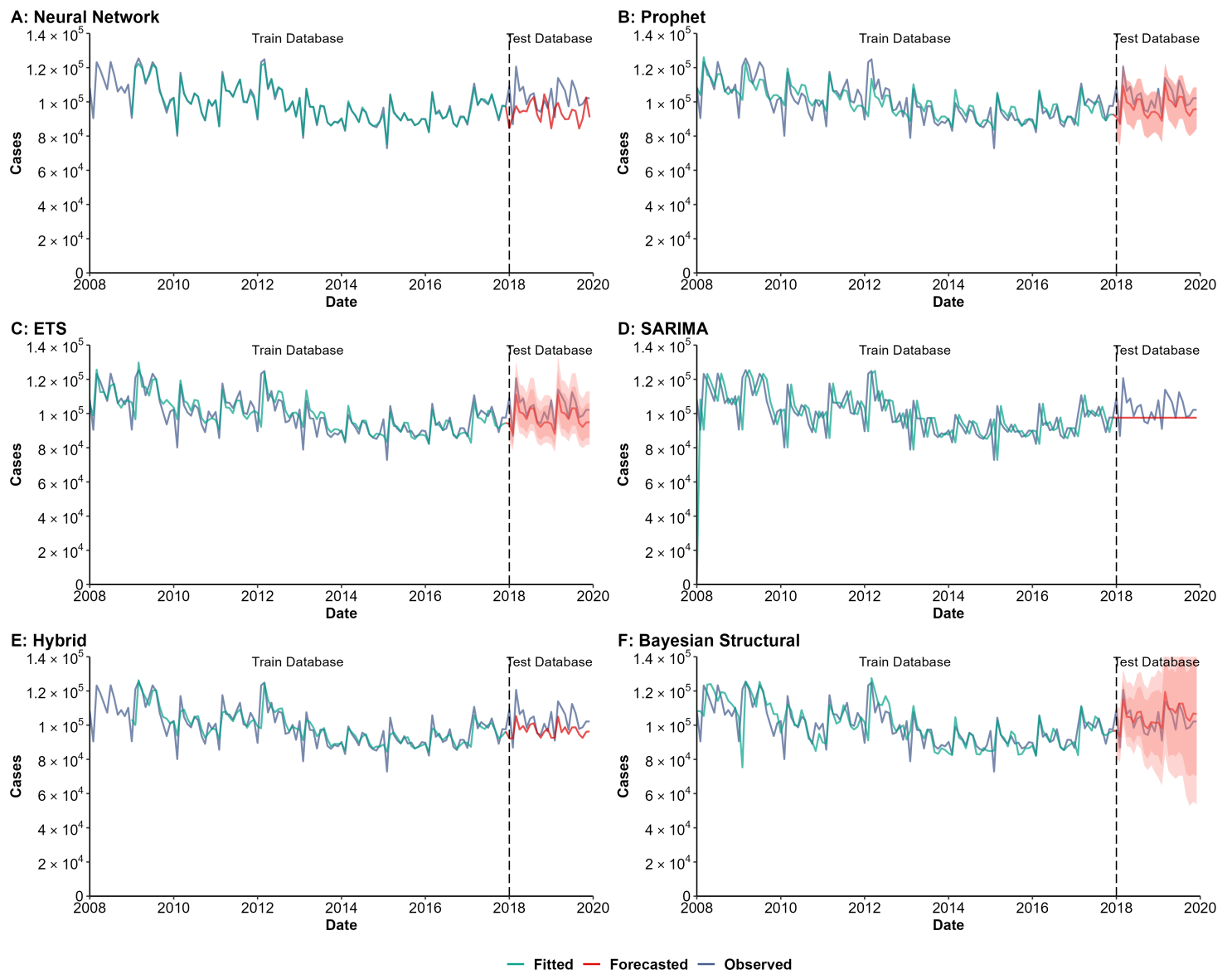
J : R_Squared of Models

| Method | Train | Test | All |
|---------------------|-------|------|------|
| Neural Network | 0.90 | 0.72 | 0.88 |
| ETS | 0.91 | 0.67 | 0.90 |
| SARIMA | 0.86 | 0.73 | 0.86 |
| Hybrid* | 0.94 | 0.71 | 0.92 |
| Bayesian Structural | 0.78 | 0.65 | 0.77 |
| Prophet | 0.83 | 0.71 | 0.82 |

*Hybrid: Combined SARIMA, ETS, STL and Neural Network model

Supplementary Fig. 31. Training and comparing variant time series models for enteric fever.

(A) Neural Network model; (B) Prophet model; (C) Exponential smoothing (ETS) model; (D) Seasonal autoregressive integrated moving average (SARIMA) model; (E) Hybrid models combining SARIMA, ETS, STL (seasonal and trend decomposition using loess), and neural network model; (F) Bayesian structural model; (G) Root mean square error (RMSE) of variant models; (H) Symmetric mean absolute percentage error (SMAPE) of variant models; (I) Mean absolute scaled error (MASE) of variant models; (J) R-squared of variant models.



G : SMAPE of Models

| Method | Train | Test | All |
|---------------------|-------|-------|------|
| Neural Network | 0.71 | 10.58 | 2.50 |
| ETS | 4.23 | 5.29 | 4.41 |
| SARIMA | 9.86 | 7.33 | 9.44 |
| Hybrid* | 3.76 | 6.81 | 4.31 |
| Bayesian Structural | 5.35 | 4.52 | 5.22 |
| Prophet | 4.53 | 5.88 | 4.76 |

*Hybrid: Combined SARIMA, ETS, STL and Neural Network model

H : RMSE of Models

| Method | Train | Test | All |
|---------------------|----------|----------|----------|
| Neural Network | 1041.08 | 12656.05 | 5478.10 |
| ETS | 6186.51 | 6740.76 | 6282.28 |
| SARIMA | 15019.03 | 9396.49 | 14236.98 |
| Hybrid* | 5523.44 | 8479.68 | 6167.26 |
| Bayesian Structural | 8381.15 | 5365.91 | 7958.34 |
| Prophet | 6389.18 | 7366.71 | 6562.22 |

*Hybrid: Combined SARIMA, ETS, STL and Neural Network model

I : MASE of Models

| Method | Train | Test | All |
|---------------------|-------|------|------|
| Neural Network | 0.10 | 1.62 | 0.35 |
| ETS | 0.51 | 0.98 | 0.78 |
| SARIMA | 0.99 | Inf | 1.16 |
| Hybrid* | 0.46 | 1.72 | 1.02 |
| Bayesian Structural | 0.65 | 0.91 | 0.83 |
| Prophet | 0.55 | 1.11 | 0.88 |

*Hybrid: Combined SARIMA, ETS, STL and Neural Network model

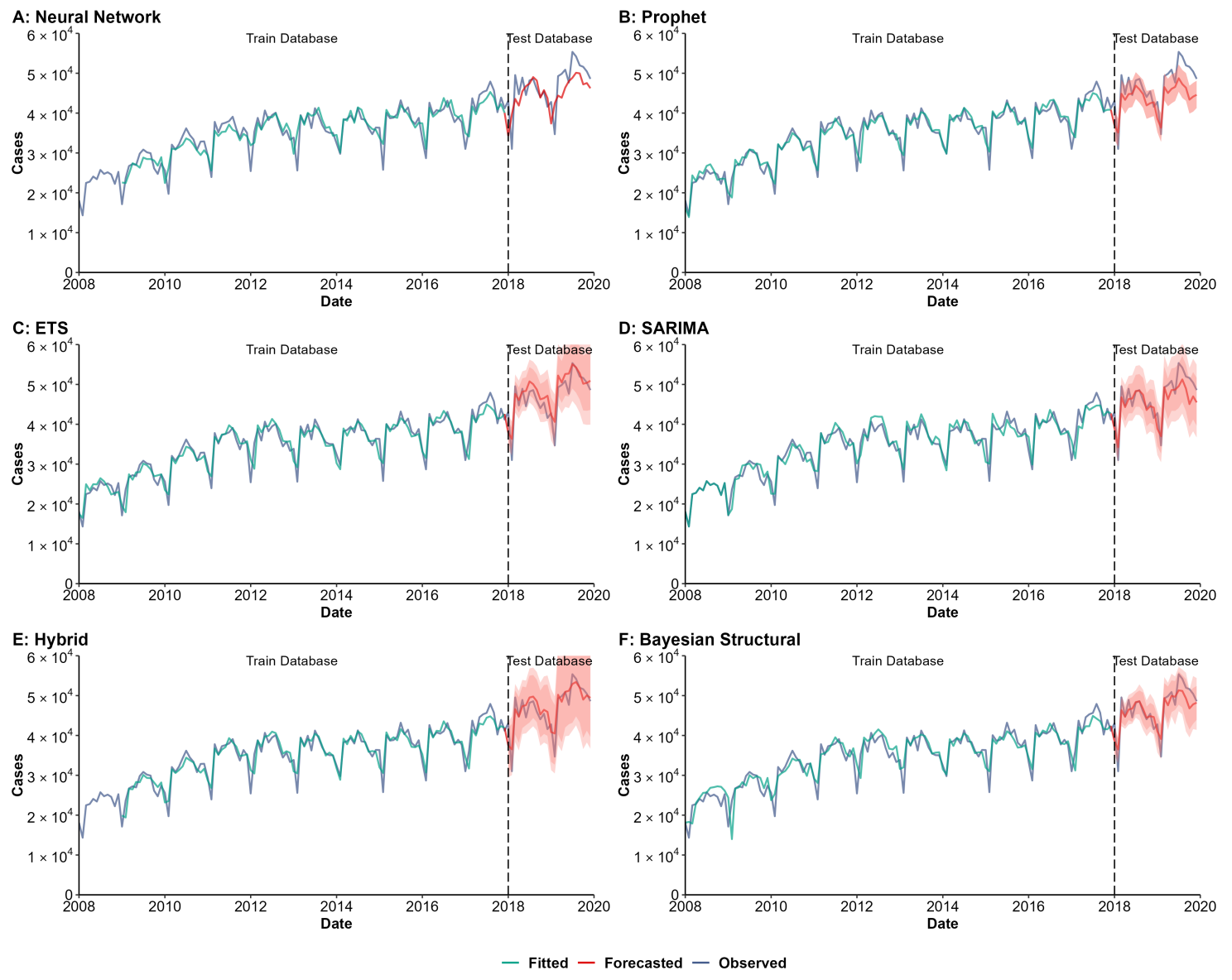
J : R_Squared of Models

| Method | Train | Test | All |
|---------------------|-------|------|------|
| Neural Network | 0.99 | 0.02 | 0.75 |
| ETS | 0.70 | 0.71 | 0.67 |
| SARIMA | 0.10 | 0.10 | 0.09 |
| Hybrid* | 0.73 | 0.48 | 0.65 |
| Bayesian Structural | 0.54 | 0.58 | 0.55 |
| Prophet | 0.67 | 0.67 | 0.64 |

*Hybrid: Combined SARIMA, ETS, STL and Neural Network model

Supplementary Fig. 32. Training and comparing variant time series models for hepatitis B.

(A) Neural Network model; (B) Prophet model; (C) Exponential smoothing (ETS) model; (D) Seasonal autoregressive integrated moving average (SARIMA) model; (E) Hybrid models combining SARIMA, ETS, STL (seasonal and trend decomposition using loess), and neural network model; (F) Bayesian structural model; (G) Root mean square error (RMSE) of variant models; (H) Symmetric mean absolute percentage error (SMAPE) of variant models; (I) Mean absolute scaled error (MASE) of variant models; (J) R-squared of variant models.



G : SMAPE of Models

| Method | Train | Test | All |
|---------------------|-------|------|------|
| Neural Network | 5.13 | 8.48 | 5.74 |
| ETS | 4.45 | 5.26 | 4.59 |
| SARIMA | 4.30 | 5.40 | 4.48 |
| Hybrid* | 4.18 | 4.90 | 4.31 |
| Bayesian Structural | 5.85 | 4.86 | 5.68 |
| Prophet | 4.08 | 8.16 | 4.76 |

*Hybrid: Combined SARIMA, ETS, STL and Neural Network model

H : RMSE of Models

| Method | Train | Test | All |
|---------------------|---------|---------|---------|
| Neural Network | 2280.48 | 4523.55 | 2824.09 |
| ETS | 1865.68 | 2960.59 | 2088.41 |
| SARIMA | 1943.45 | 2973.30 | 2149.63 |
| Hybrid* | 1821.54 | 2743.41 | 2020.68 |
| Bayesian Structural | 2469.89 | 2717.47 | 2512.84 |
| Prophet | 1755.91 | 4295.93 | 2375.96 |

*Hybrid: Combined SARIMA, ETS, STL and Neural Network model

I : MASE of Models

| Method | Train | Test | All |
|---------------------|-------|------|------|
| Neural Network | 0.79 | 1.65 | 0.94 |
| ETS | 0.45 | 0.98 | 0.70 |
| SARIMA | 0.57 | 0.84 | 0.62 |
| Hybrid* | 0.44 | 0.94 | 0.69 |
| Bayesian Structural | 0.58 | 0.99 | 0.87 |
| Prophet | 0.42 | 1.68 | 0.75 |

*Hybrid: Combined SARIMA, ETS, STL and Neural Network model

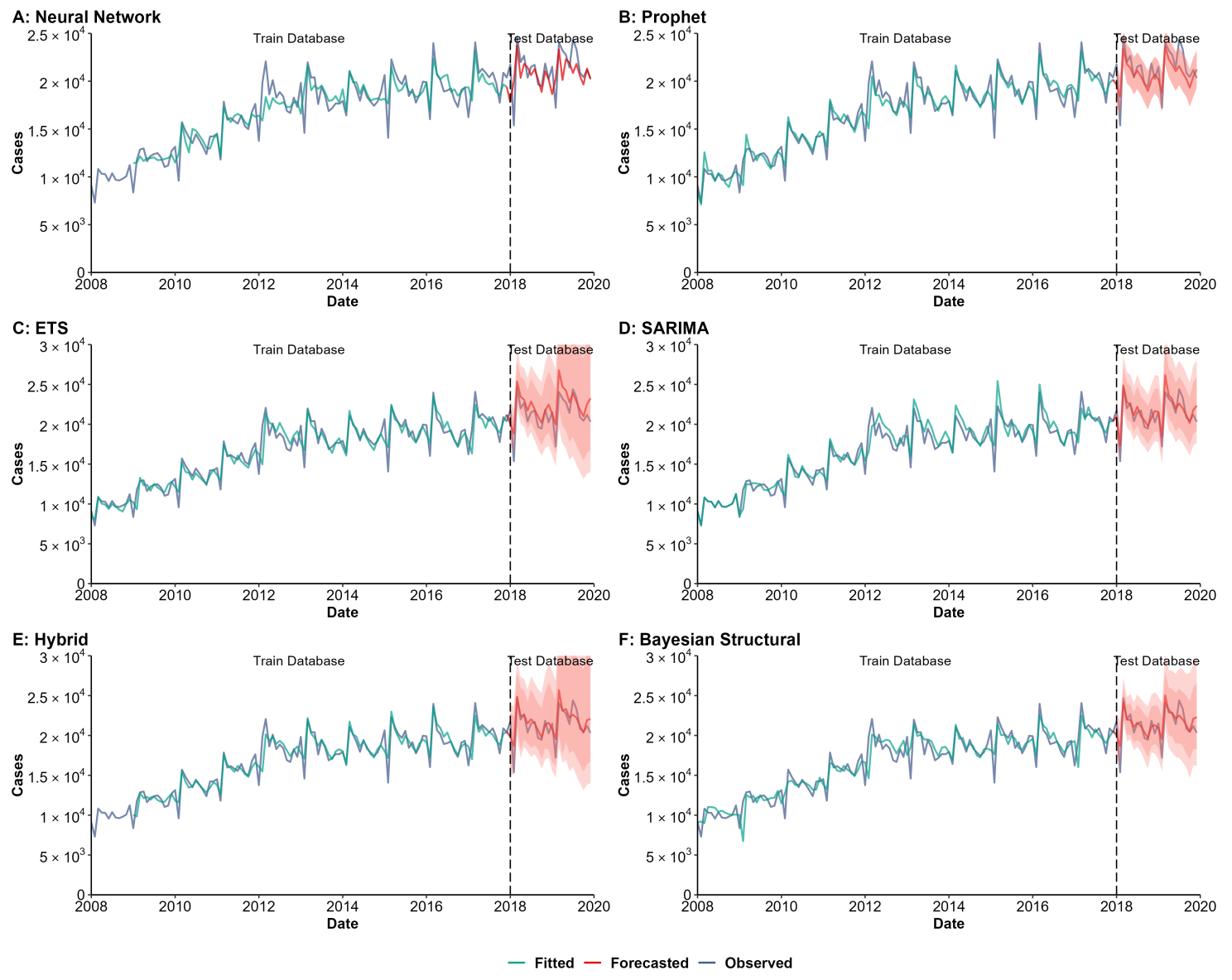
J : R_Squared of Models

| Method | Train | Test | All |
|---------------------|-------|------|------|
| Neural Network | 0.84 | 0.42 | 0.85 |
| ETS | 0.93 | 0.78 | 0.93 |
| SARIMA | 0.92 | 0.78 | 0.93 |
| Hybrid* | 0.90 | 0.76 | 0.92 |
| Bayesian Structural | 0.87 | 0.80 | 0.90 |
| Prophet | 0.93 | 0.76 | 0.93 |

*Hybrid: Combined SARIMA, ETS, STL and Neural Network model

Supplementary Fig. 33. Training and comparing variant time series models for syphilis.

(A) Neural Network model; (B) Prophet model; (C) Exponential smoothing (ETS) model; (D) Seasonal autoregressive integrated moving average (SARIMA) model; (E) Hybrid models combining SARIMA, ETS, STL (seasonal and trend decomposition using loess), and neural network model; (F) Bayesian structural model; (G) Root mean square error (RMSE) of variant models; (H) Symmetric mean absolute percentage error (SMAPE) of variant models; (I) Mean absolute scaled error (MASE) of variant models; (J) R-squared of variant models.



G : SMAPE of Models

| Method | Train | Test | All |
|---------------------|-------|------|------|
| Neural Network | 5.75 | 6.82 | 5.95 |
| ETS | 4.87 | 6.22 | 5.09 |
| SARIMA | 4.61 | 4.11 | 4.53 |
| Hybrid* | 4.41 | 4.63 | 4.45 |
| Bayesian Structural | 6.26 | 4.42 | 5.96 |
| Prophet | 4.50 | 5.35 | 4.64 |

*Hybrid: Combined SARIMA, ETS, STL and Neural Network model

H : RMSE of Models

| Method | Train | Test | All |
|---------------------|---------|---------|---------|
| Neural Network | 1313.61 | 1921.85 | 1443.39 |
| ETS | 1062.89 | 1602.86 | 1170.31 |
| SARIMA | 1076.37 | 1059.44 | 1073.56 |
| Hybrid* | 1026.21 | 1245.38 | 1069.41 |
| Bayesian Structural | 1336.63 | 1208.47 | 1316.14 |
| Prophet | 1008.31 | 1367.16 | 1076.46 |

*Hybrid: Combined SARIMA, ETS, STL and Neural Network model

I : MASE of Models

| Method | Train | Test | All |
|---------------------|-------|------|------|
| Neural Network | 0.99 | 0.87 | 0.96 |
| ETS | 0.48 | 0.82 | 0.68 |
| SARIMA | 0.61 | 0.49 | 0.59 |
| Hybrid* | 0.43 | 0.68 | 0.66 |
| Bayesian Structural | 0.59 | 0.73 | 0.94 |
| Prophet | 0.44 | 0.92 | 0.66 |

*Hybrid: Combined SARIMA, ETS, STL and Neural Network model

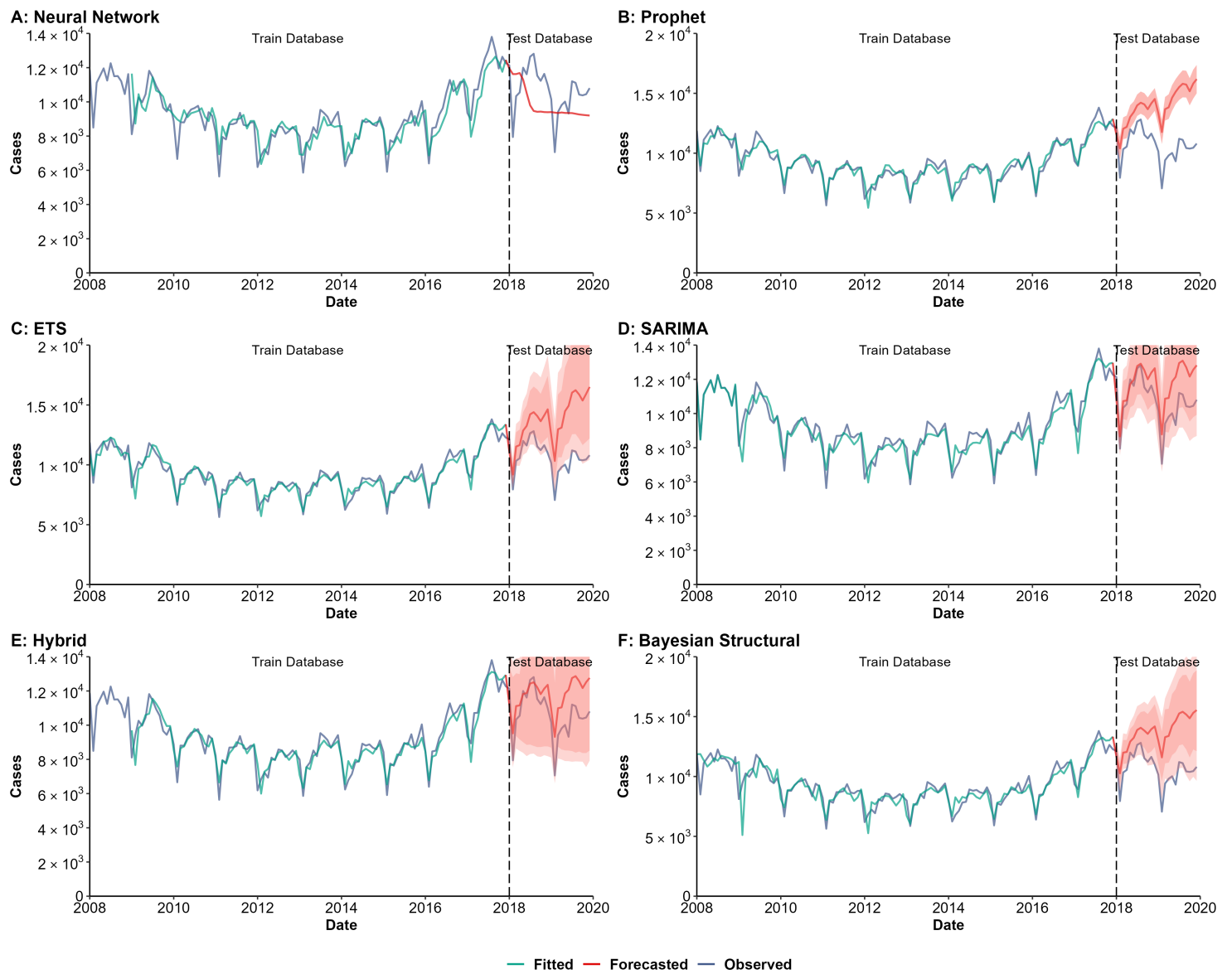
J : R_Squared of Models

| Method | Train | Test | All |
|---------------------|-------|------|------|
| Neural Network | 0.83 | 0.24 | 0.82 |
| ETS | 0.92 | 0.67 | 0.92 |
| SARIMA | 0.93 | 0.77 | 0.94 |
| Hybrid* | 0.90 | 0.68 | 0.90 |
| Bayesian Structural | 0.88 | 0.70 | 0.89 |
| Prophet | 0.93 | 0.69 | 0.93 |

*Hybrid: Combined SARIMA, ETS, STL and Neural Network model

Supplementary Fig. 34. Training and comparing variant time series models for hepatitis C.

(A) Neural Network model; (B) Prophet model; (C) Exponential smoothing (ETS) model; (D) Seasonal autoregressive integrated moving average (SARIMA) model; (E) Hybrid models combining SARIMA, ETS, STL (seasonal and trend decomposition using loess), and neural network model; (F) Bayesian structural model; (G) Root mean square error (RMSE) of variant models; (H) Symmetric mean absolute percentage error (SMAPE) of variant models; (I) Mean absolute scaled error (MASE) of variant models; (J) R-squared of variant models.



G : SMAPE of Models

| Method | Train | Test | All |
|---------------------|-------|-------|------|
| Neural Network | 6.22 | 14.29 | 7.68 |
| ETS | 4.49 | 25.52 | 8.00 |
| SARIMA | 4.50 | 11.09 | 5.60 |
| Hybrid* | 4.29 | 11.46 | 5.59 |
| Bayesian Structural | 5.78 | 25.16 | 9.01 |
| Prophet | 4.06 | 27.09 | 7.90 |

*Hybrid: Combined SARIMA, ETS, STL and Neural Network model

H : RMSE of Models

| Method | Train | Test | All |
|---------------------|--------|---------|---------|
| Neural Network | 768.47 | 1741.24 | 1017.07 |
| ETS | 527.64 | 3552.64 | 1528.25 |
| SARIMA | 531.86 | 1435.89 | 761.16 |
| Hybrid* | 512.80 | 1436.89 | 768.47 |
| Bayesian Structural | 803.90 | 3352.88 | 1553.12 |
| Prophet | 472.92 | 3665.31 | 1557.39 |

*Hybrid: Combined SARIMA, ETS, STL and Neural Network model

I : MASE of Models

| Method | Train | Test | All |
|---------------------|-------|-------|------|
| Neural Network | 0.92 | 11.29 | 1.38 |
| ETS | 0.52 | 3.43 | 1.25 |
| SARIMA | 0.58 | 1.58 | 0.76 |
| Hybrid* | 0.52 | 2.07 | 0.90 |
| Bayesian Structural | 0.67 | 4.99 | 1.37 |
| Prophet | 0.47 | 5.13 | 1.37 |

*Hybrid: Combined SARIMA, ETS, STL and Neural Network model

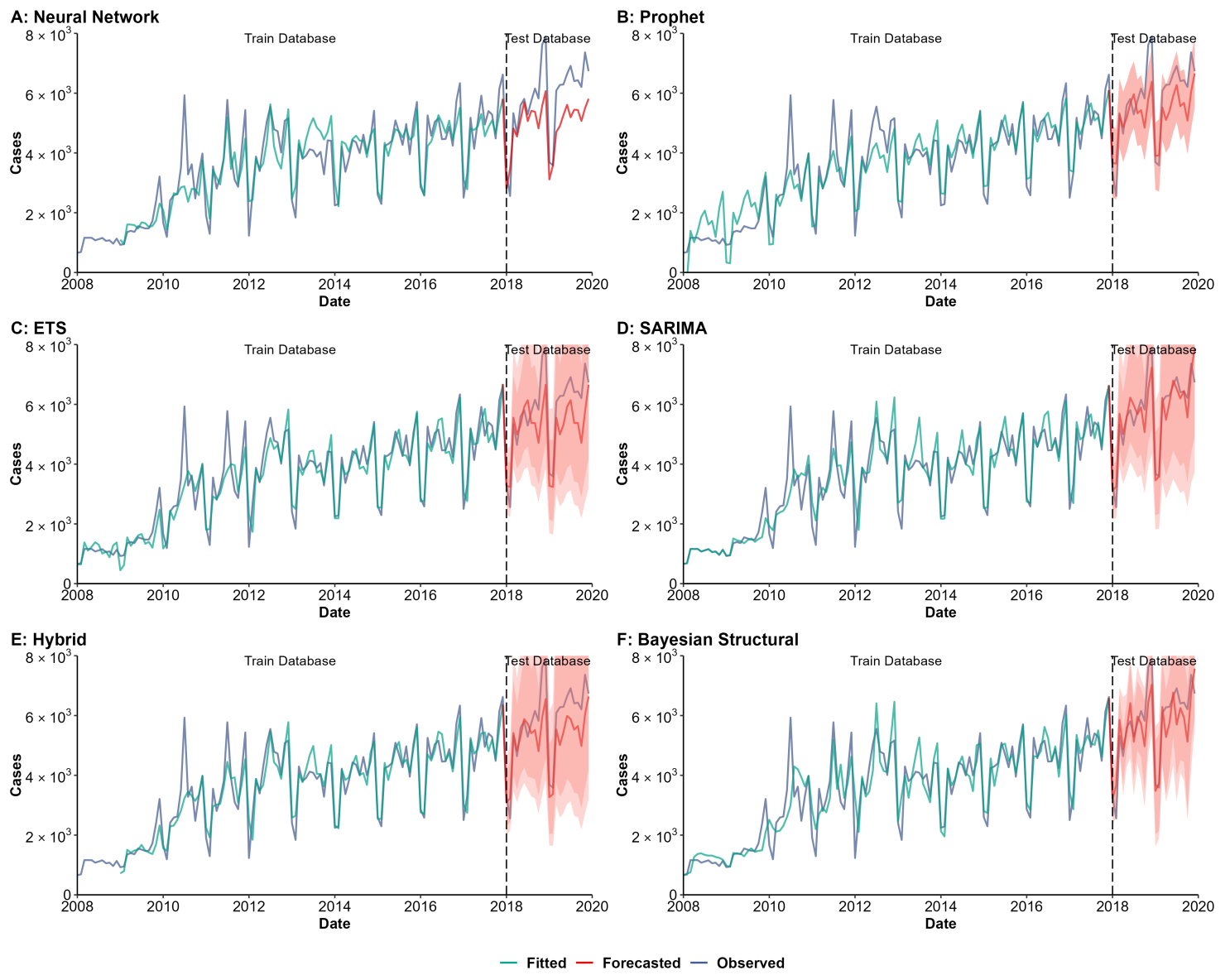
J : R_Squared of Models

| Method | Train | Test | All |
|---------------------|-------|------|------|
| Neural Network | 0.76 | 0.00 | 0.63 |
| ETS | 0.90 | 0.17 | 0.64 |
| SARIMA | 0.91 | 0.52 | 0.83 |
| Hybrid* | 0.90 | 0.51 | 0.82 |
| Bayesian Structural | 0.78 | 0.13 | 0.59 |
| Prophet | 0.92 | 0.09 | 0.60 |

*Hybrid: Combined SARIMA, ETS, STL and Neural Network model

Supplementary Fig. 35. Training and comparing variant time series models for gonorrhea.

(A) Neural Network model; (B) Prophet model; (C) Exponential smoothing (ETS) model; (D) Seasonal autoregressive integrated moving average (SARIMA) model; (E) Hybrid models combining SARIMA, ETS, STL (seasonal and trend decomposition using loess), and neural network model; (F) Bayesian structural model; (G) Root mean square error (RMSE) of variant models; (H) Symmetric mean absolute percentage error (SMAPE) of variant models; (I) Mean absolute scaled error (MASE) of variant models; (J) R-squared of variant models.



G : SMAPE of Models

| Method | Train | Test | All |
|---------------------|-------|-------|-------|
| Neural Network | 12.69 | 16.54 | 13.39 |
| ETS | 11.58 | 13.62 | 11.92 |
| SARIMA | 10.56 | 7.26 | 10.01 |
| Hybrid* | 10.25 | 12.17 | 10.60 |
| Bayesian Structural | 13.89 | 9.71 | 13.19 |
| Prophet | 19.54 | 12.87 | 18.43 |

*Hybrid: Combined SARIMA, ETS, STL and Neural Network model

H : RMSE of Models

| Method | Train | Test | All |
|---------------------|--------|---------|--------|
| Neural Network | 596.10 | 1073.93 | 707.41 |
| ETS | 495.77 | 906.91 | 584.73 |
| SARIMA | 551.30 | 518.54 | 545.98 |
| Hybrid* | 495.91 | 817.70 | 568.14 |
| Bayesian Structural | 612.22 | 659.41 | 620.33 |
| Prophet | 584.61 | 845.66 | 635.61 |

*Hybrid: Combined SARIMA, ETS, STL and Neural Network model

I : MASE of Models

| Method | Train | Test | All |
|---------------------|-------|------|------|
| Neural Network | 0.69 | 1.55 | 0.81 |
| ETS | 0.42 | 0.96 | 0.59 |
| SARIMA | 0.54 | 0.45 | 0.51 |
| Hybrid* | 0.39 | 0.92 | 0.58 |
| Bayesian Structural | 0.53 | 0.51 | 0.58 |
| Prophet | 0.55 | 1.11 | 0.70 |

*Hybrid: Combined SARIMA, ETS, STL and Neural Network model

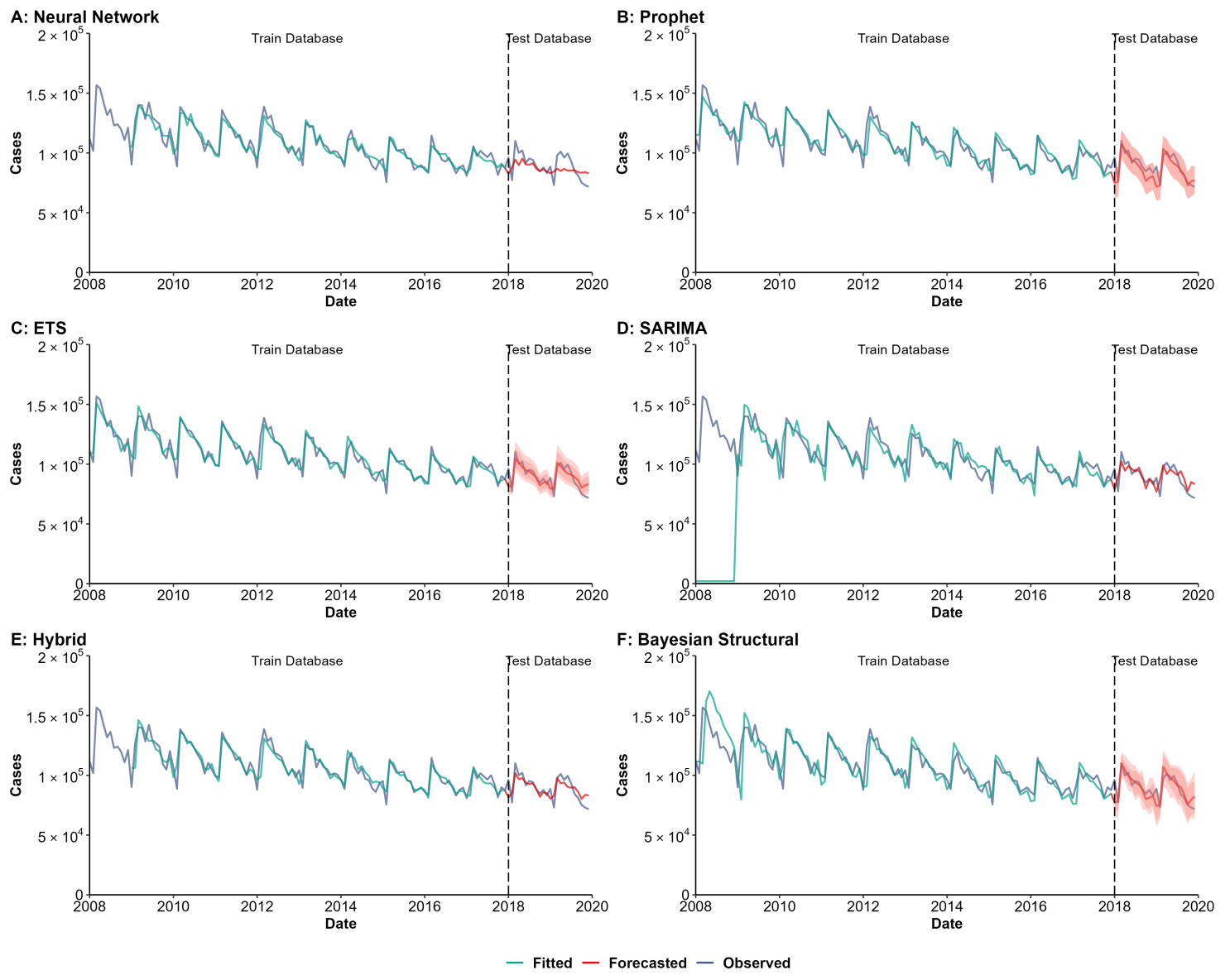
J : R_Squared of Models

| Method | Train | Test | All |
|---------------------|-------|------|------|
| Neural Network | 0.81 | 0.81 | 0.82 |
| ETS | 0.90 | 0.73 | 0.90 |
| SARIMA | 0.87 | 0.85 | 0.90 |
| Hybrid* | 0.87 | 0.83 | 0.88 |
| Bayesian Structural | 0.84 | 0.78 | 0.87 |
| Prophet | 0.86 | 0.80 | 0.87 |

*Hybrid: Combined SARIMA, ETS, STL and Neural Network model

Supplementary Fig. 36. Training and comparing variant time series models for acquired immunodeficiency syndrome (AIDS).

(A) Neural Network model; (B) Prophet model; (C) Exponential smoothing (ETS) model; (D) Seasonal autoregressive integrated moving average (SARIMA) model; (E) Hybrid models combining SARIMA, ETS, STL (seasonal and trend decomposition using loess), and neural network model; (F) Bayesian structural model; (G) Root mean square error (RMSE) of variant models; (H) Symmetric mean absolute percentage error (SMAPE) of variant models; (I) Mean absolute scaled error (MASE) of variant models; (J) R-squared of variant models.



G : SMAPE of Models

| Method | Train | Test | All |
|---------------------|-------|------|-------|
| Neural Network | 3.61 | 8.56 | 4.51 |
| ETS | 3.73 | 5.55 | 4.03 |
| SARIMA | 24.50 | 7.31 | 21.64 |
| Hybrid* | 3.85 | 6.24 | 4.28 |
| Bayesian Structural | 6.34 | 5.22 | 6.16 |
| Prophet | 4.17 | 5.62 | 4.41 |

*Hybrid: Combined SARIMA, ETS, STL and Neural Network model

H : RMSE of Models

| Method | Train | Test | All |
|---------------------|----------|---------|----------|
| Neural Network | 5048.30 | 9072.43 | 5984.72 |
| ETS | 5942.67 | 5897.21 | 5935.12 |
| SARIMA | 40903.93 | 7918.45 | 37479.69 |
| Hybrid* | 5951.85 | 6656.23 | 6085.99 |
| Bayesian Structural | 10818.75 | 6471.70 | 10223.42 |
| Prophet | 6199.41 | 6882.93 | 6318.47 |

*Hybrid: Combined SARIMA, ETS, STL and Neural Network model

I : MASE of Models

| Method | Train | Test | All |
|---------------------|-------|------|------|
| Neural Network | 0.66 | 3.25 | 0.87 |
| ETS | 0.43 | 1.10 | 0.67 |
| SARIMA | 2.03 | 0.99 | 1.90 |
| Hybrid* | 0.46 | 1.33 | 0.73 |
| Bayesian Structural | 0.76 | 0.72 | 0.79 |
| Prophet | 0.48 | 0.79 | 0.71 |

*Hybrid: Combined SARIMA, ETS, STL and Neural Network model

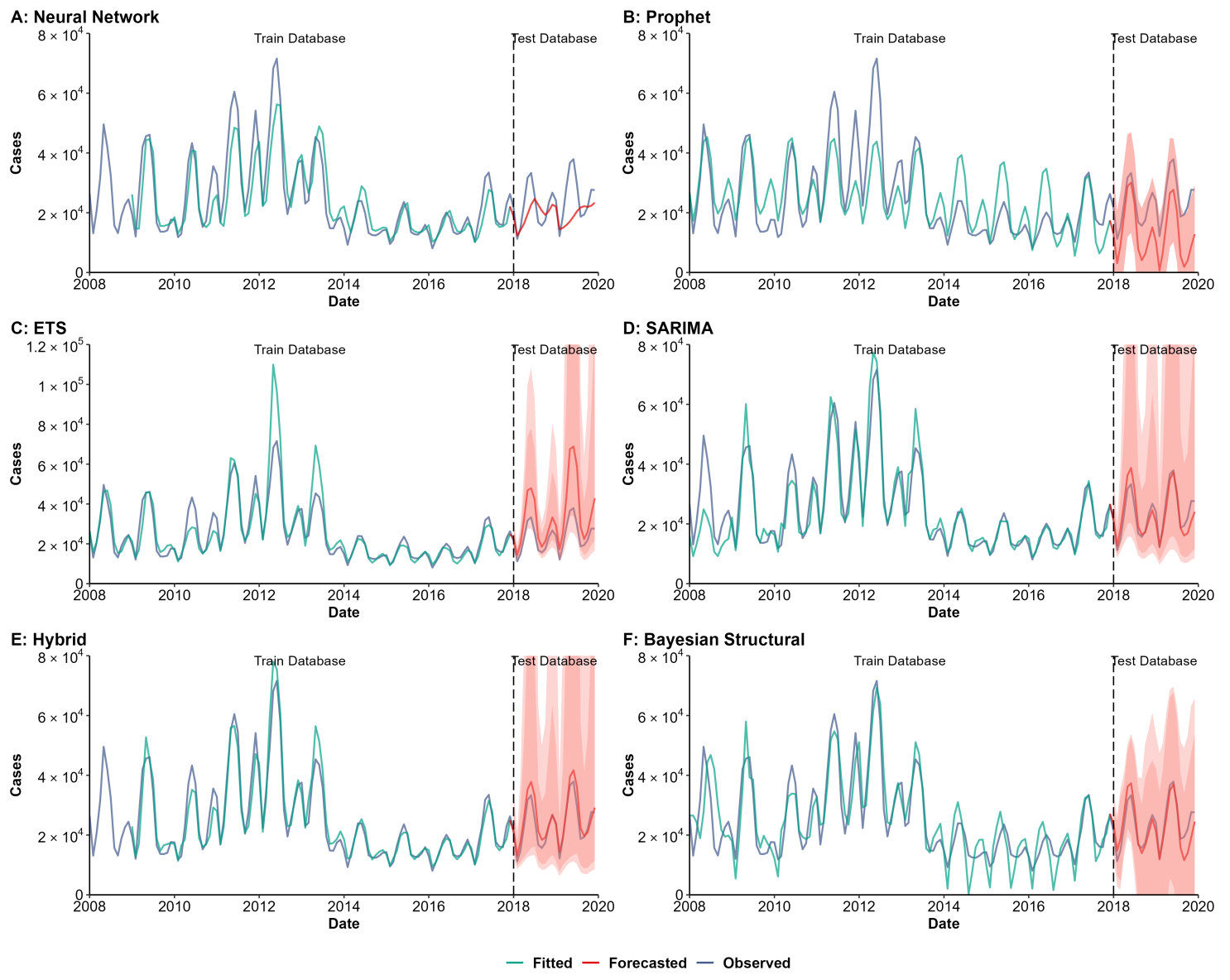
J : R_Squared of Models

| Method | Train | Test | All |
|---------------------|-------|------|------|
| Neural Network | 0.90 | 0.37 | 0.87 |
| ETS | 0.88 | 0.68 | 0.89 |
| SARIMA | 0.00 | 0.41 | 0.00 |
| Hybrid* | 0.85 | 0.63 | 0.86 |
| Bayesian Structural | 0.71 | 0.65 | 0.74 |
| Prophet | 0.87 | 0.68 | 0.87 |

*Hybrid: Combined SARIMA, ETS, STL and Neural Network model

Supplementary Fig. 37. Training and comparing variant time series models for tuberculosis.

(A) Neural Network model; (B) Prophet model; (C) Exponential smoothing (ETS) model; (D) Seasonal autoregressive integrated moving average (SARIMA) model; (E) Hybrid models combining SARIMA, ETS, STL (seasonal and trend decomposition using loess), and neural network model; (F) Bayesian structural model; (G) Root mean square error (RMSE) of variant models; (H) Symmetric mean absolute percentage error (SMAPE) of variant models; (I) Mean absolute scaled error (MASE) of variant models; (J) R-squared of variant models.



G : SMAPE of Models

| Method | Train | Test | All |
|---------------------|-------|-------|-------|
| Neural Network | 17.22 | 24.96 | 18.62 |
| ETS | 12.95 | 31.97 | 16.12 |
| SARIMA | 14.06 | 11.14 | 13.58 |
| Hybrid* | 10.19 | 10.15 | 10.18 |
| Bayesian Structural | 27.89 | 14.49 | 25.65 |
| Prophet | 27.47 | 73.75 | 35.18 |

*Hybrid: Combined SARIMA, ETS, STL and Neural Network model

H : RMSE of Models

| Method | Train | Test | All |
|---------------------|---------|----------|---------|
| Neural Network | 6262.36 | 7883.47 | 6586.85 |
| ETS | 6868.39 | 13611.02 | 8377.88 |
| SARIMA | 5460.31 | 3226.85 | 5155.70 |
| Hybrid* | 3679.01 | 3132.44 | 3585.83 |
| Bayesian Structural | 6631.07 | 3784.71 | 6247.39 |
| Prophet | 8652.71 | 11406.85 | 9169.36 |

*Hybrid: Combined SARIMA, ETS, STL and Neural Network model

I : MASE of Models

| Method | Train | Test | All |
|---------------------|-------|------|------|
| Neural Network | 0.85 | 2.96 | 1.01 |
| ETS | 0.58 | 1.09 | 0.67 |
| SARIMA | 0.51 | 0.46 | 0.50 |
| Hybrid* | 0.42 | 0.42 | 0.43 |
| Bayesian Structural | 0.77 | 0.49 | 0.65 |
| Prophet | 1.01 | 1.59 | 1.12 |

*Hybrid: Combined SARIMA, ETS, STL and Neural Network model

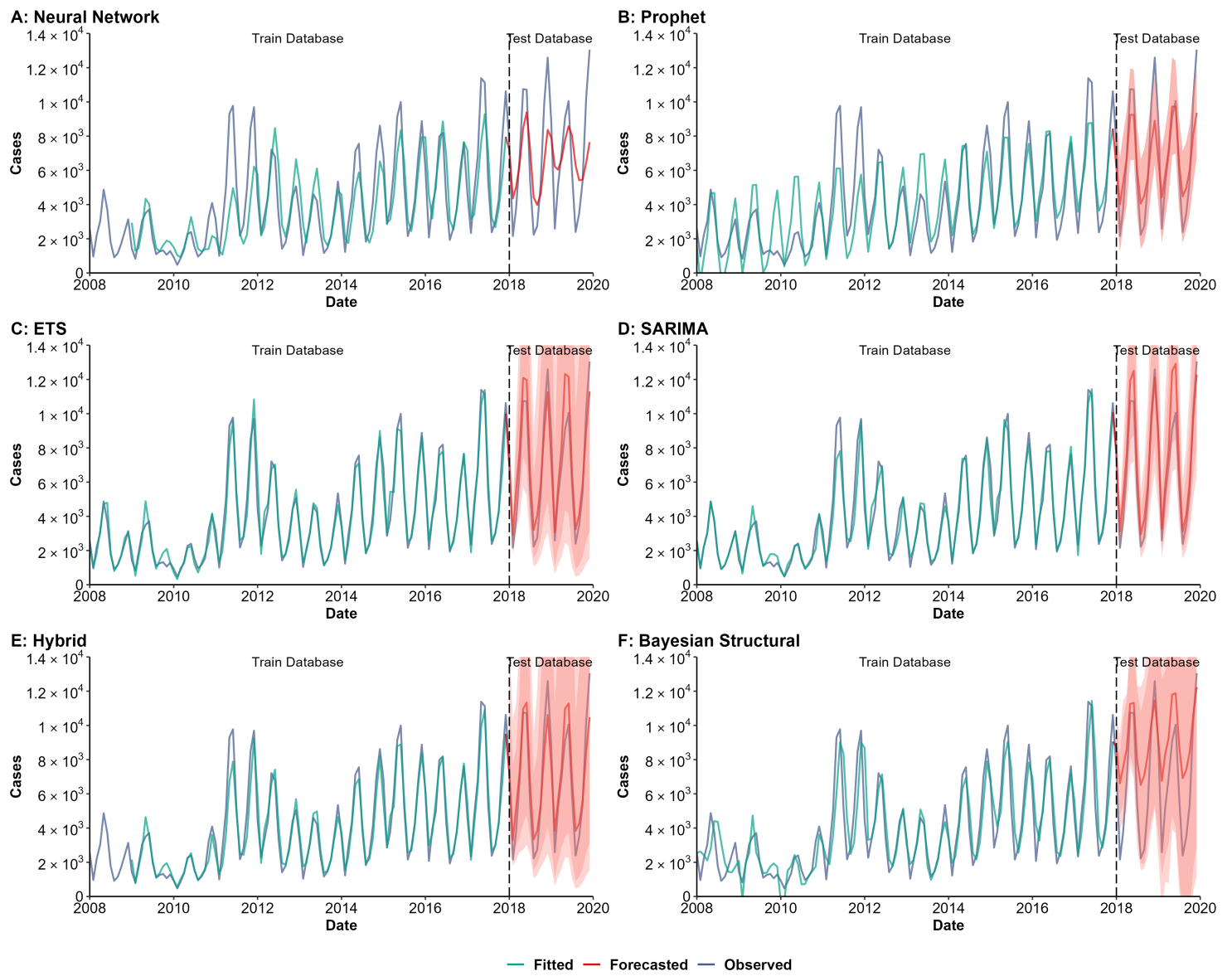
J : R_Squared of Models

| Method | Train | Test | All |
|---------------------|-------|------|------|
| Neural Network | 0.80 | 0.11 | 0.75 |
| ETS | 0.86 | 0.87 | 0.80 |
| SARIMA | 0.86 | 0.82 | 0.86 |
| Hybrid* | 0.93 | 0.91 | 0.93 |
| Bayesian Structural | 0.78 | 0.78 | 0.78 |
| Prophet | 0.59 | 0.76 | 0.51 |

*Hybrid: Combined SARIMA, ETS, STL and Neural Network model

Supplementary Fig. 38. Training and comparing variant time series models for mumps.

(A) Neural Network model; (B) Prophet model; (C) Exponential smoothing (ETS) model; (D) Seasonal autoregressive integrated moving average (SARIMA) model; (E) Hybrid models combining SARIMA, ETS, STL (seasonal and trend decomposition using loess), and neural network model; (F) Bayesian structural model; (G) Root mean square error (RMSE) of variant models; (H) Symmetric mean absolute percentage error (SMAPE) of variant models; (I) Mean absolute scaled error (MASE) of variant models; (J) R-squared of variant models.



G : SMAPE of Models

| Method | Train | Test | All |
|---------------------|-------|-------|-------|
| Neural Network | 29.94 | 32.57 | 30.42 |
| ETS | 10.94 | 18.43 | 12.19 |
| SARIMA | 10.42 | 16.31 | 11.40 |
| Hybrid* | 13.07 | 18.71 | 14.09 |
| Bayesian Structural | 28.96 | 40.55 | 30.89 |
| Prophet | 37.36 | 25.23 | 35.34 |

*Hybrid: Combined SARIMA, ETS, STL and Neural Network model

H : RMSE of Models

| Method | Train | Test | All |
|---------------------|---------|---------|---------|
| Neural Network | 1559.38 | 2412.97 | 1745.90 |
| ETS | 507.57 | 1307.01 | 706.68 |
| SARIMA | 572.96 | 1233.43 | 726.04 |
| Hybrid* | 680.15 | 1231.46 | 808.84 |
| Bayesian Structural | 1171.60 | 2831.52 | 1574.84 |
| Prophet | 1374.52 | 1738.25 | 1441.53 |

*Hybrid: Combined SARIMA, ETS, STL and Neural Network model

I : MASE of Models

| Method | Train | Test | All |
|---------------------|-------|------|------|
| Neural Network | 0.84 | 1.62 | 0.97 |
| ETS | 0.21 | 0.41 | 0.26 |
| SARIMA | 0.24 | 0.32 | 0.26 |
| Hybrid* | 0.28 | 0.44 | 0.34 |
| Bayesian Structural | 0.52 | 1.52 | 0.78 |
| Prophet | 0.63 | 0.89 | 0.69 |

*Hybrid: Combined SARIMA, ETS, STL and Neural Network model

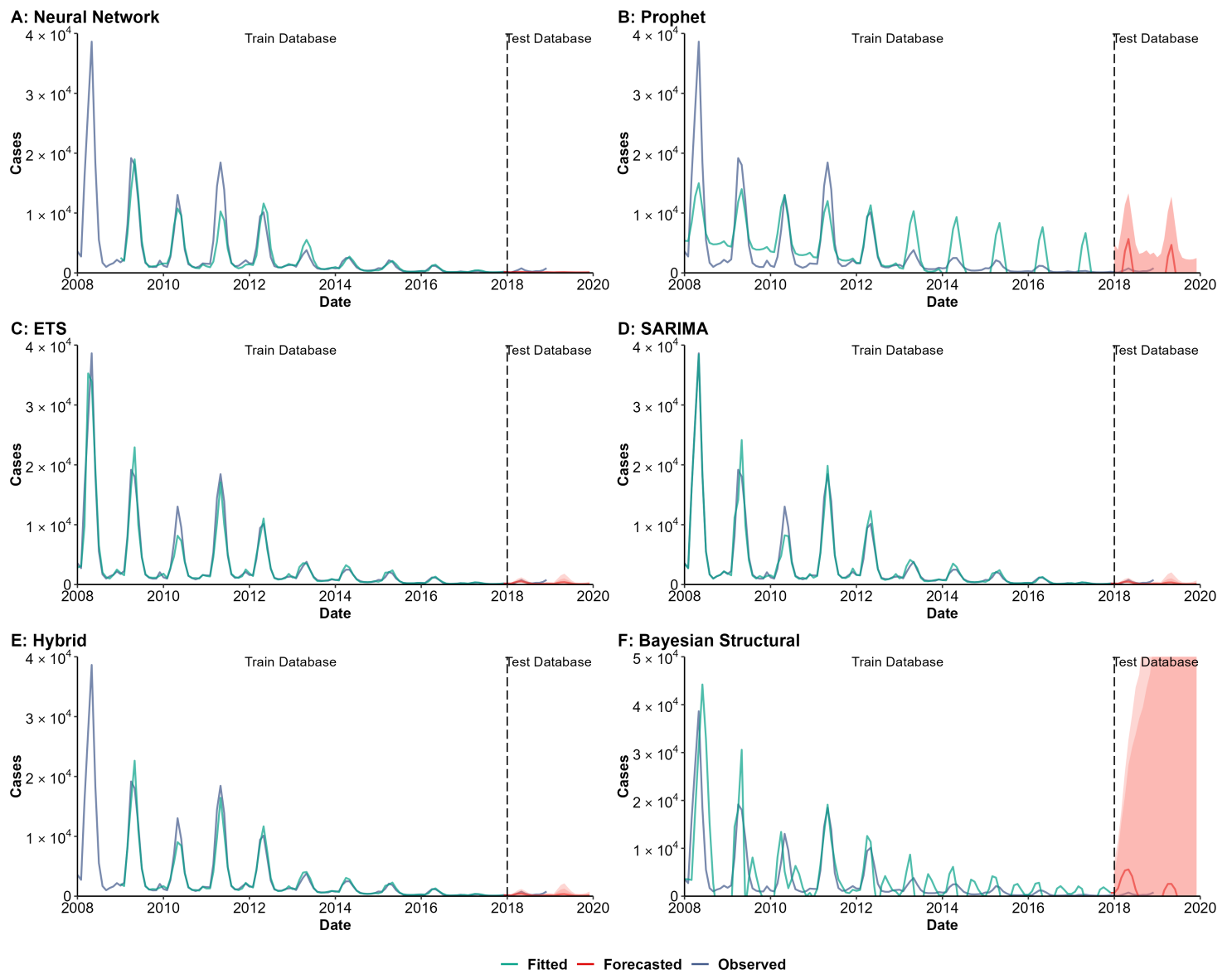
J : R_Squared of Models

| Method | Train | Test | All |
|---------------------|-------|------|------|
| Neural Network | 0.67 | 0.61 | 0.67 |
| ETS | 0.96 | 0.87 | 0.94 |
| SARIMA | 0.95 | 0.92 | 0.94 |
| Hybrid* | 0.94 | 0.89 | 0.93 |
| Bayesian Structural | 0.80 | 0.92 | 0.75 |
| Prophet | 0.73 | 0.88 | 0.77 |

*Hybrid: Combined SARIMA, ETS, STL and Neural Network model

Supplementary Fig. 39. Training and comparing variant time series models for scarlet fever.

(A) Neural Network model; (B) Prophet model; (C) Exponential smoothing (ETS) model; (D) Seasonal autoregressive integrated moving average (SARIMA) model; (E) Hybrid models combining SARIMA, ETS, STL (seasonal and trend decomposition using loess), and neural network model; (F) Bayesian structural model; (G) Root mean square error (RMSE) of variant models; (H) Symmetric mean absolute percentage error (SMAPE) of variant models; (I) Mean absolute scaled error (MASE) of variant models; (J) R-squared of variant models.



G : SMAPE of Models

| Method | Train | Test | All |
|---------------------|--------|--------|--------|
| Neural Network | 22.14 | 87.34 | 28.66 |
| ETS | 15.04 | 58.21 | 18.96 |
| SARIMA | 14.79 | 62.87 | 19.16 |
| Hybrid* | 13.87 | 62.14 | 18.70 |
| Bayesian Structural | 111.03 | 176.40 | 116.97 |
| Prophet | 98.40 | 184.97 | 106.27 |

*Hybrid: Combined SARIMA, ETS, STL and Neural Network model

H : RMSE of Models

| Method | Train | Test | All |
|---------------------|---------|---------|---------|
| Neural Network | 1574.38 | 316.31 | 1496.94 |
| ETS | 1409.08 | 234.49 | 1345.36 |
| SARIMA | 1058.88 | 243.11 | 1012.26 |
| Hybrid* | 962.14 | 246.44 | 916.09 |
| Bayesian Structural | 5302.93 | 3056.49 | 5139.45 |
| Prophet | 3850.75 | 3883.99 | 3853.78 |

*Hybrid: Combined SARIMA, ETS, STL and Neural Network model

I : MASE of Models

| Method | Train | Test | All |
|---------------------|-------|-------|------|
| Neural Network | 0.59 | 12.59 | 0.61 |
| ETS | 0.33 | 2.10 | 0.35 |
| SARIMA | 0.23 | 2.55 | 0.24 |
| Hybrid* | 0.33 | 2.99 | 0.34 |
| Bayesian Structural | 1.80 | 2.26 | 0.96 |
| Prophet | 1.43 | 2.00 | 1.49 |

*Hybrid: Combined SARIMA, ETS, STL and Neural Network model

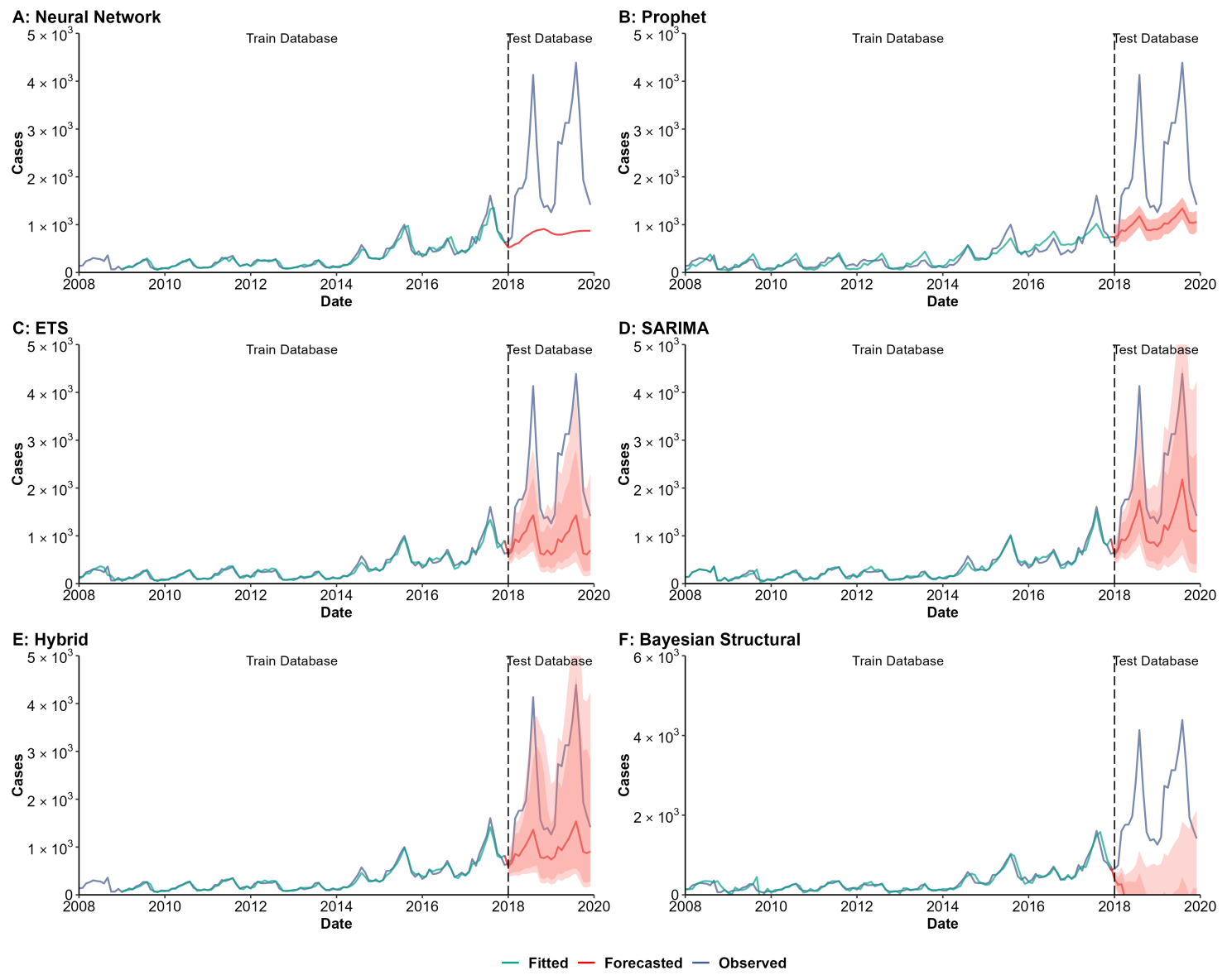
J : R_Squared of Models

| Method | Train | Test | All |
|---------------------|-------|------|------|
| Neural Network | 0.86 | 0.29 | 0.86 |
| ETS | 0.94 | 0.20 | 0.94 |
| SARIMA | 0.97 | 0.20 | 0.97 |
| Hybrid* | 0.95 | 0.23 | 0.95 |
| Bayesian Structural | 0.51 | 0.02 | 0.51 |
| Prophet | 0.56 | 0.26 | 0.53 |

*Hybrid: Combined SARIMA, ETS, STL and Neural Network model

Supplementary Fig. 40. Training and comparing variant time series models for rubella.

(A) Neural Network model; (B) Prophet model; (C) Exponential smoothing (ETS) model; (D) Seasonal autoregressive integrated moving average (SARIMA) model; (E) Hybrid models combining SARIMA, ETS, STL (seasonal and trend decomposition using loess), and neural network model; (F) Bayesian structural model; (G) Root mean square error (RMSE) of variant models; (H) Symmetric mean absolute percentage error (SMAPE) of variant models; (I) Mean absolute scaled error (MASE) of variant models; (J) R-squared of variant models.



G : SMAPE of Models

| Method | Train | Test | All |
|---------------------|-------|--------|-------|
| Neural Network | 12.75 | 83.99 | 25.70 |
| ETS | 14.60 | 76.57 | 24.93 |
| SARIMA | 13.86 | 54.60 | 20.65 |
| Hybrid* | 11.44 | 69.55 | 22.00 |
| Bayesian Structural | 23.53 | 187.05 | 50.78 |
| Prophet | 29.54 | 65.67 | 35.56 |

*Hybrid: Combined SARIMA, ETS, STL and Neural Network model

H : RMSE of Models

| Method | Train | Test | All |
|---------------------|--------|---------|---------|
| Neural Network | 70.07 | 1720.43 | 736.33 |
| ETS | 62.62 | 1523.42 | 624.56 |
| SARIMA | 59.63 | 1221.93 | 501.81 |
| Hybrid* | 50.95 | 1470.03 | 628.52 |
| Bayesian Structural | 90.84 | 4006.62 | 1637.80 |
| Prophet | 118.75 | 1489.20 | 617.55 |

*Hybrid: Combined SARIMA, ETS, STL and Neural Network model

I : MASE of Models

| Method | Train | Test | All |
|---------------------|-------|-------|------|
| Neural Network | 0.67 | 55.29 | 5.05 |
| ETS | 0.55 | 7.91 | 3.05 |
| SARIMA | 0.54 | 4.87 | 2.14 |
| Hybrid* | 0.44 | 8.94 | 3.26 |
| Bayesian Structural | 0.78 | 19.78 | 6.38 |
| Prophet | 1.14 | 17.72 | 4.23 |

*Hybrid: Combined SARIMA, ETS, STL and Neural Network model

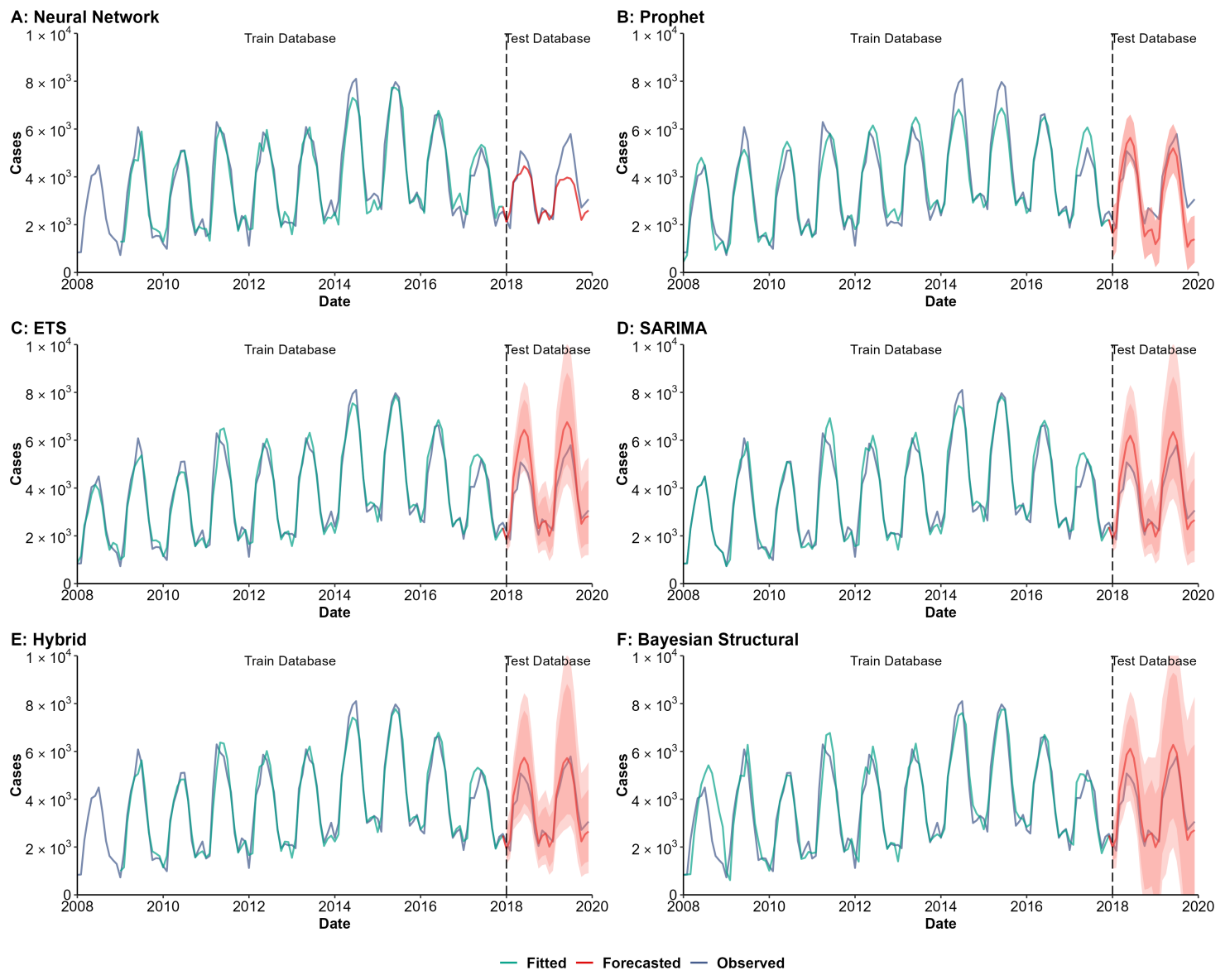
J : R_Squared of Models

| Method | Train | Test | All |
|---------------------|-------|------|------|
| Neural Network | 0.94 | 0.18 | 0.55 |
| ETS | 0.95 | 0.77 | 0.76 |
| SARIMA | 0.95 | 0.91 | 0.89 |
| Hybrid* | 0.97 | 0.92 | 0.79 |
| Bayesian Structural | 0.90 | 0.09 | 0.39 |
| Prophet | 0.81 | 0.84 | 0.75 |

*Hybrid: Combined SARIMA, ETS, STL and Neural Network model

Supplementary Fig. 41. Training and comparing variant time series models for pertussis.

(A) Neural Network model; (B) Prophet model; (C) Exponential smoothing (ETS) model; (D) Seasonal autoregressive integrated moving average (SARIMA) model; (E) Hybrid models combining SARIMA, ETS, STL (seasonal and trend decomposition using loess), and neural network model; (F) Bayesian structural model; (G) Root mean square error (RMSE) of variant models; (H) Symmetric mean absolute percentage error (SMAPE) of variant models; (I) Mean absolute scaled error (MASE) of variant models; (J) R-squared of variant models.



G : SMAPE of Models

| Method | Train | Test | All |
|---------------------|-------|-------|-------|
| Neural Network | 12.14 | 14.48 | 12.56 |
| ETS | 9.62 | 15.38 | 10.58 |
| SARIMA | 9.00 | 13.31 | 9.72 |
| Hybrid* | 8.87 | 10.70 | 9.20 |
| Bayesian Structural | 15.36 | 12.61 | 14.90 |
| Prophet | 11.07 | 28.19 | 13.92 |

*Hybrid: Combined SARIMA, ETS, STL and Neural Network model

H : RMSE of Models

| Method | Train | Test | All |
|---------------------|--------|--------|--------|
| Neural Network | 476.32 | 721.75 | 529.47 |
| ETS | 402.21 | 796.37 | 490.42 |
| SARIMA | 427.34 | 619.30 | 464.87 |
| Hybrid* | 383.89 | 431.13 | 392.90 |
| Bayesian Structural | 683.38 | 583.40 | 667.76 |
| Prophet | 509.86 | 879.70 | 587.89 |

*Hybrid: Combined SARIMA, ETS, STL and Neural Network model

I : MASE of Models

| Method | Train | Test | All |
|---------------------|-------|------|------|
| Neural Network | 0.47 | 1.29 | 0.56 |
| ETS | 0.37 | 0.78 | 0.46 |
| SARIMA | 0.37 | 0.66 | 0.42 |
| Hybrid* | 0.35 | 0.54 | 0.40 |
| Bayesian Structural | 0.58 | 0.63 | 0.60 |
| Prophet | 0.47 | 0.96 | 0.58 |

*Hybrid: Combined SARIMA, ETS, STL and Neural Network model

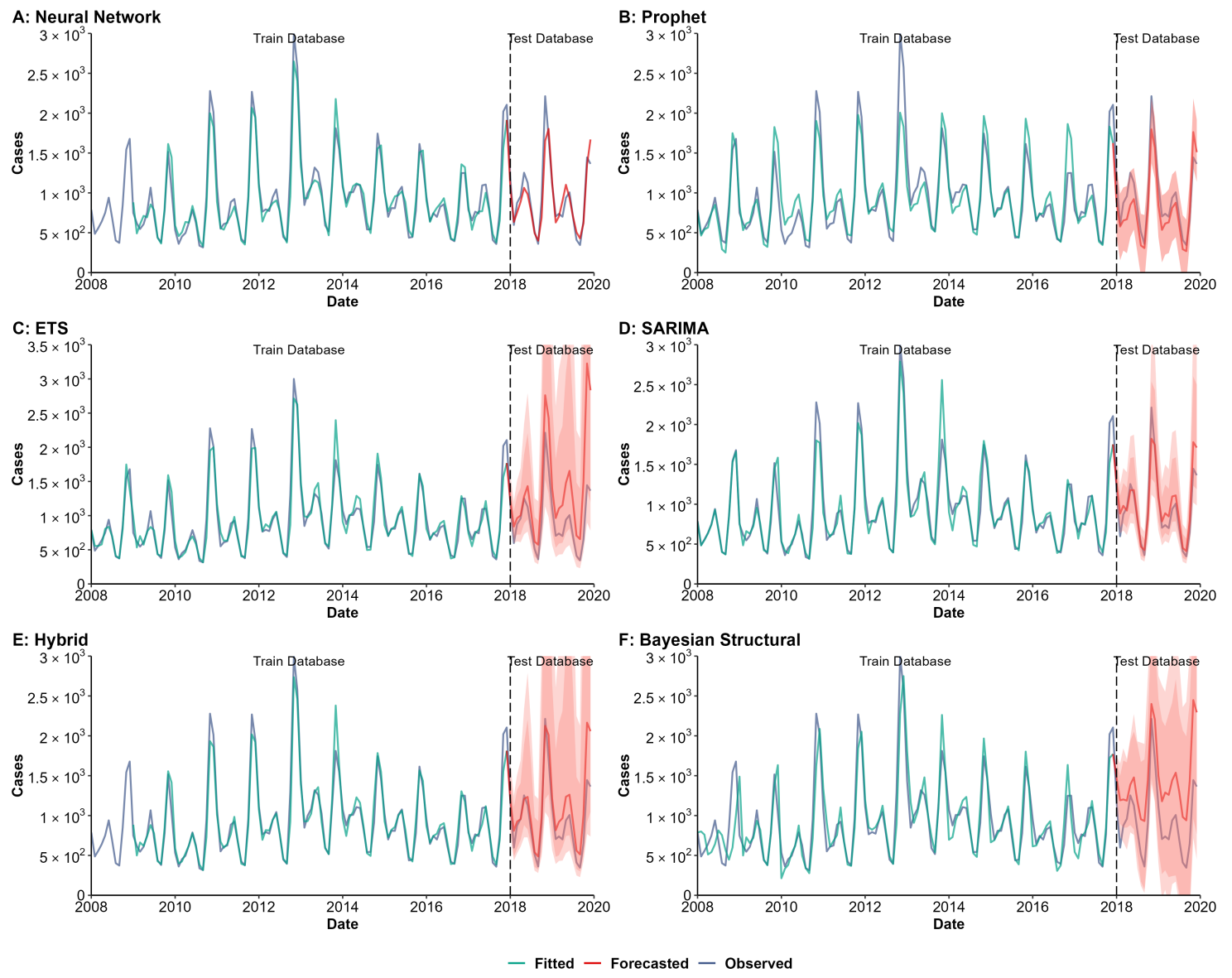
J : R_Squared of Models

| Method | Train | Test | All |
|---------------------|-------|------|------|
| Neural Network | 0.93 | 0.81 | 0.91 |
| ETS | 0.95 | 0.94 | 0.93 |
| SARIMA | 0.95 | 0.93 | 0.94 |
| Hybrid* | 0.95 | 0.92 | 0.95 |
| Bayesian Structural | 0.86 | 0.93 | 0.86 |
| Prophet | 0.92 | 0.82 | 0.89 |

*Hybrid: Combined SARIMA, ETS, STL and Neural Network model

Supplementary Fig. 42. Training and comparing variant time series models for brucellosis.

(A) Neural Network model; (B) Prophet model; (C) Exponential smoothing (ETS) model; (D) Seasonal autoregressive integrated moving average (SARIMA) model; (E) Hybrid models combining SARIMA, ETS, STL (seasonal and trend decomposition using loess), and neural network model; (F) Bayesian structural model; (G) Root mean square error (RMSE) of variant models; (H) Symmetric mean absolute percentage error (SMAPE) of variant models; (I) Mean absolute scaled error (MASE) of variant models; (J) R-squared of variant models.



G : SMAPE of Models

| Method | Train | Test | All |
|---------------------|-------|-------|-------|
| Neural Network | 9.74 | 12.02 | 10.15 |
| ETS | 9.05 | 37.05 | 13.72 |
| SARIMA | 8.90 | 12.89 | 9.57 |
| Hybrid* | 7.92 | 19.72 | 10.07 |
| Bayesian Structural | 16.77 | 47.16 | 21.84 |
| Prophet | 14.22 | 21.09 | 15.37 |

*Hybrid: Combined SARIMA, ETS, STL and Neural Network model

H : RMSE of Models

| Method | Train | Test | All |
|---------------------|--------|--------|--------|
| Neural Network | 129.17 | 165.65 | 136.53 |
| ETS | 138.60 | 611.14 | 279.75 |
| SARIMA | 151.85 | 162.02 | 153.59 |
| Hybrid* | 127.49 | 266.81 | 162.00 |
| Bayesian Structural | 235.53 | 541.45 | 308.37 |
| Prophet | 207.85 | 204.60 | 207.31 |

*Hybrid: Combined SARIMA, ETS, STL and Neural Network model

I : MASE of Models

| Method | Train | Test | All |
|---------------------|-------|------|------|
| Neural Network | 0.32 | 0.41 | 0.33 |
| ETS | 0.29 | 0.98 | 0.45 |
| SARIMA | 0.29 | 0.44 | 0.31 |
| Hybrid* | 0.26 | 0.60 | 0.32 |
| Bayesian Structural | 0.50 | 1.77 | 0.65 |
| Prophet | 0.45 | 0.61 | 0.48 |

*Hybrid: Combined SARIMA, ETS, STL and Neural Network model

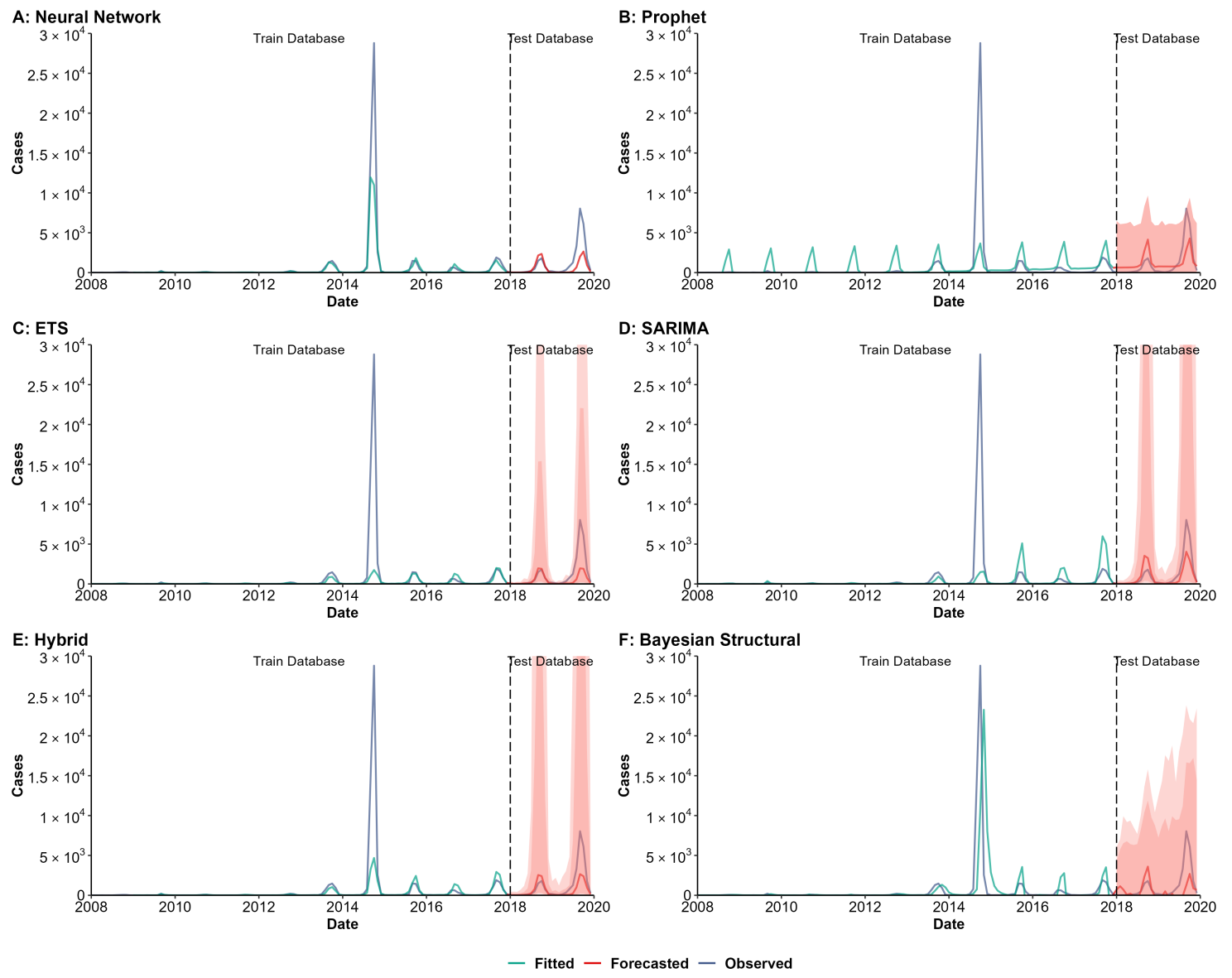
J : R_Squared of Models

| Method | Train | Test | All |
|---------------------|-------|------|------|
| Neural Network | 0.94 | 0.86 | 0.93 |
| ETS | 0.92 | 0.70 | 0.76 |
| SARIMA | 0.91 | 0.88 | 0.90 |
| Hybrid* | 0.94 | 0.84 | 0.89 |
| Bayesian Structural | 0.78 | 0.79 | 0.67 |
| Prophet | 0.82 | 0.87 | 0.82 |

*Hybrid: Combined SARIMA, ETS, STL and Neural Network model

Supplementary Fig. 43. Training and comparing variant time series models for hemorrhagic fever with renal syndrome (HFRS).

(A) Neural Network model; (B) Prophet model; (C) Exponential smoothing (ETS) model; (D) Seasonal autoregressive integrated moving average (SARIMA) model; (E) Hybrid models combining SARIMA, ETS, STL (seasonal and trend decomposition using loess), and neural network model; (F) Bayesian structural model; (G) Root mean square error (RMSE) of variant models; (H) Symmetric mean absolute percentage error (SMAPE) of variant models; (I) Mean absolute scaled error (MASE) of variant models; (J) R-squared of variant models.



G : SMAPE of Models

| Method | Train | Test | All |
|---------------------|--------|--------|--------|
| Neural Network | 32.55 | 80.31 | 41.23 |
| ETS | 60.01 | 73.88 | 62.32 |
| SARIMA | 64.04 | 57.21 | 62.90 |
| Hybrid* | 48.62 | 69.78 | 52.47 |
| Bayesian Structural | 116.22 | 137.74 | 119.80 |
| Prophet | 150.99 | 109.97 | 144.15 |

*Hybrid: Combined SARIMA, ETS, STL and Neural Network model

H : RMSE of Models

| Method | Train | Test | All |
|---------------------|---------|---------|---------|
| Neural Network | 1740.62 | 1564.42 | 1709.94 |
| ETS | 2773.70 | 1648.69 | 2619.97 |
| SARIMA | 2873.25 | 1225.84 | 2670.22 |
| Hybrid* | 2582.23 | 1474.07 | 2418.81 |
| Bayesian Structural | 2967.59 | 1848.96 | 2812.22 |
| Prophet | 2733.37 | 1408.61 | 2560.63 |

*Hybrid: Combined SARIMA, ETS, STL and Neural Network model

I : MASE of Models

| Method | Train | Test | All |
|---------------------|-------|------|------|
| Neural Network | 0.74 | 1.70 | 0.96 |
| ETS | 0.71 | 2.17 | 2.92 |
| SARIMA | 1.98 | 1.02 | 1.69 |
| Hybrid* | 0.65 | 1.60 | 1.73 |
| Bayesian Structural | 1.29 | 1.34 | 1.17 |
| Prophet | 1.50 | 1.58 | 1.52 |

*Hybrid: Combined SARIMA, ETS, STL and Neural Network model

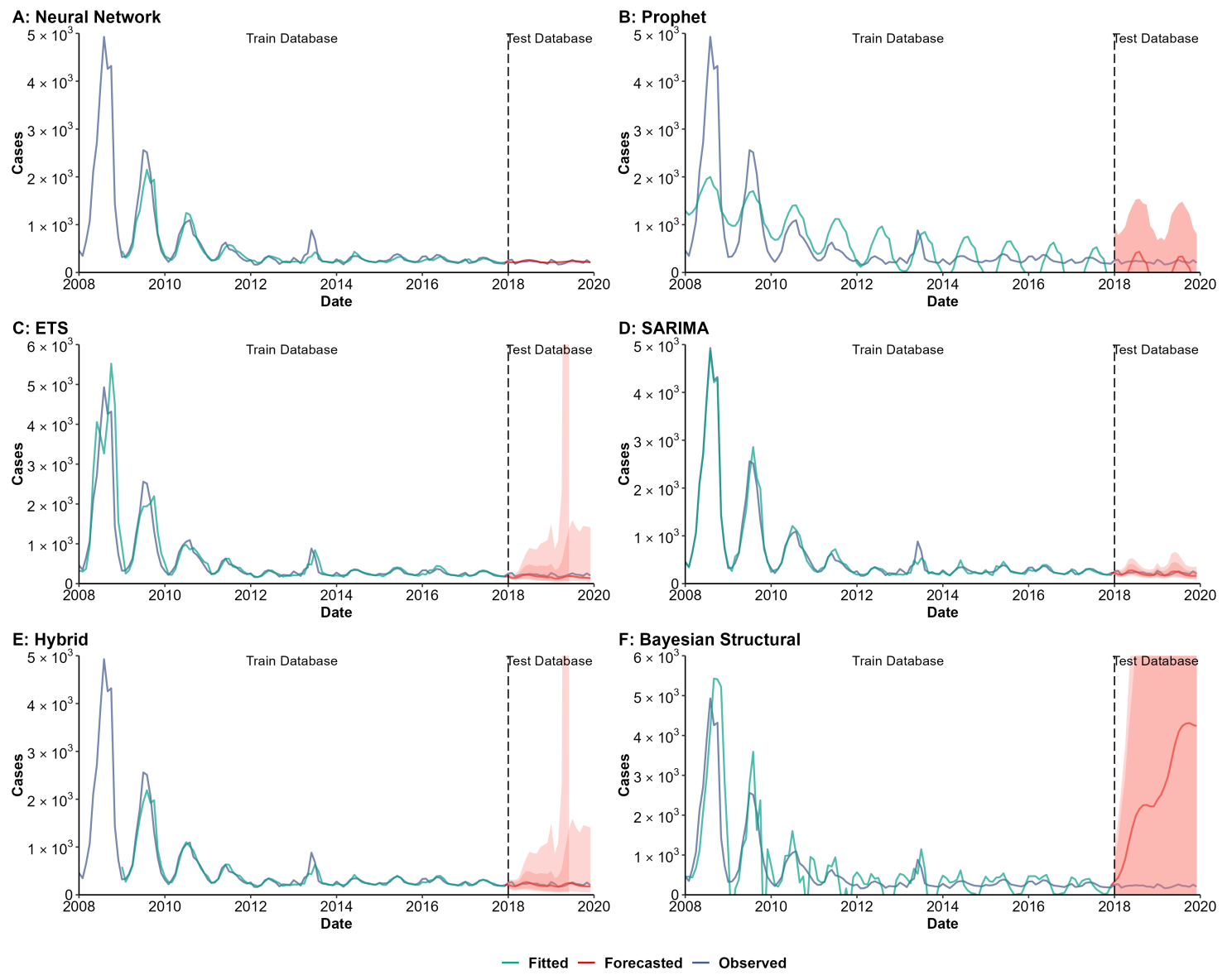
J : R_Squared of Models

| Method | Train | Test | All |
|---------------------|-------|------|------|
| Neural Network | 0.86 | 0.58 | 0.84 |
| ETS | 0.28 | 0.59 | 0.29 |
| SARIMA | 0.06 | 0.66 | 0.11 |
| Hybrid* | 0.60 | 0.62 | 0.57 |
| Bayesian Structural | 0.17 | 0.21 | 0.17 |
| Prophet | 0.14 | 0.53 | 0.17 |

*Hybrid: Combined SARIMA, ETS, STL and Neural Network model

Supplementary Fig. 44. Training and comparing variant time series models for dengue fever.

(A) Neural Network model; (B) Prophet model; (C) Exponential smoothing (ETS) model; (D) Seasonal autoregressive integrated moving average (SARIMA) model; (E) Hybrid models combining SARIMA, ETS, STL (seasonal and trend decomposition using loess), and neural network model; (F) Bayesian structural model; (G) Root mean square error (RMSE) of variant models; (H) Symmetric mean absolute percentage error (SMAPE) of variant models; (I) Mean absolute scaled error (MASE) of variant models; (J) R-squared of variant models.



G : SMAPE of Models

| Method | Train | Test | All |
|---------------------|-------|--------|-------|
| Neural Network | 15.18 | 10.57 | 14.34 |
| ETS | 17.98 | 27.30 | 19.53 |
| SARIMA | 12.43 | 15.32 | 12.91 |
| Hybrid* | 11.52 | 13.11 | 11.81 |
| Bayesian Structural | 68.73 | 153.70 | 82.89 |
| Prophet | 81.68 | 126.76 | 89.20 |

*Hybrid: Combined SARIMA, ETS, STL and Neural Network model

H : RMSE of Models

| Method | Train | Test | All |
|---------------------|--------|---------|---------|
| Neural Network | 143.37 | 28.45 | 130.25 |
| ETS | 404.63 | 61.48 | 370.23 |
| SARIMA | 108.42 | 39.92 | 100.31 |
| Hybrid* | 118.88 | 36.39 | 108.65 |
| Bayesian Structural | 595.78 | 2665.33 | 1216.47 |
| Prophet | 594.28 | 401.53 | 566.73 |

*Hybrid: Combined SARIMA, ETS, STL and Neural Network model

I : MASE of Models

| Method | Train | Test | All |
|---------------------|-------|-------|------|
| Neural Network | 0.91 | 3.19 | 0.96 |
| ETS | 0.91 | 3.48 | 0.88 |
| SARIMA | 0.33 | 1.53 | 0.36 |
| Hybrid* | 0.56 | 1.62 | 0.67 |
| Bayesian Structural | 2.00 | 13.03 | 1.88 |
| Prophet | 2.32 | 2.27 | 2.63 |

*Hybrid: Combined SARIMA, ETS, STL and Neural Network model

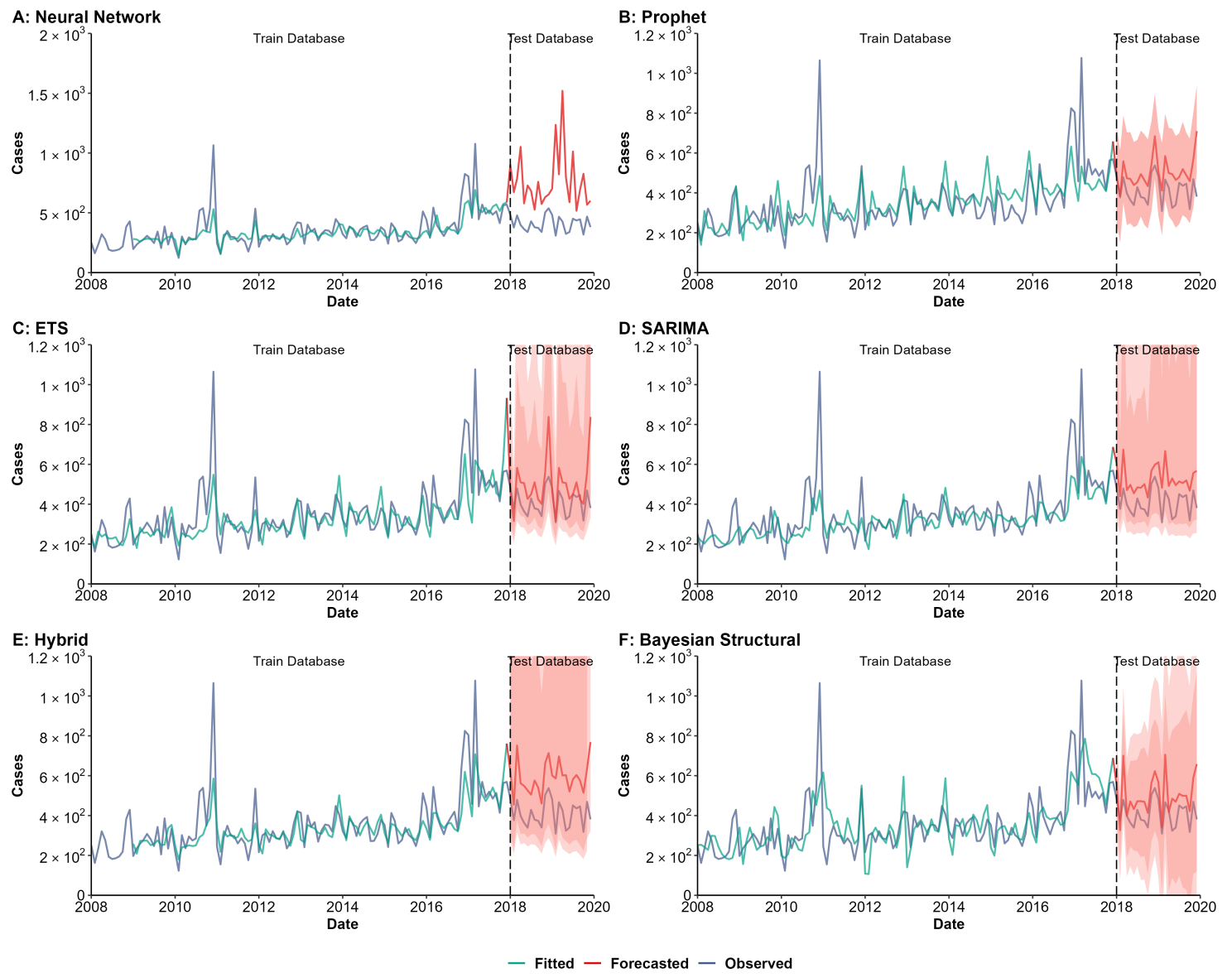
J : R_Squared of Models

| Method | Train | Test | All |
|---------------------|-------|------|------|
| Neural Network | 0.89 | 0.09 | 0.90 |
| ETS | 0.82 | 0.14 | 0.82 |
| SARIMA | 0.98 | 0.11 | 0.98 |
| Hybrid* | 0.92 | 0.13 | 0.92 |
| Bayesian Structural | 0.69 | 0.01 | 0.26 |
| Prophet | 0.52 | 0.05 | 0.49 |

*Hybrid: Combined SARIMA, ETS, STL and Neural Network model

Supplementary Fig. 45. Training and comparing variant time series models for malaria.

(A) Neural Network model; (B) Prophet model; (C) Exponential smoothing (ETS) model; (D) Seasonal autoregressive integrated moving average (SARIMA) model; (E) Hybrid models combining SARIMA, ETS, STL (seasonal and trend decomposition using loess), and neural network model; (F) Bayesian structural model; (G) Root mean square error (RMSE) of variant models; (H) Symmetric mean absolute percentage error (SMAPE) of variant models; (I) Mean absolute scaled error (MASE) of variant models; (J) R-squared of variant models.



G : SMAPE of Models

| Method | Train | Test | All |
|---------------------|-------|-------|-------|
| Neural Network | 14.39 | 56.86 | 22.11 |
| ETS | 18.03 | 20.39 | 18.42 |
| SARIMA | 19.26 | 25.02 | 20.22 |
| Hybrid* | 15.36 | 36.33 | 19.18 |
| Bayesian Structural | 23.15 | 20.69 | 22.74 |
| Prophet | 19.67 | 20.28 | 19.77 |

*Hybrid: Combined SARIMA, ETS, STL and Neural Network model

H : RMSE of Models

| Method | Train | Test | All |
|---------------------|--------|--------|--------|
| Neural Network | 95.96 | 433.61 | 204.25 |
| ETS | 109.02 | 139.10 | 114.58 |
| SARIMA | 110.36 | 125.18 | 112.96 |
| Hybrid* | 96.63 | 193.75 | 120.27 |
| Bayesian Structural | 119.46 | 117.68 | 119.17 |
| Prophet | 112.35 | 113.36 | 112.52 |

*Hybrid: Combined SARIMA, ETS, STL and Neural Network model

I : MASE of Models

| Method | Train | Test | All |
|---------------------|-------|------|------|
| Neural Network | 1.31 | 1.35 | 1.32 |
| ETS | 0.68 | 0.82 | 0.95 |
| SARIMA | 1.51 | 1.54 | 1.52 |
| Hybrid* | 0.58 | 2.09 | 1.34 |
| Bayesian Structural | 0.83 | 0.82 | 1.06 |
| Prophet | 0.73 | 1.25 | 1.00 |

*Hybrid: Combined SARIMA, ETS, STL and Neural Network model

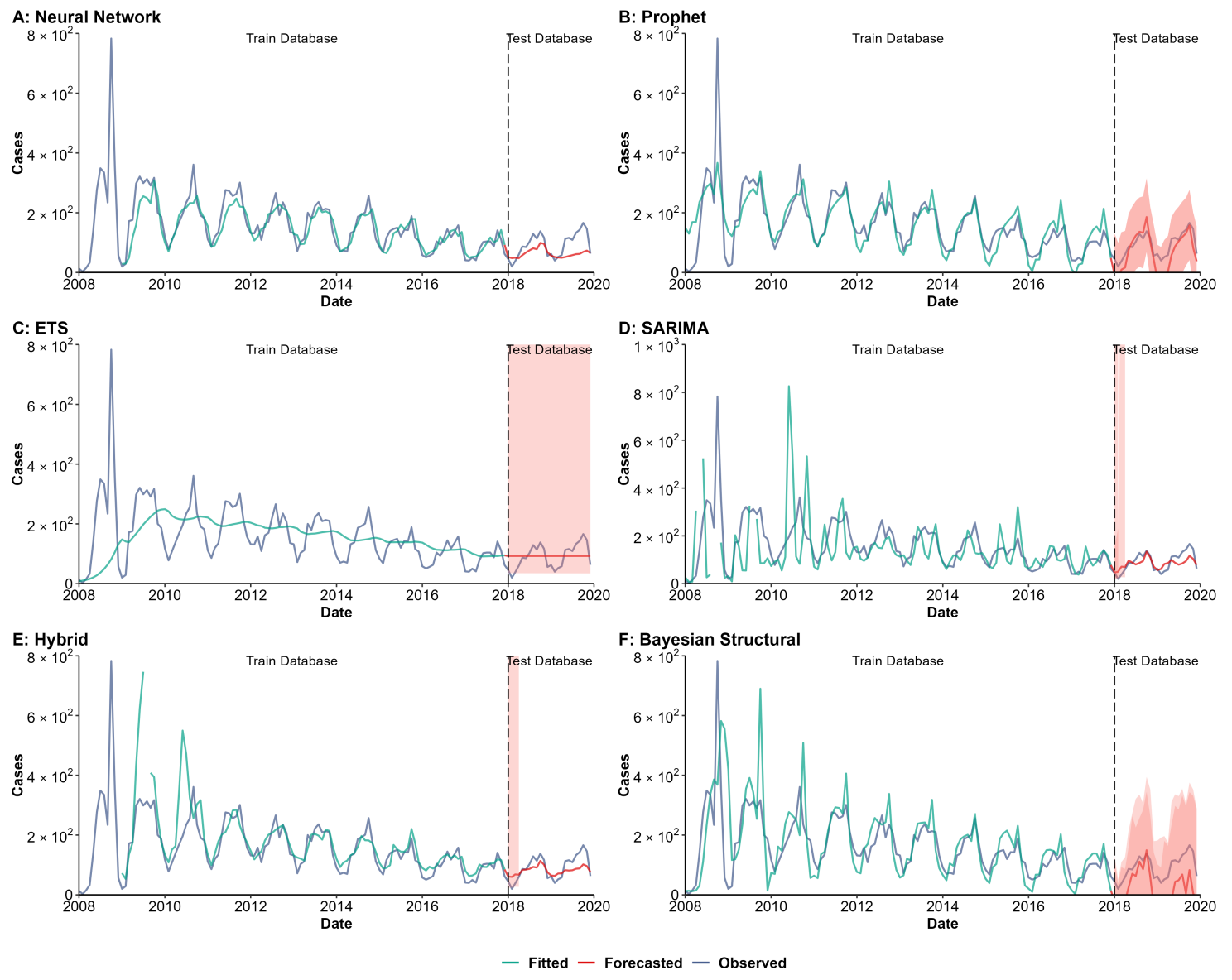
J : R_Squared of Models

| Method | Train | Test | All |
|---------------------|-------|------|------|
| Neural Network | 0.66 | 0.00 | 0.17 |
| ETS | 0.50 | 0.25 | 0.42 |
| SARIMA | 0.52 | 0.51 | 0.40 |
| Hybrid* | 0.64 | 0.34 | 0.40 |
| Bayesian Structural | 0.42 | 0.45 | 0.41 |
| Prophet | 0.44 | 0.30 | 0.40 |

*Hybrid: Combined SARIMA, ETS, STL and Neural Network model

Supplementary Fig. 46. Training and comparing variant time series models for echinococcosis.

(A) Neural Network model; (B) Prophet model; (C) Exponential smoothing (ETS) model; (D) Seasonal autoregressive integrated moving average (SARIMA) model; (E) Hybrid models combining SARIMA, ETS, STL (seasonal and trend decomposition using loess), and neural network model; (F) Bayesian structural model; (G) Root mean square error (RMSE) of variant models; (H) Symmetric mean absolute percentage error (SMAPE) of variant models; (I) Mean absolute scaled error (MASE) of variant models; (J) R-squared of variant models.



G : SMAPE of Models

| Method | Train | Test | All |
|---------------------|-------|--------|-------|
| Neural Network | 19.06 | 40.05 | 22.88 |
| ETS | 43.26 | 42.22 | 43.09 |
| SARIMA | 42.25 | 28.28 | 39.85 |
| Hybrid* | 23.23 | 30.53 | 24.57 |
| Bayesian Structural | 39.33 | 131.59 | 54.71 |
| Prophet | 32.34 | 74.13 | 39.31 |

*Hybrid: Combined SARIMA, ETS, STL and Neural Network model

H : RMSE of Models

| Method | Train | Test | All |
|---------------------|--------|-------|--------|
| Neural Network | 38.50 | 43.52 | 39.46 |
| ETS | 103.91 | 40.12 | 96.26 |
| SARIMA | 116.52 | 27.73 | 106.68 |
| Hybrid* | 78.30 | 30.21 | 71.94 |
| Bayesian Structural | 99.99 | 85.32 | 97.70 |
| Prophet | 61.06 | 40.85 | 58.18 |

*Hybrid: Combined SARIMA, ETS, STL and Neural Network model

I : MASE of Models

| Method | Train | Test | All |
|---------------------|-------|----------|-------|
| Neural Network | 1.09 | 5.40 | 1.30 |
| ETS | 1.42 | 37811.26 | 16.10 |
| SARIMA | 0.92 | 1.59 | 0.94 |
| Hybrid* | 1.19 | 3.31 | 1.19 |
| Bayesian Structural | 1.26 | 1.83 | 1.03 |
| Prophet | 0.82 | 0.99 | 0.95 |

*Hybrid: Combined SARIMA, ETS, STL and Neural Network model

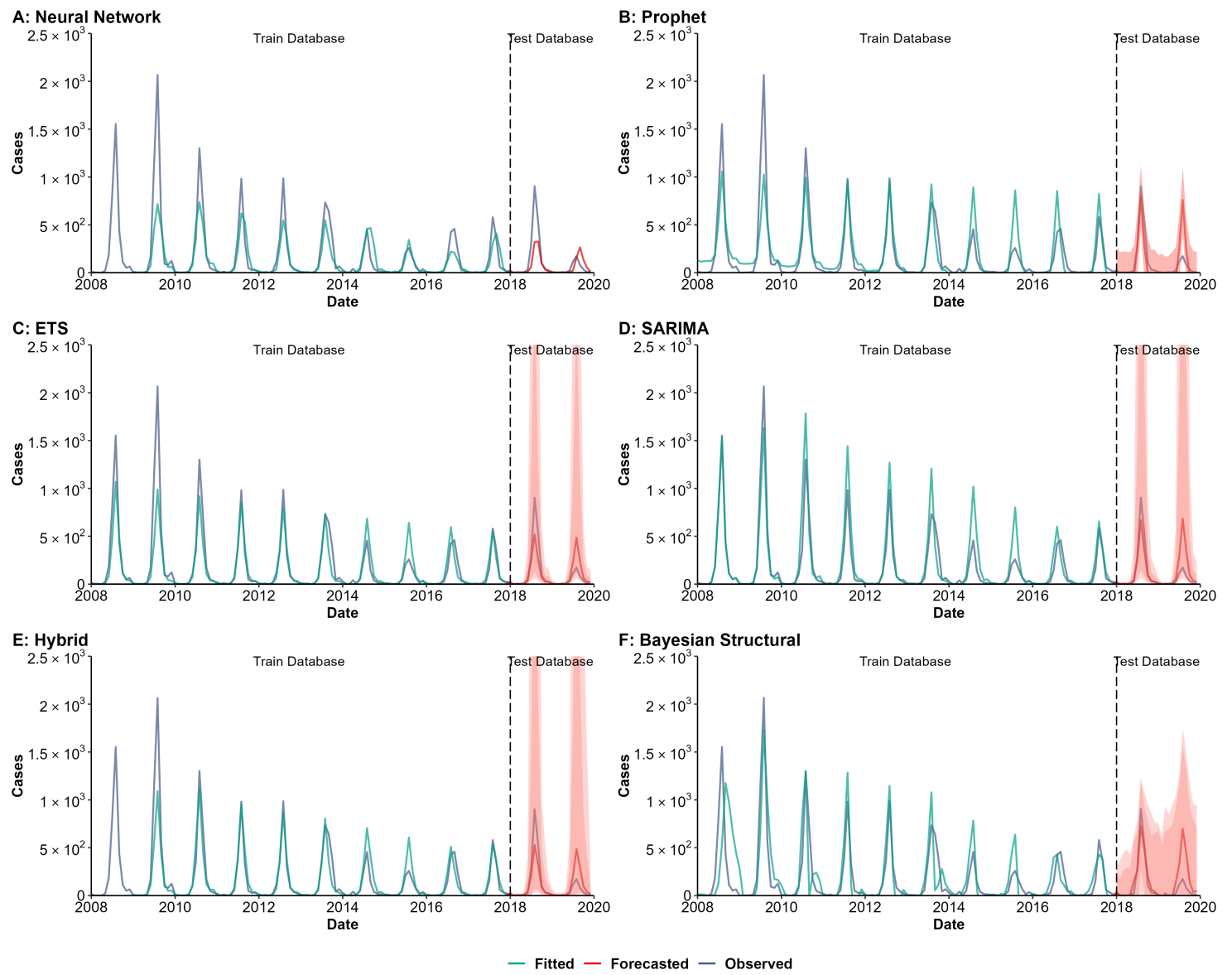
J : R_Squared of Models

| Method | Train | Test | All |
|---------------------|-------|------|------|
| Neural Network | 0.75 | 0.38 | 0.74 |
| ETS | 0.05 | 0.29 | 0.09 |
| SARIMA | 0.11 | 0.64 | 0.14 |
| Hybrid* | 0.57 | 0.80 | 0.59 |
| Bayesian Structural | 0.40 | 0.54 | 0.44 |
| Prophet | 0.63 | 0.80 | 0.65 |

*Hybrid: Combined SARIMA, ETS, STL and Neural Network model

Supplementary Fig. 47. Training and comparing variant time series models for typhus.

(A) Neural Network model; (B) Prophet model; (C) Exponential smoothing (ETS) model; (D) Seasonal autoregressive integrated moving average (SARIMA) model; (E) Hybrid models combining SARIMA, ETS, STL (seasonal and trend decomposition using loess), and neural network model; (F) Bayesian structural model; (G) Root mean square error (RMSE) of variant models; (H) Symmetric mean absolute percentage error (SMAPE) of variant models; (I) Mean absolute scaled error (MASE) of variant models; (J) R-squared of variant models.



G : SMAPE of Models

| Method | Train | Test | All |
|---------------------|--------|--------|--------|
| Neural Network | 56.47 | 71.44 | 59.20 |
| ETS | 45.10 | 66.28 | 48.63 |
| SARIMA | 50.29 | 66.36 | 52.97 |
| Hybrid* | 46.67 | 61.37 | 49.34 |
| Bayesian Structural | 120.67 | 116.21 | 119.93 |
| Prophet | 114.71 | 165.91 | 123.24 |

*Hybrid: Combined SARIMA, ETS, STL and Neural Network model

H : RMSE of Models

| Method | Train | Test | All |
|---------------------|--------|--------|--------|
| Neural Network | 186.43 | 142.46 | 179.24 |
| ETS | 155.98 | 123.15 | 151.00 |
| SARIMA | 147.68 | 137.83 | 146.09 |
| Hybrid* | 138.15 | 120.42 | 135.10 |
| Bayesian Structural | 239.91 | 150.99 | 227.51 |
| Prophet | 173.93 | 180.99 | 175.13 |

*Hybrid: Combined SARIMA, ETS, STL and Neural Network model

I : MASE of Models

| Method | Train | Test | All |
|---------------------|-------|------|------|
| Neural Network | 0.89 | 1.25 | 0.94 |
| ETS | 0.40 | 0.70 | 0.51 |
| SARIMA | 0.36 | 0.57 | 0.38 |
| Hybrid* | 0.39 | 0.69 | 0.46 |
| Bayesian Structural | 0.88 | 0.64 | 0.70 |
| Prophet | 0.66 | 0.93 | 0.71 |

*Hybrid: Combined SARIMA, ETS, STL and Neural Network model

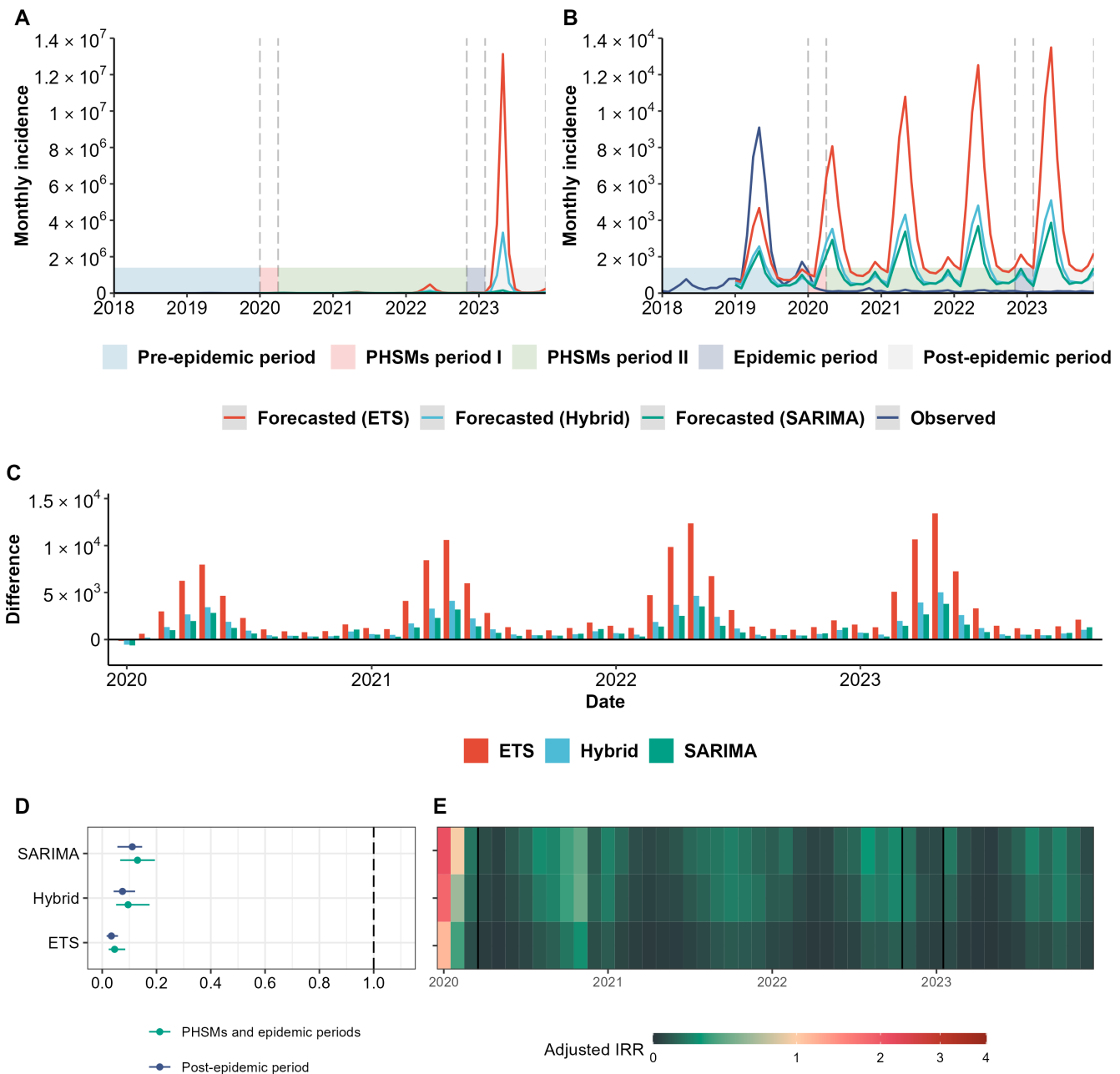
J : R_Squared of Models

| Method | Train | Test | All |
|---------------------|-------|------|------|
| Neural Network | 0.74 | 0.64 | 0.73 |
| ETS | 0.82 | 0.64 | 0.81 |
| SARIMA | 0.85 | 0.60 | 0.83 |
| Hybrid* | 0.82 | 0.66 | 0.81 |
| Bayesian Structural | 0.56 | 0.61 | 0.57 |
| Prophet | 0.72 | 0.63 | 0.69 |

*Hybrid: Combined SARIMA, ETS, STL and Neural Network model

Supplementary Fig. 48. Training and comparing variant time series models for Japanese encephalitis (JE).

(A) Neural Network model; (B) Prophet model; (C) Exponential smoothing (ETS) model; (D) Seasonal autoregressive integrated moving average (SARIMA) model; (E) Hybrid models combining SARIMA, ETS, STL (seasonal and trend decomposition using loess), and neural network model; (F) Bayesian structural model; (G) Root mean square error (RMSE) of variant models; (H) Symmetric mean absolute percentage error (SMAPE) of variant models; (I) Mean absolute scaled error (MASE) of variant models; (J) R-squared of variant models.



Supplementary Fig. 49. Training and comparing variant time series models for rubella.

(A) The forecasted number of rubella cases in the China from 2020 to 2023 trained on 2008-2019 data. (B) The forecasted number of rubella cases in the China from 2019 to 2023 trained on 2008-2018 data. (C) The difference between the forecasted incidence and the observed incidence of rubella in the China from 2020 to 2023, based on the model trained on 2008-2018 data. (D) The adjusted incidence relative ratio (IRR) distribution of rubella during different period which split by October 2022. (E) The changes of adjusted IRR of rubella during different period.